PERFUSION BIOREACTOR FOR TISSUE-ENGINEERED BLOOD VESSELS

A Thesis
Presented to
The Academic Faculty

By

Chrysanthi Williams

In Partial Fulfillment
of the Requirements for the Degree
Doctor of Philosophy in Bioengineering

Georgia Institute of Technology
December, 2003

PERFUSION BIOREACTOR FOR TISSUE-ENGINEERED BLOOD VESSELS

Approved by:

Dr. Timothy M. Wick, Advisor

Dr. Don Giddens

Dr. Pete Ludovice

Dr. Harish Radhakrishna

Dr. Athanassios Sambanis

Date Approved 12/03/03

To My Parents, Zafeiria and Panagiotis, and Husband, Kenneth

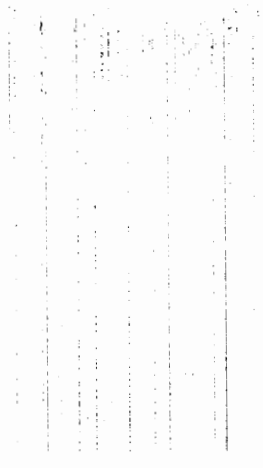

ACKNOWLEDGEMENTS

I would like to express my sincere appreciation and gratitude to my advisor and mentor, Dr. Timothy M. Wick, for entrusting me with a challenging project and teaching me how to be an independent researcher. He taught me how to strive for excellence in my academic pursuits and helped me develop critical thinking skills. I would also like to thank my committee members, Drs. Don P. Giddens, Pete Ludovice, Harish Radhakrishna and Athanassios Sambanis for their assistance and input in this work. Special thanks to Tracey Couse, the IBB histologist, for her help and genuine friendship and support.

I would also like to thank Dr. Sunil Saini for his wonderful friendship and for setting an example of a great investigator, as well as Matt Wagner, Padmini Rangamani, and many others in IBB for their friendship and support.

My sincerest thanks go to my parents for their unconditional and eternal love and support. Their memory is always with me and has given me the strength to complete this work. I am also grateful to my grandmother for her faith in God. She taught me how to always be grateful for what I have and never give up. Special thanks to my husband, Ken Williams, for his love and support through the hard times. His encouragement and example of hard work helped me attain my goals.

TABLE OF CONTENTS

LIST OF TABLES

LIST OF FIGURES

LIST OF ABBREVIATIONS

CABG	Coronary Artery Bypass Graft
$CHCl_3$	Methylene Chloride
DAB	p-Dimethylaminobenzaldehyde
DI	Deionized
DMEM	Dulbecco's Modified Eagle Medium
DMMB	Dimethylmethylene Blue
DNA	Deoxyribonucleic Acid
DS	Dual Seeding
EC	Endothelial Cells/Endothelialization
ECM	Extracellular Matrix
EDTA	Ethylenediaminetetraacetic Acid
EGF	Epidermal Growth Factor
ePTFE	Expanded Polytetrafluoroethylene
FBS	Fetal Bovine Serum
FDA	Food and Drug Administration
FGF	Fibroblast Growth Factor
Fn	Fibronectin
GAG	Glycosaminoglycan
H&E	Hematoxylin and Eosin
HASMC	Human Aortic Smooth Muscle Cells
HCl	Hydrochloric Acid
HEPES	N-(2-hydroxyethyl)piperazine-N(2-ethanesulfonic acid)

HMDS	Hexamethyldisilazane
L/G	Lactate/Glucose
NaCl	Sodium Chloride
NaOH	Sodium Hydroxide
OD	Optical Density
PBE	Phosphate Buffered Saline/EDTA
PBS	Phosphate Buffered Saline
PCL	Poly-ε-caprolactone
PECAM	Platelet Endothelial Cell Adhesion Molecule
PGA	Polyglycolic Acid
PHA	Polyhydroxyalkanoate
PLGA	Poly-Lactic-co-Glycolic Acid
PLLA	Poly-L-lactic Acid
PTCA	Percutaneous Transluminal Coronary Angioplasty
RASMC	Rat Aortic Smooth Muscle Cells
SMA	Smooth Muscle α-Actin
SMC	Smooth Muscle Cells
SS	Single Seeding
VCAM	Vascular Endothelial Cell Adhesion Molecule
vWF	Von Willebrand Factor

SUMMARY

Limited availability of autologous small diameter vessels needed for bypass surgery in the coronary and peripheral circulation has motivated research toward creating tissue-engineered vascular grafts. Bioreactors have recently been acknowledged as an integral part of vascular tissue engineering due to their numerous capabilities. Indeed, bioreactors can be used to impart biochemical and mechanical stimuli similar to those observed in vivo, improve nutrient transport compared to static cultures, and significantly increase tissue production in a reproducible and controllable manner.

The goal of this work was to develop a scaleable perfusion bioreactor for the production of small diameter arterial constructs. The compact bioreactor is composed of modules arranged in series so that one construct is mounted in each module and all constructs are exposed to the same environment. The bioreactor has two independent flow loops, one through the construct lumen and one on the external surface. Both flow loops were used to seed bovine aortic smooth muscle cells (SMC) on porous polyglycolic acid non-woven felts under dynamic conditions; bovine aortic endothelial cells (EC) were introduced through the lumen at later culture times.

In single (lumen only) seeding, SMC ($0.9x10^6$ cells/ml) were perfused reciprocally through the scaffold lumen at a low flow rate for 24 hours, and a fresh SMC suspension ($0.9x10^6$ cells/ml) was seeded under the same conditions for an additional 24 hours. During these 48 hours, the external surface of the scaffolds was supplied with culture medium by a peristaltic pump. In dual (lumen and external surface) seeding,

SMC were seeded (as previously described) for 24 hours, and then a fresh SMC suspension ($0.9x10^6$ cells/ml) was perfused on the external surface of the scaffold for 24 hours while culture medium was perfused through the lumen by a peristaltic pump. After seeding, medium was delivered through both the lumen and the external surface of the scaffold at 1.5 Hz by a peristaltic pump during growth. For both single- and dual-seeded constructs, an EC suspension ($0.1x10^6$ cells/ml) was perfused through the construct lumen reciprocally by a dual syringe pump at 4 ml/min two days prior to harvest (late endothelialization) as described previously for SMC suspension.

Cell seeding efficiency was 13% for both protocols; cell density was $739x10^6$ and $776x10^6$ cells per g of tissue; collagen was 586 and 741 μg; and glycosaminoglycan content was 9 mg per construct (for both), in single and dual seeding, respectively. Even though biochemical analysis data were comparable for both protocols, histological analysis showed more collagen and elastin in dual-seeded constructs. Furthermore, handling ability of dual-seeded constructs, i.e. constructs' structural integrity, was superior to that of single-seeded constructs, so ring tensile tests were performed on dual-seeded constructs. Ultimate tensile strength of dual-seeded constructs was 2% of the ultimate tensile strength of native bovine aortic tissue.

To test the hypothesis that early EC seeding will enhance arterial construct growth by increasing SMC proliferation and matrix production, 25-day experiments were performed where dual-seeded constructs were seeded with EC after 10 days of SMC culture (early endothelialization) versus 23 days of SMC culture (late endothelialization). Long term co-culture (15 days) of EC and SMC resulted in significantly higher cell number ($27x10^6$ cells versus $16x10^6$ cells, respectively), but lower collagen (2% versus

4% of the dry weight) and GAG content (37% versus 44% of the dry weight) compared to short term co-culture (2 days). These results show that EC regulate SMC functions and control the amount of extracellular matrix produced. This finding gives tissue engineers one more parameter that can be adjusted for optimal growth of vascular grafts in vitro. Specifically, increasing EC seeding density would decrease EC and SMC proliferation (proliferating EC increase SMC proliferation) and possibly enhance SMC extracellular matrix production.

Development of robust bioreactors and bioprocessing technologies is essential to produce functional tissue-engineered constructs to meet clinical demands. Since bioreactor biomechanical environment controls cell differentiation and construct development, bioreactor design must be addressed in the early stages of tissue engineering research. A scaleable perfusion bioreactor has been developed in this work for the simultaneous growth of multiple vascular grafts under similar conditions. This bioreactor allowed for the sequential seeding of SMC and EC and incorporated construct biomechanical stimulation (shear stress and pulsatility); therefore the bioreactor is a significant contribution towards attaining engineered vascular tissue with complex architecture and differentiated function.

CHAPTER I

INTRODUCTION

Since 1918, cardiovascular disease has been the No. 1 killer in the United States, claiming 1.4 million persons in 2000 alone, with 54% of the deaths due to coronary heart disease (CHD) (American Heart Association, 2003). Coronary arteries supply blood to the myocardium of the heart, and CHD occurs due to cholesterol-lipid-calcium deposits on the inner walls that narrow the vessel lumen and prevent adequate blood supply. Current therapies focus on either removing these deposits (laser angioplasty, atherectomy), expanding the narrowed arteries (balloon angioplasty), or bypassing the occluded region using a native vessel or an engineered vascular graft. Each of these approaches has limitations. For example, removing the deposits or expanding the arteries leads to restenosis with time, and bypass surgery is an invasive procedure that carries serious risks, such as heart attack, stroke, or even death. Native vessels that are used as substitutes have limited availability, and synthetic grafts used to replace small diameter arteries induce clotting and fail.

Significant work has been performed toward the design of biomaterials to serve as small diameter conduits. Since the blood-contacting surface of biomaterials often induces clotting, researchers have incorporated heparin to prevent coagulation, seeded the inner surfaces with endothelial cells that among other functions provide the anti-thrombogenic properties of native vessels, and/or modified the surface otherwise. Although some of these approaches have been successful short term, complications such as thrombosis, infection, and graft failure arise with time.

An alternative to synthetic grafts is the development of completely biological or tissue-engineered replacement arteries. These grafts are composed of cells residing in a biodegradable or biologic scaffold that dissolves over time in culture and is replaced by the cell-synthesized matrix. Through this approach, the graft eventually mimics the architecture of native vessels, which are composed of different cell types (endothelial cells, smooth muscle cells, fibroblasts), and their matrix and have a very organized and specific structure. The underlying concept is that with time no foreign material will be present, and the occluded vessel will have been replaced with living tissue composed of cells and their extracellular matrix.

Engineering of arterial constructs in vitro requires biochemical and mechanical cues that can be imparted by bioreactors. Bioreactors improve nutrient delivery to the growing tissues by culture medium perfusion, can provide pulsatile shear stress, tension and pressure to mimic the in vivo mechanical environment, and increase tissue production in a reproducible manner compared to static cultures. The bioreactor design described in this thesis has incorporated these characteristics and is used to address issues related to dynamic cell seeding and SMC-EC co-culture conditions.

Aortic smooth muscle and endothelial cells are seeded into biodegradable polymeric scaffolds in a dual perfusion bioreactor to address fundamental questions about arterial tissue growth and differentiation. This bioreactor has two independent flows: through the lumen of the tubular constructs and on their external surface. The utility of this attribute was studied by seeding both surfaces of a scaffold with smooth muscle cells (dual seeding) and comparing the results with single seeding (through the lumen only). Both smooth muscle and endothelial cells were seeded on the scaffolds under dynamic

conditions in the same bioreactor without compromising sterility. Dynamic seeding not only renders the bioprocess of arterial construct development time- and cost-efficient, but also allows for the seeding of multiple cell types at different times in culture, an important step toward the engineering of tissues with multi-layered architecture. Additionally, this scaleable bioreactor enables the production of multiple grafts at a time, which is a step toward addressing scale-up related issues.

The specific aims of this thesis are:

1. *Cell and porous biodegradable scaffold evaluation in static experiments in terms of cell attachment and proliferation to identify cell/polymer combination for bioreactor culture.*

Static seeding experiments of aortic smooth muscle cells in various biodegradable polymer matrices helped reveal a cell-matrix combination with potential for use as a small caliber blood vessel substitute. A decision was based on important parameters, such as cell attachment, distribution, and proliferation. Growth of human and animal aortic smooth muscle cells in poly(L-lactic acid) (PLLA), poly(ε-caprolactone) (PCL), and poly(glycolic acid) (PGA) was compared, and the chosen cell-scaffold combination was used to validate the bioreactor system. Additionally, different polymer surface modifications were investigated to improve cell attachment and proliferation. These static experiments focused on identifying a cell-matrix combination supporting high cell attachment and proliferation, which was then used in dynamic bioreactor experiments. An exhaustive search of all possible combinations of cell types, polymers and surface modifications was not performed. Rather, the goal here was to select a biodegradable

polymer scaffold that supports cell attachment and proliferation for use in bioreactor experiments.

Dynamic experiments in the bioreactor system required the development of tubular polymeric scaffolds with uniform properties. Tubular PLLA and PCL scaffolds were prepared with compression molding and casting, while PGA felts were sutured across their length to create a tubular scaffold. However, based on static seeding experiments, PGA scaffolds were selected for bioreactor experiments and tubular PLLA and PCL scaffolds were not tested in the bioreactor.

2. *Design and validation of a dual perfusion bioreactor for the long term growth of small diameter arterial constructs.*

This aim involved the design and development of a dual perfusion bioreactor system that can accommodate seeding and growth of several constructs at a time in a homogeneous biochemical environment and closely mimic the physiologic flow environment of a native artery. Both the seeding, growth and maturation of the graft took place in the same vessel thereby minimizing handling and contamination risk. The design also allowed for the mechanical preconditioning of the constructs with pulsatile shear stress to enhance matrix synthesis and cell differentiation.

PGA scaffolds were mounted in the bioreactor and seeded with aortic smooth muscle and endothelial cells. Primary objectives were uniform SMC distribution, high cell proliferation, robust extracellular matrix production (collagen and elastin), and smooth muscle cell differentiation. Short and long term experiments showed that

dynamic cell seeding, cell attachment, uniform cell distribution, differentiation, high proliferation, and extracellular matrix production can be achieved in the bioreactor.

3. *Comparison of single (lumen only) versus dual (lumen and external surface) cell seeding in the bioreactor and their effect on cell proliferation, differentiation, distribution, and extracellular matrix production.*

This bioreactor is the first system that has the ability to seed smooth muscle cells both on the external and the lumen surface of scaffolds under dynamic conditions, and be used for long term growth of arterial constructs. This attribute is the result of dual perfusion of both surfaces via two independent flow loops. To investigate whether dual seeding of smooth muscle cells has an advantage over single seeding in terms of cell attachment, distribution and proliferation, we directly compared the two protocols in 25-day bioreactor experiments. Harvested constructs were also analyzed for tissue differentiation and extracellular matrix content.

4. *Comparison of early (10 days) versus late (23 days) endothelialization of SMC-seeded constructs in the bioreactor and their effect on cell proliferation, differentiation, distribution, and extracellular matrix production.*

Dynamic cell seeding in the bioreactor allowed the comparison of early versus late endothelialization on arterial construct development. The effect of short term (2 days in late endothelialization) versus long term (15 days in early endothelialization) co-culture of smooth muscle and endothelial cells on arterial construct growth and differentiation was studied in 25-day bioreactor experiments. In these experiments, smooth muscle cells

were seeded onto PGA scaffolds with the dual seeding protocol and endothelial cells were introduced through the lumen after 10 or 23 days. Endothelial cells recruit pericytes/smooth muscle cells during vasculogenesis/angiogenesis in vivo and provide cues that regulate smooth muscle cell migration, proliferation, and differentiation. However, most tissue engineering approaches seed endothelial cells toward the end of the in vitro culture, thereby inhibiting long term interactions between the two cell types.

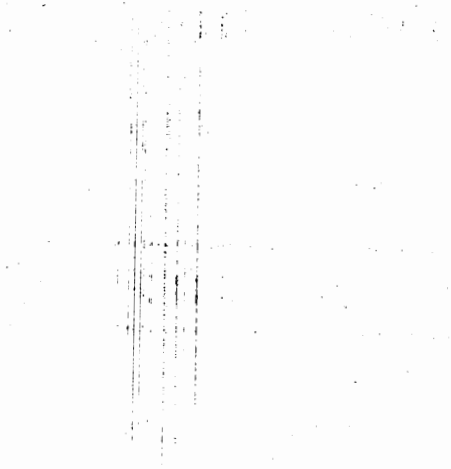

CHAPTER II

BACKGROUND

II.1 Anatomy and Physiology of an Artery

II.1.1 Cellular Components

An arterial wall is composed of three layers (Figure 2.1). The inner layer, tunica intima, is a monolayer of endothelial cells (EC) "glued" together by a polysaccharide matrix and separated from the next layer by a thick elastic band, the internal elastic lamina. The internal elastic lamina is interrupted by fenestrae, through which smooth muscle cells may migrate from the media into the intima, and form contacts with endothelial cells. The middle layer, tunica media, is mainly composed of smooth muscle cells (SMC), collagenous connective tissue, and elastic fibers. The components of the extracellular matrix (ECM) between the smooth muscle cells help in minimizing energy loss during pressure changes that occur during the pulsatile flow of blood. The media is separated from the adjacent outer layer by another thick elastic band, the external elastic lamina. The outer layer, tunica adventitia, consists of connective tissue, provides rigidity, and aids in maintaining the shape of blood vessels and anchoring them to the surrounding tissues (Ku, 2000; Wight, 1996). Because diffusion of oxygen from the lumen to the outer layers of the media is inadequate in the largest caliper vessels, small arterioles arising in the adventitia send vascular branches (vasa vasorum, or vessels of the vessels) into the outer one-half to two-thirds of the media.

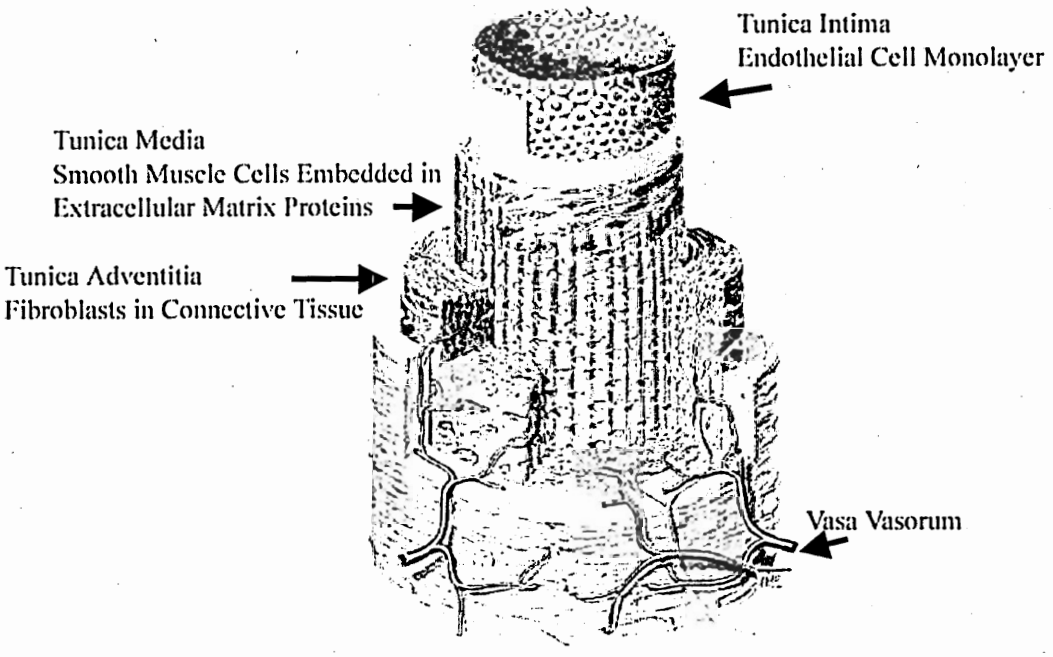

Figure 2.1 Multi-Layered Architecture of the Arterial Wall.
Adapted from Kangasniemi and Opas (Kangasniemi and Opas, 1997).

Each layer and cell type has specific functions and serves distinct purposes. Endothelial cells (EC) form a monolayer that lines the entire vascular system and have a remarkable capacity to adjust their number and arrangement to suit local requirements. EC are polygonal, elongated cells that have many pinocytotic vesicles and form junctional complexes with their neighbors. They uniquely contain Weibel-Palade bodies, 0.1 μm wide, 3 μm long membrane-bound structures that represent the storage organelle for von Willebrand factor (vWF) (Cotran et al., 1994). EC are involved in extending (angiogenesis) and remodeling the blood vessel network, thereby effecting tissue growth and repair. As a semipermeable membrane, the endothelium controls the transfer of small and large molecules into the arterial wall and through the walls of capillaries and venules. In most regions, the intercellular junctions are normally impermeable to such

molecules, but the relatively labile junctions between EC may widen under the influence of hemodynamic factors and vasoactive agents. EC play an important role in tissue homeostasis, fibrinolysis and coagulation, vasotone regulation, growth regulation of other cell types, and blood cell activation and migration during physiological and pathological processes (Risau, 1995; Shireman and Pearce, 1996).

Vascular smooth muscle cells perform many functions, including vasoconstriction and dilation in response to normal or pharmacological stimuli; synthesis of various types of collagen, elastin, and proteoglycans; elaboration of growth factors and cytokines; and migration and proliferation. Resting vascular SMCs are spindle-shaped, with single, elongated nuclei, resembling fibroblasts. The contractile function of SMC is mediated by cytoplasmic filaments that contain actin and myosin.

Smooth muscle cells are capable of expressing a range of phenotypes or alterations in character (Chamley-Campbell and Campbell, 1981; Owens, 1995; Thyberg et al., 1990). Modulations in cell phenotype may occur as a result of cell-cell interactions, alterations of extracellular matrix, or in response to other signals such as hormones (Stegemann and Nerem, 2003). At one end of this phenotypic spectrum are SMC in contractile state with 80-90% of the cytoplasmic volume occupied with contractile apparatus (Tagami et al., 1986). Organelles such as rough endoplasmic reticulum, Golgi, and free ribosomes are few in number and located in the perinuclear region. SMC in the contractile phenotypic state exhibit reduced proliferation and matrix production. At the other end of the spectrum is the synthetic state, which is seen in development, repair, and pathological conditions. SMC with synthetic phenotype proliferate and actively produce extracellular matrix proteins, and their cytoplasm

contains few filament bundles but large amounts of rough endoplasmic reticulum, Golgi, and free ribosomes (Ross, 1971). Aortic SMC in synthetic state synthesize four-fold the amount of collagen and five-fold the amount of sulfated glycosaminoglycans compared to contractile SMC, whereas the amount of noncollagen protein synthesized doubles under the same conditions. These increases are not related to cell proliferation since synthetic state cells are maintained in a quiescent growth state in these experiments (Campbell, 1985). Contractile SMC switch to a more synthetic phenotype in vitro (Thyberg et al., 1985), and this change may be irreversible depending on the culture conditions (Chamley-Campbell and Campbell, 1981; Stadler et al., 1989).

Fibroblasts and SMC share several functions such as collagen, elastin, and proteoglycan synthesis or contractile activities. In the normal adult, some of these functions are specifically exerted by the fibroblast (e.g. collagen synthesis) or the SMC (e.g. contractility), but during development or pathological conditions this can change. SMC secrete collagen during development and during the formation of an atheromatous plaque, whereas contractility may be exerted by fibroblasts during wound healing, resulting in wound contraction (Desmouliere and Gabbiani, 1995). Therefore, fibroblasts can acquire SMC-like features during wound contraction and disease and express SMC-specific markers in particular situations.

II.1.2 Smooth Muscle Cell-Endothelial Cell Interactions

EC are believed to recruit SMC-pericytes to newly-formed blood vessels during vasculogenesis (Hungerford and Little, 1999). A recent study suggests that a small percentage of primary EC may give rise to SMC via transdifferentiation in vitro (Frid et

al., 2002). However, the origin of these SMC-like cells remains unclear, and bone marrow-derived progenitor cells may be implicated. Although further work is required to establish whether transdifferentiation of EC into SMC is possible, these two cell types are clearly interacting significantly in vivo. EC used to be regarded solely as a lining of all blood vessels that forms a barrier to blood. However, it is now known that EC are involved in numerous cell signaling pathways and communicate with SMC via heterocellular junctions and other mediators (Davies, 1986). Intermittent fenestrations in the internal elastic lamina are 0.5-1.5 μm in large vessels and 0.1-0.45 μm in capillaries, thereby allowing direct contact between the two cell types (Saunders and D'Amore, 1992). EC-SMC co-culture experiments have revealed an EC effect on SMC proliferation, migration (Casscells, 1992), phenotype, and extracellular matrix production.

Smooth muscle cell proliferation depends on the endothelial cell (EC) proliferative state and EC can be either stimulators or inhibitors (Campbell and Campbell, 1986; Casscells, 1992). Synthetic smooth muscle cells in the presence of proliferating endothelium have an increased proliferation rate, whereas confluent, quiescent endothelium inhibits SMC proliferation. EC co-cultured with SMC across a 10-μm thick porous polycarbonate membrane induce SMC proliferation (Waybill et al., 1997; Waybill and Hopkins, 1999), but in another study, where a 13-μm thick polyethylene terephthalate membrane was used, this effect was decreased with time and led to growth inhibition by day 4 (Fillinger et al., 1993). Respectively, SMC inhibit EC proliferation in vitro when the two cell types are in direct contact but not when they are separated by 1-2 mm (Orlidge and D'Amore, 1987). Conditioned medium from EC-SMC

co-cultures also inhibits EC proliferation to the same degree as direct contact co-culture itself, due to activated transforming growth factor-β production (Antonelli-Orlidge et al., 1989). Three-dimensional co-culture studies of EC and SMC in collagen gels show that SMC affect not only EC proliferation but also EC alignment and elongation (Imberti et al., 2002; Ziegler et al., 1995). Therefore, cell signaling between EC and SMC is a two-way communication.

Also, EC affect SMC extracellular matrix deposition. Bovine aortic endothelial cell conditioned medium in rabbit aortic smooth muscle cell 2-D cultures stimulates glycosaminoglycans synthesis up to 120% within 24 hours by the SMC (Merrilees et al., 1990) and keeps the SMC in a differentiated, contractile phenotype. In a different study with pig and rat aortic EC and SMC, hyaluronic acid and sulfated glycosaminoglycans production increases in co-culture compared to separate cultures of the two cell types (Merrilees and Scott, 1981). In contrast, collagen synthesis and collagen type I expression decrease in EC-SMC in vitro co-culture models (Powell et al., 1997). EC have also been shown to increase gene expression of vascular endothelial growth factor, platelet-derived growth factors AA and BB, and transforming growth factor β, and decrease expression of basic fibroblast growth factor in co-cultured SMC (Heydarkhan-Hagvall et al., 2003).

These co-culture studies reveal strong interactions between EC and SMC that are dependent on co-culture method and cell densities in vitro. This communication occurs through mediators released into the surrounding medium or through direct cell-cell contact in vivo, and is an important factor in the control of blood vessel growth, remodeling, and function.

II.1.3 Extracellular Matrix Composition

The extracellular matrix (ECM) interacts with vascular cells to regulate their adhesion (Clyman et al., 1990), migration (Rocnik et al., 1998) and proliferation (Carey, 1991), and with plasma proteins, growth factors, cytokines, and enzymes. One of the main functions of the ECM is providing the mechanical integrity of the blood vessel. Each layer of the vessel wall has a different ECM composition that dictates the layer's mechanical properties. The intima is viscoelastic and compressible due to the high content of proteoglycans and hyaluronan. The adventitia is rich in fibrillar collagen, which results in a rigid structure.

The principal source of collagens in the intima and media is the SMC. The predominant vascular collagens are types I and III, which are organized into distinct fibrillar bundles thus providing tensile strength to the tissue. In the normal arterial wall, types I and III collagens are organized into distinct fibrillar bundles, wedged either between elastic fibers in elastic arteries or organized into "nests" surrounding medial smooth muscle cells in muscular arteries. Type IV and VIII collagens are present within vascular basement membranes beneath EC and surrounding SMC. These molecules interact with other molecules and form networks that serve as an anchoring substrate for vascular cells and as a permeability barrier to plasma proteins. Type V collagen is present in small amounts and co-distributes with collagen type I. Type VI collagen is another minor vascular collagen that forms high molecular weight aggregates from small collagen monomers by self-association and disulfide bonding. SMC regulate collagen synthesis in the media by cell growth rate, different factors and cytokines, and the nature

of the ECM substrate. Endothelial cells also synthesize various collagen types, particularly during angiogenesis (Wight, 1996).

Another major extracellular matrix component of blood vessels is elastin, which provides the elasticity needed to accommodate both pressure changes arising from the pulsatile nature of blood flow as well as the hemodynamic changes created on the vascular walls by the blood flow. SMC secrete the precursor tropoelastin together with a 67kDa elastin-binding protein that associates with the cell surface through a specific membrane protein. This 67kDa protein has lectin-binding sites that interact with microfibrillar proteins and a hydrophobic domain that binds hydrophobic sequences within the elastin peptide. The elastic fibers are arranged into concentric sheets or lamellae that separate the intima from the media layer (i.e. internal elastic lamina), the media from the adventitia (i.e. external elastic lamina), and the concentric layers of smooth muscle. The elastic lamellae are often interconnected by radially oriented elastic fibers to facilitate the transfer of stress thoughout the vessel wall.

SMC are surrounded by a basal lamina that contains collagen type IV, proteoglycans, glycosaminoglycans, and glycoproteins. SMC synthesize a spectrum of glycosaminoglycans (GAG) including hyaluronic acid, heparan sulfate, dermatan sulfate, and chondroitin sulfates (Wight, 1989). These GAG, except for hyaluronic acid, do not exist as free chains but are covalently bound to protein to form proteoglycan macromolecules, which may further link with hyaluronic acid to form very large proteoglycan aggregates (Merrilees, 1985). Proteoglycans and hyaluronan are hydrophilic molecules that trap water in the vascular wall and participate in the regulation of vascular permeability, lipid metabolism, hemostasis, and thrombosis. In addition, they

interact with vascular cells, growth factors and cytokines to regulate vascular cell adhesion, migration and proliferation (Wight, 1989). Vascular cells synthesize glycoproteins, such as fibronectin, laminin, thrombospondin, tenascin, and osteopontin, that regulate the extracellular matrix integrity and provide a variety of substrates for the cells of the vascular wall (Wight, 1996).

II.2 Atherosclerosis

To this point, the discussion has primarily focused on healthy arteries. In disease, however, artery morphology, properties, and function change significantly. The most serious disease is atherosclerosis, which is a form of arteriosclerosis (hardening of the arteries). Atherosclerosis is a multi-factorial disease and is influenced by diet, cigarette smoking, diabetes, high blood pressure, and exercise (Burke et al., 1997). Several theories have been formulated to explain the localized nature of atherosclerosis. Fluid mechanical theories predict that atherogenesis occurs in areas that have a relatively complex geometry, a fairly large Reynolds number, and a lower than average wall shear stress throughout the pulsatile cycle (Giddens et al., 1990; Ku et al., 1985; Lieber and Giddens, 1990). Flow in these areas is complex, unsteady, and sometimes turbulent. Solid mechanical views blame sites of high stress, such as bifurcations, and constricted or dilated areas. A blood vessel that is under internal pressure and longitudinal stretch experiences stress concentration under the following conditions: increased radius of curvature, saddle shape, areas in the neighborhood of a small side branch, and when there is bending of the wall (Fung, 1996).

The disease begins with the focal eccentric accumulation of lipid in the intima with intracellular lipid visible mainly in macrophages and smooth muscle cells with time. This leads to the formation of a fatty streak, which is composed of SMC, matrix fibers, and lipids. At a later stage, the fatty streak becomes the preatheroma, which contains multiple extracellular lipid pools, as well as collagen and elastin fibers accumulated beneath the endothelium. The subendothelial zone may subsequently become more organized to form the fibrous cap, which resembles the normal media layer in structure and thickness, and does not contain any macrophages or lipids. As the lipid pools coalesce into lipid cores, the intima becomes disorganized, and this lesion type is termed an atheroma. As the disease develops, the lesion becomes stratified due to the increasing amount of fibrous tissue in deep and superficial layers, and the localization of lipid cores between the fibrous regions, forming fibroatheromas (Glagov et al., 1995). However as the lesion enlarges, the artery also enlarges by an outward bulging of the wall beneath the growing plaque to compensate for the narrowing that has occurred. Lumen stenosis becomes evident when the plaque takes up approximately 40% or more of the lumen area (Bassiouny et al., 1997).

Intimal thickening or hyperplasia could also be a response to vascular intimal injury. When the vascular wall is injured, SMC proliferate in and migrate from the media to the intima, and synthesize extracellular matrix proteins. SMC undergo dedifferentiation, lose their ability to contract, gain the capacity to divide, and increase ECM synthesis (Assoian and Marcantonio, 1996). SMC residing in the intima lose their thick myosin-containing filaments and greatly increase the amount of organelles involved in protein synthesis, such as rough endoplasmic reticulum and Golgi apparatus. The

migratory and proliferative activity of SMC is regulated by both growth promoters, such as platelet-derived growth factor, basic fibroblast growth factor, and interleukin 1, and inhibitors, such as heparan sulfate, nitric oxide, and transforming growth factor-β. Intimal SMC may return to a nonproliferative state when either the overlying endothelial layer is re-established or the abnormal chronic endothelial stimulation ceases.

II.3 Current Therapies

Atheromas in advanced disease almost always undergo patchy or massive calcification, and atherosclerotic lesions cause clinical disease by one of the following mechanisms: slow narrowing of the intima that results in ischemia of the tissues perfused by the involved vessels; sudden occlusion of the lumen by superimposed thrombosis or hemorrhage into an atheroma; thrombosis followed by embolism; weakening of the wall of a vessel, causing an aneurysm or rupture (Schoen, 1994).

Several approaches are taken to treat atherosclerotic cardiovascular disease of small caliber arteries (<6 mm), and the most common ones are briefly described next.

Balloon angioplasty or percutaneous transluminal coronary angioplasty (PTCA) is a procedure used to dilate narrowed arteries. A catheter is inserted with a deflated balloon at its tip into the narrowed vessel, the balloon is inflated, compressing the plaque and enlarging the inner diameter of the artery, and then the balloon is deflated and the catheter removed. About 70-90% of these procedures also involve the placement of a stent, which is a wire mesh tube that is initially collapsed to a small diameter, placed over a balloon catheter and moved into the area of the blockage. When the balloon is inflated, the stent expands, locks in place and holds the artery open. The three most prevalent

stent designs are slotted tubes (a metal tube from which most of the material is removed, resulting in a lattice-like structure), coiled stents (continuous coiled wire), and wire mesh stents (knitted metal wire) (Szycher, 1998).

Concerns with stents include injury to the vessel wall during insertion, and acute thrombosis or intimal hyperplasia as consequences of injury (Didisheim and Watson, 1996). Acute thrombosis occurs within hours in 1% of the stenting procedures and is almost always due to incomplete stent expansion and vessel dissection. Subacute thrombosis, on the other hand, can occur up to 30 days later, after patients have been discharged from the hospital, and lead to ischemia and death (Kutryk, 1999). Patients who have undergone stent procedures are given chronic anti-coagulants, and in about one third of the cases restenosis occurs within approximately 6 months of the procedure. A novel method called brachytherapy has recently been developed to reduce the recurrence of stenosis after successful treatment of in-stent stenosis. Brachytherapy involves the delivery of gamma and beta radiation to coronary arteries so as to inhibit cellular proliferation that causes stenosis, and the Food and Drug Administration (FDA) recently approved two such devices. Irradiation of blood vessels has previously been thought, however, to induce aneurysm formation and delayed oncogenesis in the neighboring soft tissue (Sapirstein et al., 2001).

Laser angioplasty is a technique that aims at recanalizing occlusions that cannot be crossed with conventional balloon angioplasty guidewires and uses a catheter with a laser at the tip, which emits pulsating beams of light that vaporize the plaque (Sanborn, 1989). The first laser device for coronary arteries was approved by the FDA in 1992.

Coronary atherectomy uses either a laser catheter or a rotating shaver that shaves off the plaque. Reported complications related to rotational atherectomy include vasospasm, perforations, and atrioventricular block (Reisman, 1997).

Coronary artery bypass graft operation (CABG), first performed in 1964, is an invasive procedure, which is done to reroute, or "bypass", blood around occluded arteries and improve the supply of blood and oxygen to the heart. Grafts commonly used include the great saphenous vein from the leg, internal mammary artery from the chest, radial artery from the arms, and sometimes arteries from the stomach. Although 70-82% of the saphenous vein substitutes remain patent (i.e. do not fail) in 5 years (Lytle et al., 1985), stenosis due to intimal hyperplasia, which is a flow-restricting lesion, and limited availability are important limitations. Internal mammary and radial arteries are often used in the coronary circulation and are preferred for key artery branches because they tend to remain open longer but also have limited availability (Cameron et al., 1996; Conte, 1998). Although bypass surgery is a very common procedure, it carries some serious risks, such as heart attack, stroke or even death.

II.4 Engineered Vascular Grafts

Autologous vascular grafts are currently the gold standard for the replacement of small diameter arteries (3-6 mm diameter), but their limited availability creates a large need for other types of grafts. Consequently, synthetic materials, such as Dacron, expanded polytetrafluoroethylene (ePTFE), polyetherurethane, poly(lactic acid), poly(glycolic acid) and their copolymers, have also been evaluated extensively. Although Dacron (polyethylene terephthalate fiber) and ePTFE have been successful in

vascular applications requiring large diameter substitutes, they fail rapidly due to occlusion when placed in low-flow vascular segments. Therefore, researchers have modified the surface properties of synthetic materials to reduce their thrombogenicity by modifying surface chemical groups, grafting peptides (Ko and Iwata, 2002; Mann et al., 1999), proteins (Ye et al., 2000), growth factors (Greisler et al., 1996), heparin, or treating the surface with plasma (Lee et al., 2000; Marois et al., 1999). A popular approach has been the endothelialization of the lumen of the grafts, i.e. seeding with endothelial cells, so as to reduce the thrombogenic properties of the synthetic materials (Deutsch et al., 1999). There are two strategies for autologous EC extraction and seeding: single stage seeding, in which EC are extracted and used immediately for seeding, and two stage, in which serial passaging is used to increase cell number prior to seeding (Seifalian et al., 2002; Tiwari et al., 2001). Single stage seeding is suitable for patients suffering from acute coronary ischemia, and an ~76% clot-free graft surface has been obtained using this technique in 8-week canine experiments (Herring et al., 1978). The basic limitations of this technique are autologous cell harvesting and cell detachment from the surface of the synthetic materials. Although materials are typically coated with extracellular matrix proteins to increase the adherence of endothelial cells, some proteins induce platelet adherence as well. Genetically modified SMC have also been considered as an alternative to EC. SMC were transduced with endothelial nitric oxide synthase to depress growth and appear promising as cardiovascular prostheses linings (Scott-Burden et al., 1996). Alternatively, biological materials that have been decellularized offer promise compared to synthetic biomaterials. Schmidt and Baier have written a thorough review of acellular grafts made of biologic materials such as allografts (glutaraldehyde-

treated human umbilical veins), and xenografts (porcine small intestinal submucosa) (Hiles et al., 1995; Roeder et al., 1999) that have been decellularized to reduce the host immune response (Schmidt and Baier, 2000). Complications with these materials include long term degradation, dilation, aneurysm formation, calcification, and glutaraldehyde cytotoxicity (Conte, 1998).

An increasing number of researchers support the idea of developing a living blood vessel substitute that closely mimics the native arteries. A living vascular graft will have the ability to respond to hemodynamic changes and other stimuli, remodel, and self-heal. Among the desired properties of a blood vessel substitute are adequate mechanical strength, controllable adaptation to changing hemodynamics, compliant elasticity, zero tolerance for failure, long term fatigue strength and durability, low thrombogenicity, biocompatibility, easy handling, and low cost.

Since the innovative work of Weinberg and Bell (Weinberg and Bell, 1986), who created a vascular graft by seeding collagen gels with endothelial cells, smooth muscle cells and fibroblasts, different groups have taken different approaches in the quest of optimal materials and graft structure (Niklason, 1999; Ratcliffe, 2000). Following Weinberg's model, Tranquillo et al. (Tranquillo et al., 1996) developed a media-equivalent composed of rat smooth muscle cells and collagen using an electromagnetic field to circumferentially align smooth muscle cells, which is hypothesized to increase the construct's mechanical strength. Seliktar et al. studied the effects of mechanically preconditioning collagen seeded with smooth muscle cells at 1 Hz frequency up to 8 days (Seliktar et al., 2000). SMC were circumferentially aligned across the construct wall, and ultimate stress and material modulus were significantly increased compared to static

cultures. Berglund et al. crosslinked collagen type I gels with glutaraldehyde, ultraviolet radiation, and dehydrothermal treatments to increase mechanical strength while maintaining cell viability (Berglund et al., 2003). Although collagen gel matrices offer a "cell-friendly" environment for attachment and migration, the mechanical strength of the resulting constructs is greatly inferior to that of native vessels (Berglund et al., 2003; Girton et al., 2000). To overcome the inadequate strength of collagen gels while using a biological milieu for tissue development, fibrin gels have been used. SMC cultured in fibrin gels upregulated collagen production compared to cells in collagen gels, which was further enhanced by addition of transforming growth factor-β, insulin, and plasmin (Grassl et al., 2002; Neidert et al., 2002).

Huynh et al. (Huynh et al., 1999) used submucosal collagen isolated from porcine small intestine coated with type I bovine collagen and treated the inner surface with heparin-benzalkonium to prevent coagulation. The collagen layers were cross-linked to increase the mechanical strength and the grafts remained patent and thrombi-free up to 13 weeks when implanted in rabbits. However, the response of the human cardiovascular system to animal collagens remains unknown.

It is important to distinguish between the collagen matrix secreted by cells and the collagen gels that are used as matrices for cell seeding. The collagen, usually type I, found in the collagen gels has undergone a number of processing steps, such as digestion, mixing with an acid, and neutralizing with a base, which polymerizes it into a hydrogel network. It is very likely that the resulting collagen fibril architecture differs from that of the collagen secreted by cells, which may affect the mechanical properties of the cell-seeded gels. Specifically, cells may degrade the collagen gel they are embedded into, in

an effort to remodel and replace it with their matrix. It has been shown that matrix metalloproteases are present and active in type I collagen gels, and that mechanical preconditioning increases the amount of active enzymes (Seliktar, 2000). Therefore, although native collagen contributes to the mechanical strength of the vessel wall, cell-seeded collagen gels have inferior mechanical properties.

A unique approach was taken by L'Heureux et al. (L'Heureux et al., 1998), who created a tissue-engineered blood vessel made exclusively of cultured human cells and their matrix without any synthetic biomaterials. Human vascular smooth muscle cells were cultured to produce a cohesive cellular sheet (media layer) that was wrapped around a mandrel, and a similar sheet of human skin fibroblasts was subsequently wrapped around the media to produce the adventitia. After a minimum of 8 weeks maturation, the mandrel was removed and the lumen was seeded with human umbilical vein endothelial cells (intima). The overall culture period was 3 months, excluding cell expansion. The resulting graft had burst strength of over 2,000 mmHg and good handling and suturability when implanted in a canine model. The media layer was also tested with pharmacological stimuli and showed contractile/relaxation responses (L'Heureux et al., 2001). Although this technique has been very successful, the overall development time is long, and scale-up capabilities do not appear straightforward.

An analogous approach was taken by Campbell et al. who developed grafts in the recipient's peritoneal cavity (Campbell et al., 1999). Silastic tubing was inserted in the peritoneal cavity of rats or rabbits, granulation tissue was formed on the tubing surface, the tubing was removed, and the graft was everted and implanted in the host's carotid artery or abdominal aorta. The intima of the grafts was populated with mesothelial cells

and the media with myofibroblasts. Although this innovative method of graft development needs to be further evaluated in long term in vivo experiments to establish patency, it bypasses complicated cell and scaffold sourcing-related issues.

Much of the work in the engineering of vascular grafts has focused on the use of biodegradable polymeric scaffolds. The main advantage of these matrices is that they provide the initial strength necessary for implantation while being biodegradable (Table 2.1). The obvious disadvantage is that they are synthetic biomaterials that may elicit an immune response. Semicrystalline polymers such as polyglycolic (PGA) and poly-L-lactic acid (PLLA) degrade by bulk hydrolysis. Degradation occurs first in the amorphous domains, which are more accessible to water, and crystallinity gradually increases resulting in a highly crystalline material that is much more resistant to hydrolysis than the starting material. The increase in crystallinity is believed to occur due to an increased mobility of the partially degraded polymer chains, which enables a realignment of the polymer chains into a more ordered crystalline state (Anderson, 1995). PLGA copolymers degrade via nonspecific hydrolytic scission of their ester bonds to carbon dioxide and water. Other factors such as pH, heat, and carboxypeptidases may also contribute to the degradation process. In vivo and in vitro experiments with PLGA copolymers have studied their degradation and biocompatibility (Lu et al., 2000). PLGA degradation particles have a crystalline-like morphology with sharp edges and folds and range in size from 4 to 30 μm (Cordewener et al., 2000). PLLA is thought to degrade via simple hydrolysis, whereas PGA may also be subjected to enzyme-mediated hydrolysis. PGA fragments are brought into the cells via phagocytosis and degrade intracellularly by

Table 2.1 Properties of PCL, PLLA and PGA Scaffolds.
Asterisk indicates that heat of fusion varies with the degree of crystallinity for semi-crystalline polymers such as PLLA and PGA.

	Poly(ε-caprolactone) PCL	Poly(L-lactic acid) PLLA	Poly(glycolic acid) PGA
Structure	-[-CO-$(CH_2)_5$-O-]$_n$-	-[-O-CH(CH_3)-CO-]$_n$-	-[-O-CH_2-CO-]$_n$-
Solvents	Methylene chloride Chloroform Hexafluoro-isopropanol Acetone	Methylene chloride Chloroform Hexafluoro-isopropanol	Hexafluoro-isopropanol Hexafluoroacetone sesquihydrate

	PCL	PLLA	PGA
Melting temperature, T_m (°C)	57	175	225
Glass transition temperature, T_g (°C)	-62	65	35
Heat of fusion (J/g)	34	30*	71*
Crystallinity (%)	57	35	35-75
Specific gravity	1.11	1.2-1.3	1.5-1.7
Tensile strength (MPa)	16	69-103	69-138
Modulus (MPa)	400	3446	6893

simple hydrolysis. Some of the glycolate produced is excreted directly in the urine while the remaining glycolate is oxidized to glyoxylate which is then converted to glycine, serine, and pyruvate. Finally, pyruvate enters the Krebs cycle (Hollinger and Battistone, 1986). PGA absorption is 6-17 weeks and the tensile strength falls to about 10% after 3 weeks. Only mild inflammatory responses have been caused by PLGA polymers and in some instances phagocytic and giant cells have been observed. PLGA polymers have been approved by the Food and Drug Administration as suture materials, bone plates and screws, and cardiovascular woven meshes. Thus, these polymers have been used in various tissue engineering applications.

Biodegradable polymeric scaffolds have been used successfully in vascular tissue engineering. Shum-Tim et al. developed an autologous (ovine) aorta by seeding a polyglycolic acid (PGA)-polyhydroxyalkanoate (PHA) composite biomaterial with a mixture of endothelial cells, smooth muscle cells, and fibroblasts (Shum-Tim et al., 1999). PGA meshes, which are highly porous biodegradable matrices, were surrounded by three layers of PHA that is also a biodegradable but impermeable biomaterial that has longer degradation time than PGA and can withstand systemic pressure. In vivo experiments were carried out for up to 5 months without any postoperative anticoagulant administration.

Niklason et al. seeded PGA scaffolds with bovine aortic smooth muscle cells in a bioreactor system for 8 weeks under pulsatile conditions and subsequently applied bovine aortic endothelial cells for 3 days with continuous flow (Niklason et al., 1999). The resulting endothelium stained positive for von Willebrand factor and platelet endothelial cell adhesion molecule (PECAM), and the smooth muscle cells expressed smooth muscle

α-actin and calponin. The grafts showed high SMC density and collagen production, had burst pressure of over 2000 mmHg, and contracted in response to serotonin, endothelin-1, and prostaglandin F_{2a}. Pulsatility had a positive effect on wall thickness, collagen production, and suture retention strength. Culture medium was supplemented with ascorbic acid, copper ion, and amino acids to support matrix production, which resulted in vessels with higher burst strength. Implantation of scaffolds seeded with autologous EC and SMC and cultured in vitro under pulsatile flow into the right saphenous artery of miniature swine resulted in patent grafts after four weeks although decreased flow was observed. Limitations of this approach were low elastin production compared to that of native vessels and the presence of de-differentiated SMC around residual polymer fragments.

Hoerstrup et al. coated PGA meshes with a thin layer of poly-4-hydroxybutyrate, seeded them with ovine myofiblasts under static conditions for 4 days, seeded them subsequently with ovine endothelial cells, and cultured them in a pulse duplicator bioreactor for up to 28 days (Hoerstrup et al., 2001). DNA and collagen content increased continuously to 21 days but small amounts of matrix were produced which resulted in low mechanical strength. In a separate study with human cells, culture conditions were optimized with ascorbic acid and basic fibroblast growth factor for increased collagen production (Hoerstrup et al., 2000).

Shin'oka et al. (Shin'oka et al., 2001) implanted a polycaprolactone-polylactic acid copolymer reinforced with woven PGA and seeded with autologous cells in the right pulmonary artery of a four-year-old girl in Japan, and seven months later there was no evidence of graft occlusion or aneurysm formation. Although the demands for a blood

vessel substitute of the pulmonary circulation are not as high as those for the systemic circulation, the successful implantation of a completely tissue-engineered graft in humans is still a very exciting accomplishment.

In summary, significant advances have been made towards the development of a small caliber blood vessel substitute and many of the desired properties have already been obtained. Grafts with high tissue density (cells and extracellular matrix), differentiated cells, responsive to pharmacological stimuli, and with high burst pressure strength have been developed, and short term in vivo experiments have been performed.

However, significant limitations exist and further research is required for the development of patent grafts suitable for human implantation. EC are typically introduced into the vascular wall models late in culture and long term SMC-EC interactions have not been studied in a 3D dynamic culture environment. This thesis addresses the long term effect of EC on SMC proliferation, matrix production and differentiation in a perfusion bioreactor.

II.5 Bioreactors for Vascular Graft Development

It can be seen from the above discussion that significant advances have been made towards the development of a small diameter vascular graft, although the challenges remain substantial. Development of vascular substitutes is time-consuming and in most of the cases one graft is produced at a time. This approach raises the issue of how efficient and cost-effective the process can be, and also how reproducibility can be ensured (Ratcliffe and Niklason, 2002). Tissue engineering studies have elucidated the importance of bioreactors in improving cell seeding, extracellular matrix production, and

tissue architecture and differentiation compared to static culture techniques (Carrier et al., 2002; Davisson et al., 2002; Pei et al., 2002).

Few bioreactor systems are currently available for the development of conduits, and even fewer perfusion bioreactors. One of these systems engineered by Niklason et al. is composed of four bioreactors assembled in parallel, a medium reservoir, a pulsatile pump, and a compliance chamber (Niklason et al., 2001; Niklason et al., 1999). Each bioreactor is a chamber, in which highly distensible silicone tubing is inserted through the lumen of the polymer scaffold. Mixing is achieved through stirrer bars and magnetic stirplates, each scaffold is seeded initially with a SMC suspension for 30 min, each chamber is filled with culture medium and pulsatile flow is introduced through the silicone tubing. After 8 weeks the silicone tubing is removed, and flow of the medium is applied directly through the construct. Subsequently, EC suspension is injected into the lumen, and cells are allowed to adhere for 90 min under static conditions. Flow rates are then increased over a 3-day culture period from 0.033 to 0.1 ml/s. Although this bioreactor has several advantages such as continuous perfusion and pulsatile flow capabilities, it also has limitations. Each chamber operates independently, which could result in different constructs growing in different biochemical environments. In addition, SMC seeding involves opening the chamber and pipeting the cell suspension on each scaffold. Endothelial cell seeding appears to be conducted in a similar manner, although the authors do not provide a clear description of the method used. Bioreactor opening may compromise asepsis, and this bioreactor design can lead to variations from construct to construct that would be very costly in a large-scale production facility.

Commercially available spinner flasks (Bellco Glass, Inc.) have also been used for long term (7 weeks) culture of rat SMC into PGA matrices bonded with PLLA (Kim and Mooney, 1998b). SMC were seeded into the scaffolds by placing them on an orbital shaker at 100 rpm for 24 hours, and the seeded constructs were then transferred to the spinner flasks and cultured at 40 rpm. SMC proliferated in the bonded scaffolds and produced elastin over the 7-week culture time. Thus, cell seeding and construct growth took place in two different systems: an orbital shaker and a spinner flask, respectively. However, scale-up of construct production in spinner flasks is complicated.

Seliktar developed a dynamic mechanical conditioning bioreactor, in which up to four constructs can be mounted on an expandable silicone sleeve (Seliktar, 2000). The intraluminal pressure was regulated to produce a 10% cyclic change in the outer diameter of each silicone tube, and it was shown that mechanical preconditioning of collagen gels seeded with rat aortic SMC improves their mechanical strength and histological organization (Seliktar et al., 2000). Although this system is not used for the seeding phase of vascular graft development, it has the potential to be used for growth.

Kim et al. compared three different methods of seeding rat aortic cells on PGA matrices: static (culture dishes), stirred (spinner flasks), and agitated (50 ml tubes on orbital shaker) (Kim et al., 1998). The dynamic seeding methods yielded constructs with higher cell density, more uniformly distributed cell population, and greater elastin deposition compared to static.

Burg et al. also compared static (petri dish), dynamic (spinner flask), and perfusion bioreactor seeding of PGA meshes with rat aortic endothelial cells, by seeding under static or dynamic conditions for 24 hrs, followed by a maturation phase of 6 days

in a static, in a dynamic, or in a bioreactor system (Burg et al., 2000). The perfusion bioreactor system was adapted from the commercially available CellMax Quad unit (Cellco, Germantown, MD) that consists of a chamber, in which multiple circular scaffolds can be placed. This bioreactor design exposes each scaffold to a slightly different environment, and it is therefore not optimal. Nevertheless, it was found that dynamic seeding followed by a bioreactor maturation phase yielded scaffolds with the best cellular attachment and distribution and the highest metabolic activity.

A dual perfusion bioreactor was developed to endothelialize the lumen of PTFE grafts under fluid flow (Dunkern et al., 1999). EC suspension filled the chamber, the bioreactor was rotated for 4 hours at 0.3 rpm, and there was a 16-hour static incubation to ensure cell attachment. Therefore, this bioreactor was used successfully for the seeding of PTFE grafts with EC but is a one-chamber design that could be difficult to scale-up due to the rotation component.

Recently, a hybridization oven has been used for dynamic cell seeding of porous polymer scaffolds with ovine myofibroblasts (Nasseri, 2003). Scaffolds and cell suspension were placed either into 50-ml polypropylene tubes or hybridization glass bottles and rotated at 5 rpm for 24 hours. This technique has the disadvantage of the absence of gas exchange; the authors are working on a design modification that will allow continuous oxygenation. Nevertheless, this work shows that dynamic cell seeding is clearly preferred for tissue engineering applications because it results in uniform cell distribution.

In summary, there is strong evidence that supports the hypothesis that dynamic seeding produces constructs with higher cell densities, uniform cell distribution, higher

metabolic activity, and superior mechanical strength. Main bioreactor design limitations are lack of scale-up, reproducibility, and ease of bioreactor assembly and operation.

These findings have been the underlying basis of this thesis that takes vascular tissue engineering technology further by addressing unmet bioprocessing-related needs, such as scale-up capability, reproducibility, and process monitoring. More specifically, it describes a dual perfusion bioreactor system that supports the dynamic seeding and growth of multiple grafts in a similar biochemical and biomechanical environment, thereby addressing current limitations of static systems.

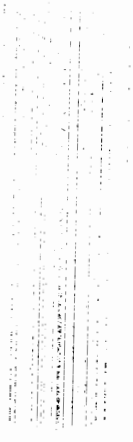

CHAPTER III

MATERIALS AND METHODS

Unless otherwise stated, reagents were obtained from Sigma-Aldrich Chemical Company (St. Louis, MO) and tissue culture supplies from VWR Scientific (Suwannee, GA).

III.1 Cell Sourcing

Human aortic smooth muscle cells (HASMC) were purchased from Clonetics® (BioWhittaker, Inc., San Diego, CA) and used between passage 6 and 10. HASMC were cultured in complete culture medium A that consisted of MCDB 131 (Mediatech Inc., Herndon, VA) supplemented with 10% fetal bovine serum (Mediatech, Inc.), 1% penicillin-streptomycin, 1% of 200mM L-glutamine, 10 ng/ml human epidermal growth factor and 2 ng/ml basic human fibroblast growth factor (PeproTech, Inc., Rocky Hill, NJ). Rat aortic smooth muscle cells (RASMC) generously provided by Dr. Robert M. Nerem (Georgia Institute of Technology, Atlanta, GA) were cultured in medium A and used at passage 6. Bovine aortic endothelial cells (EC) generously provided by Dr. Robert M. Nerem (Georgia Institute of Technology) were cultured in Dulbecco's Modified Eagle's Medium (DMEM) (medium B) with high glucose, supplemented with 10% fetal bovine serum (Mediatech, Inc.) and 1% penicillin-streptomycin, and used at passage 9. Bovine aortic smooth muscle cells (SMC) were isolated from young calves' thoracic aortas that were obtained by overnight delivery from Lampire Biologicals, Inc. (Pipersville, PA) and immersed in Hanks' balanced saline solution containing 1%

penicillin-streptomycin. The adventitia was peeled away and the artery was excised longitudinally with the lumen exposed. Endothelial cells were removed by gentle scraping with a scalpel blade. The media layer was cut into 1-2 mm cubes and placed in complete culture medium C at 37°C in a 95% air/5% CO_2 incubator for 2 days. Complete culture medium C consisted of MCDB 131 (Mediatech Inc.) supplemented with 10% fetal bovine serum (Mediatech, Inc.), 1% penicillin-streptomycin, 0.5 μg/ml fungizone (Gibco, Grand Island, NY), 25 mM HEPES buffer, 10 ng/ml human epidermal growth factor, 2 ng/ml basic human fibroblast growth factor (PeproTech, Inc.), 160 μg/ml L-ascorbic acid, 1% of 200mM L-glutamine, 92 μg/ml L-proline, 60 μg/ml glycine, 71 μg/ml L-alanine, and 2.9 ng/ml cupric sulfate (Niklason et al., 1999).

Smooth muscle cells were isolated from the media layer cubes by overnight digestion at 37°C and 95% air/5% CO_2 in 1 mg/ml fresh collagenase type II solution (300 units/mg, Worthington Biochemical Corp., Lakewood, NJ) in culture medium C. Following digestion, smooth muscle cells were washed in culture medium, plated in T-75 cm^2 or T-175 cm^2 tissue culture flasks, expanded in culture and used in bioreactor experiments at or below passage 3. SMC used in some static seeding experiments were cultured in culture medium D that was similar to C except that DMEM was used instead of MCDB 131. The culture medium was switched back to MCDB 131 after it was observed that DMEM hardly changes color when pH is decreased.

III.2 Cell Counting Methods

Cultured cells were detached from the culture flasks with Trypsin/EDTA (Gibco) and counted with a hemacytometer (Hausser Scientific, Horsham, PA) or a Coulter

Multisizer II Counter (Beckman Coulter, Inc., Fullerton, CA). In the hemacytometer method, the cell suspension was centrifuged at 1000 rpm for 5 min in a GS-6R centrifuge (Beckman Coulter, Inc.), the supernatant medium was discarded and the cell pellet was resuspended in a small volume of medium depending on the expected cell number. A 25 μl sample of the cell suspension was placed in a 1.5 ml microcentrifuge tube and mixed typically with 75 μl of 0.4 % Trypan Blue (x4 dilution). A 10 μl sample of this solution was then carefully added to each side of the hemacytometer, and the viable cells were counted in the four corner squares of each side of the hemacytometer (including cells touching the top and left borders). Live cells appeared refractile and colorless in contrast to dead cells that took up the blue dye. The live cell number was determined by the following steps: (1) averaging the cell number between the two sides of the hemacytometer; (2) dividing by 4 to get the number in one grid; (3) multiplying by the dilution factor; (4) multiplying by 10,000 to obtain the number of cells in 1 ml; (5) multiplying by the volume of medium that the 25 μl sample was aspirated from.

Cells suspended in culture medium after static seeding of scaffolds were also counted using the Coulter Multisizer II. The cell suspension was centrifuged at 10,000 rpm for 2 min in a Sorvall® RMC 14 centrifuge (Du Pont Medical Products, Wilmington, DE), the supernatant was discarded, and the cell pellet was resuspended in 200 μl of culture medium. The sample was then placed in counting containers with 20 ml of sterile PBS and ran through the instrument along with a PBS only control sample.

III.3 Biodegradable Scaffolds

Poly-ε-caprolactone (PCL) and poly-L-lactic acid (PLLA) scaffolds were used solely in static seeding experiments, whereas polyglycolic acid (PGA) scaffolds were used in both static seeding experiments as disks and in bioreactor experiments in tubular form.

PCL (Birmingham Polymers Inc., Birmingham, AL) with 1-1.3 dL/g inherent viscosity in methylene chloride ($CHCl_3$) at 30°C and 92,300 number average molecular weight was used to prepare porous polymer scaffolds for static seeding experiments with salt-polymer casting and particulate leaching (Mikos et al., 1994). Sodium chloride (NaCl) crystals were ground using an analytical mill (Tekmar, Cincinnatti, OH) and separated according to size in a sieve shaker (W.S. Tyler, Mentor, OH). Scaffold porosity was determined as the ratio of g of salt to the total weight of polymer and salt. Scaffolds with 92% porosity were prepared by dissolving 0.4 g PCL in 5.5 ml methylene chloride (Fisher Scientific, Pittsburgh, PA), pouring the solution in 50 mm Teflon® dishes (Cole-Parmer, Vernon Hills, IL), and adding 4.6 g of NaCl crystals ranging in size from 150 to 250 μm after the polymer had dissolved in $CHCl_3$. The salt particles were stirred vigorously with a thin metal rod to distribute them evenly in the solution, and the mixture was allowed to sit in a fume hood for 24-48 hours to evaporate the solvent. Scaffolds with different pore sizes were also prepared by adding 106-150 μm size NaCl crystals. Following evaporation of the solvent, cylindrical shaped scaffolds were punched out using either a 4.8 mm or 10 mm die and placed in glass beakers with deionized (DI) water. The beakers were placed on a shaker set at 100 rpm and the salt was leached out by washing for 2-3 days in DI water that was replaced 2-3 times a day. The removal of

the salt crystals resulted in a porous polymer structure with increased surface area for cell attachment. The scaffolds were then dried in a laminar flow hood (Thermo Forma, Marietta, OH), and those not meeting the desired dimensions (thickness: 2 ± 0.2 mm, diameter: (4.8 or 10) ± 0.2 mm) were discarded. Scaffolds were then mounted onto thin plastic shims using drops of silicone glue (DAP Inc., Baltimore, MD). The shims were cut from 76.2 μm plastic sheets (Precision Brand Products, Downers Grove, IL) and rounded off with a scalpel blade. Sterilization of the scaffolds took place in a laminar flow hood by one 30 min wash in 70% ethanol followed by three 10 min washes with sterile DI water. The sterilized scaffolds were dried in a laminar flow hood for 4-5 hours. Dried scaffolds were further sterilized by UV light exposure in a laminar flow hood for 20 min on each side. UV light may lead to partial degradation (Hutmacher et al., 1996) but 20-min exposure did not appear to macroscopically alter the scaffolds.

PLLA (Polysciences Inc., Warrington, PA) with 50,000 number average molecular weight was used to produce porous scaffolds for static seeding experiments and was prepared similarly to PCL with 150-250 μm pore size.

Biodegradable PGA disks (Advanced Tissue Sciences, LaJolla, CA) were generously donated by Robert M. Nerem (Georgia Institute of Technology) and used in static seeding experiments. The disks were 24x6 mm and packaged and presterilized in Petri dishes.

Biodegradable polyglycolic acid (PGA) non-woven felts obtained from Albany International (Mansfield, MA) were used in bioreactor experiments. These felts were 97% porous, 5 mm thick, and had a bulk density of 61 mg/cm^3. Sheets of PGA approximately 19x50 mm were sutured into tubes 4.5mm inner diameter (ID) by 50mm

long using 6-0 PGA (Dexon) sutures (Davis and Geck Inc., Manati, Puerto Rico). Scaffolds were sterilized by immersion in 70% ethanol for 30 min, washed three times in sterile DI water for 10 min each, and air-dried overnight in a laminar flow hood. Sterile scaffolds were prewetted in complete culture medium C overnight prior to experiments to increase protein adsorption and hydrophilicity.

III.4 Polymer Scaffold Surface Modifications

Biodegradable scaffolds (PCL and PLLA) used in static seeding experiments were treated with sodium hydroxide (Gao et al., 1998) and extracellular matrix proteins (fibronectin, collagen and gelatin) to increase hydrophilicity thereby increasing cell attachment and spreading (Nikolovski and Mooney, 2000; Tjia et al., 1999).

Sterilized scaffolds were treated with 1N NaOH solution for 30-60 sec, washed with sterilized DI water 4 times for 10 min each and incubated overnight with basal DMEM. Fibronectin-treated scaffolds were incubated overnight with 1 $\mu g/\mu l$ human plasma fibronectin (Invitrogen, Carlsbad, CA) in DMEM. Collagen pretreatment consisted of overnight incubation of scaffolds with 300 μl of Vitrogen® 100 (type I bovine collagen) (Cohesion Technologies, Inc., Palo Alto, CA) followed by 4 washes with phosphate buffered saline (PBS) solution for 10 min each. Small volumes of Vitrogen® 100 were used to cover the surface of the polymer and to allow the solution to evaporate overnight. Scaffolds were also coated overnight with 4% type A porcine skin gelatin solution diluted in PBS.

III.5 Static Seeding Experimental Setup

Static seeding experiments were designed to assess smooth muscle cell proliferation and collagen deposition in different biodegradable polymer scaffolds to reveal a cell-matrix combination for bioreactor experiments and vascular graft development. Sterilized polymer scaffolds were glued to the bottom of 24- or 48-well dishes with silicone glue. In initial experiments in 24-well dishes (well diameter = 16 mm) with 4.8 mm diameter scaffolds, 25 μl of the cell suspension (5,000 to 400,000 cells per scaffold) was pipetted on top of each scaffold, 30 μl of medium was added after 3 hours, and 300 μl after 5 hours (from time = 0 hr). A major limitation of this method was that the liquid drop of the cell suspension would not stay on the hydrophobic scaffold surface, which allowed cells to be plated on the dish surface. In addition, medium pH would drop rapidly because of the high cell concentration in the small medium volume. Therefore, these seeding and nutrient limitations led to an improved seeding technique, in which the scaffold diameter was increased to 10 mm and 48-well culture dishes were used (well diameter = 10 mm). In these experiments, cells were suspended in 1 ml of medium and culture medium was replaced every 48 hr. Harvested constructs were rinsed in PBS and frozen at -20°C until further analysis. Additional construct samples were sectioned for histological analysis or used in viability assays with confocal microscopy.

III.6 Tubular Scaffold Development

Two different molds were developed for the generation of tubular PCL and PLLA scaffolds. The first method is based on polymer casting in a Teflon® mold composed of a vertical inner rod surrounded by an outer tube and a base that supports the whole

structure (Figure 3.1). Both the rod and the lumen of the tube are covered with Bytac® adhesive film, which is an aluminum foil covered with a non-stick film of Teflon®. This adhesive film allows the simple removal of the scaffold from the mold without fracture. Polymer pellets were dissolved in methylene chloride, and salt particles of known size were added to the solution (to provide 90% porosity) that was then cast in the 2 mm gap formed between the inner rod and the outer tube. Polymer casting took place in a fume hood, which accelerated solvent evaporation, and after three days the outer tube was removed and the inner rod with the scaffold was left in the fume hood for an additional 24 hours. The scaffold was then removed from the mold, placed in DI water on a shaker for 24 hours to leach the salt, and dried in a fume hood.

The second method is based on compression molding. The die was placed in a hot press that has adjustable temperature, pressure, and vacuum. The mold design itself is enhanced so that nine scaffolds can be made simultaneously under identical conditions (Figure 3.2). Although the mold has many components and is composed of 4 different plates and 11 rods, the operating principle is simple: crushed scaffolds made of polymer and salt in 1:9 ratio were placed at the bottom of the lower plate; the upper plate was placed on top, and the nine rods were inserted in the gaps. Two thinner plates were placed one at the bottom and one at the top, and two rods were inserted through all the plates at opposite sides to ensure alignment of the assembled die. The mold was then placed in the press, heated above the polymer's melting temperature, and pressurized to aid the flow of the polymer in the gap between the rods and the walls of each slot. Vacuum was also applied to prevent the formation of air bubbles. PLLA scaffolds were

fabricated with this technique under the following conditions: Temperature (T) = 350 °F, Force = 2 tons, Time (t) = 10 min.

The plates and rods of the mold are made of an aluminum alloy and stainless steel, respectively. To prevent polymer adherence to the mold, the metal surfaces were initially sprayed with a lubricant. However, the presence of lubricant in the scaffold is undesirable, so the mold design was improved by inserting Teflon® tubing into the slots of the bottom plate. This modification prevented the polymer from sticking to the aluminum but not to the rods. In addition, another limitation of this design is corrosion of the aluminum alloy that can be easily avoided by fabricating stainless steel plates.

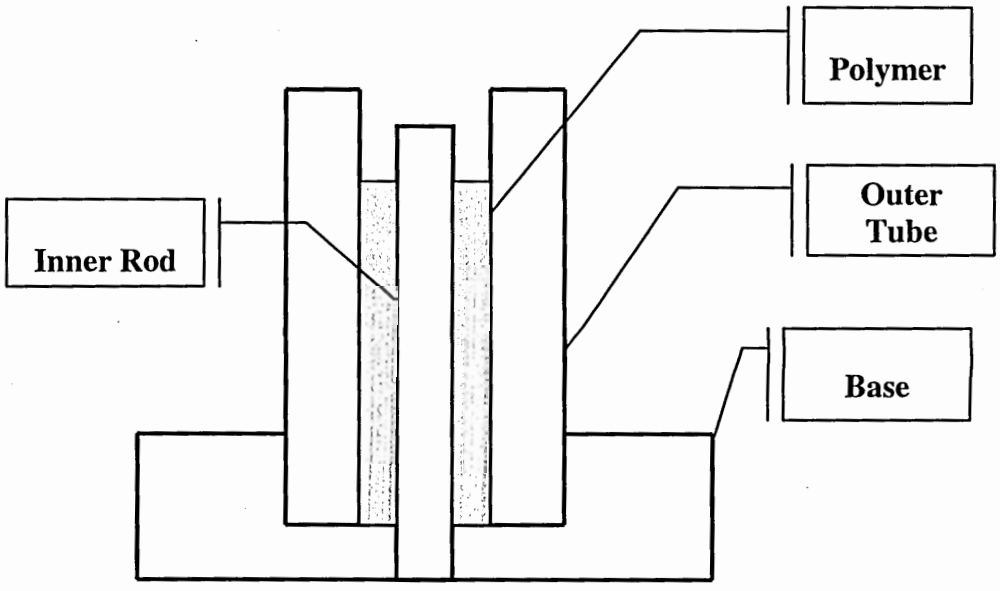

Figure 3.1 Schematic Showing 2D Slice of Teflon® Mold.

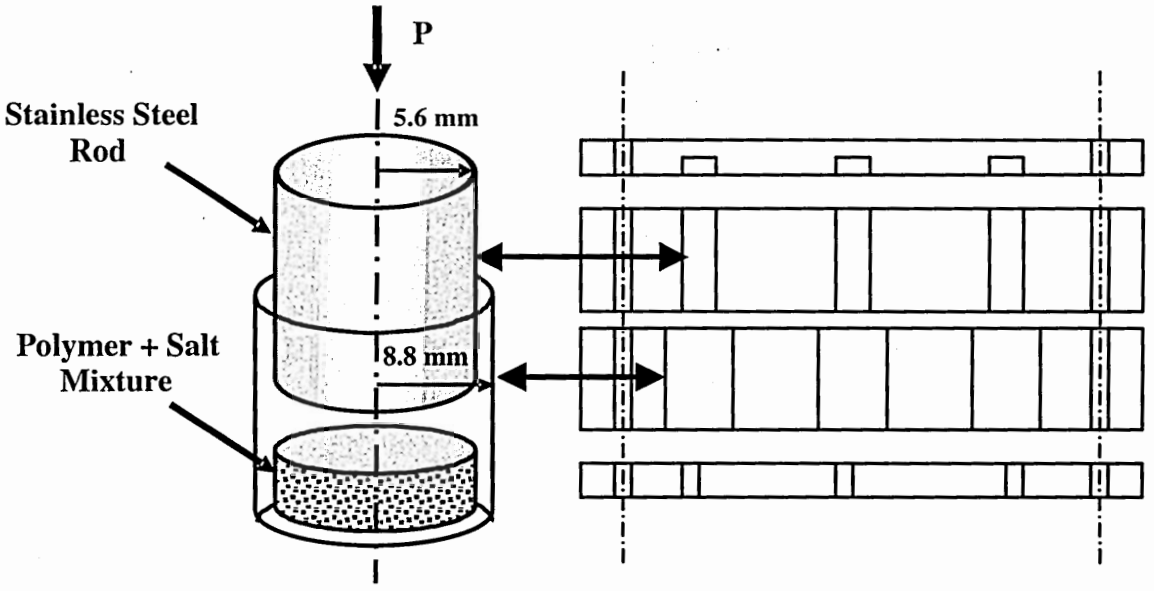

Figure 3.2 Schematic of Compression Die and Operating Principle.

III.7 Perfusion Bioreactor Design

The design of a scaleable perfusion bioreactor for the development of small diameter tissue-engineered arterial constructs was one of the main goals of this thesis. The following design criteria were deemed crucial:

(1) Scaleable bioreactor to support the development of multiple arterial constructs. The bioreactor is composed of modules assembled in series; therefore, multiple constructs can be cultured in one bioreactor under the same conditions.

(2) Dual perfusion of the lumen and the external surface of the constructs. The purpose of dual perfusion is multifold. First, it improves transport of nutrients to and waste products from the arterial constructs. Although the adventitia of blood vessels is not in contact with blood in vivo, the vasa vasorum supplies that tissue with nutrients. Therefore, external perfusion of the arterial constructs mimics the in vivo environment. Second, the external flow loop can be used for cell seeding. This advantage was tested in

experiments, where both the lumen and the external surface of PGA scaffolds were seeded with SMC (dual seeding) and compared to single seeding, in which only the lumen was seeded with SMC.

(3) Ability to seed cells under dynamic conditions in the bioreactor at different culture times. Dual perfusion allows dynamic cell seeding both through the lumen and on the external surface of the construct. Cell suspension was flown reciprocally by a dual syringe pump to maximize cell adherence and increase seeding efficiency. Dynamic cell seeding automates this bioprocess, thereby making it more time- and cost-efficient compared to other cell seeding techniques that are more labor-intensive. Furthermore, it allows sequential seeding of different cell types at different culture times. This attribute was exploited by seeding EC through the construct lumen at later times.

(4) Compact, easy to assemble, autoclavable, light, leakproof, and transparent design to facilitate use.

Cylindrical bioreactors consisting of modules (Figure 3.3) flanked by two head plates (Figure 3.4) were made from hand-blown glass. Modules were made from glass flanges (Chemglass Scientific Apparatus, Vineland, NJ) that had inner and outer diameter of 52 mm and 57 mm, respectively. Module length was initially 83 mm and was reduced in later experiments to 45 mm to minimize the medium volume inside each module and to create a more compact design.

Scaffolds were mounted on two glass ports inserted through opposite sides of the module walls to provide medium perfusion through the lumen (Figure 3.3). Lumen flow allowed for efficient and dynamic cell seeding, nutrient delivery, and mechanical stimulation (shear stress and pulsatile flow). Each glass flange had a precision-formed O-

ring groove that allowed the head plate to form a tight seal with the module via an O-ring. Bioreactor components were held together by clamps (Chemglass) (Figure 3.4). Head plates were made from a glass flange that had been closed off at one end and had a 6.35 mm OD glass port inserted through the face to allow medium flow around the external surface of the constructs for nutrient delivery. This external flow can also be used for cell seeding. All interior corners were rounded to reduce stagnation regions and facilitate medium flow. A custom built 2 L medium reservoir was used to facilitate simultaneous perfusion of multiple constructs (Figure 3.5). The reservoir contained several 6.35 mm hose barb outlet ports for tubing connections and a male luer fitting, on which a 0.2 μm syringe filter was attached for gas exchange.

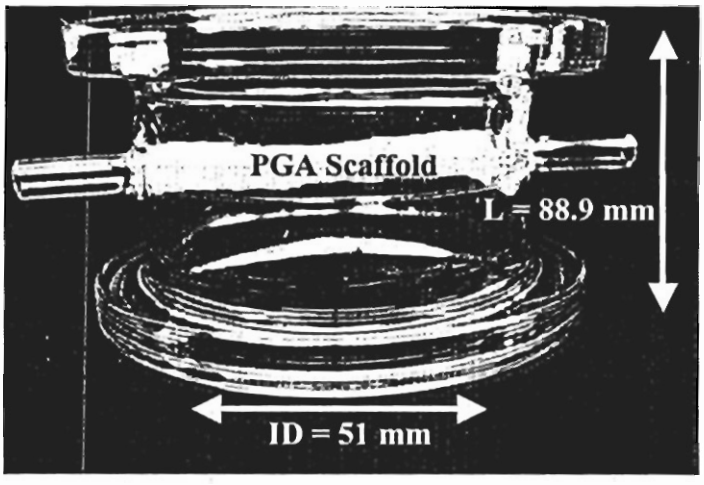

Figure 3.3 Bioreactor Module Schematic.
Pólyglycolic acid scaffold mounted in a one-module bioreactor.

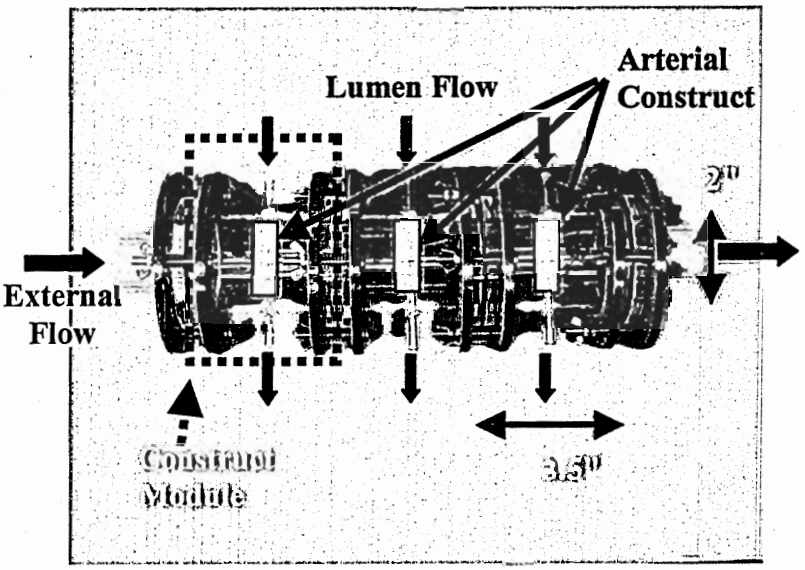

Figure 3.4 Three-Module Bioreactor Schematic.
Three module bioreactor showing lumen and external flow direction (Arrows).

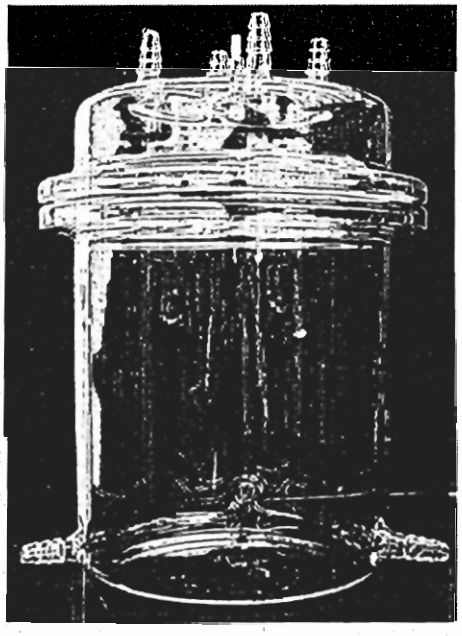

Figure 3.5 Medium Reservoir Bottle and Lid Featuring Multiple Hose Barb Connectors.

III.8 Bioreactor Assembly and Operation

All bioreactor glass components were pretreated with Sigmacote® to prevent cell adhesion and steam autoclaved for 20 min at 121°C and 2.2 atm. All other flow loop components were steam sterilized as above, and the bioreactor was assembled aseptically under a laminar flow hood. PGA scaffolds were prewetted in culture medium overnight at room temperature (Kim et al., 1999b). A PGA scaffold was mounted on the glass ports in each bioreactor module and held in place by cable ties. The medium reservoir was filled with 1 L of complete culture medium and sealed with a lid that had four hose barb connectors. One of the connectors was used for air exchange in the incubator by attaching a 0.2 μm filter. The other three connectors were used to pump culture medium between the reservoir and the bioreactor modules. To seed the polymer scaffold, SMC suspension (0.9×10^6 cells/ml) was pumped reciprocally through the lumen by a dual syringe pump (Harvard Apparatus Inc., Holliston, MA) at 4 ml/min for 24 hours; medium was pumped continuously over the external surface of the scaffold by a peristaltic pump at 30-40 ml/min (Cole-Parmer Instrument Co., Vernon Hills, IL) (Figure 3.6). In a three-module bioreactor experiment, the syringe pump flow was divided into thirds so that all three constructs could be seeded with SMC simultaneously.

During bioreactor operation, 1 L of medium was replaced in the reservoir every 4-7 days in a laminar flow hood, and the bioreactor was reperfused with the fresh medium. The bioreactor and all accessories and pumps were maintained in an incubator at 37°C and 95% air/5% CO_2.

Flow through the lumen was monitored by Gilmont® flowmeters (Cole-Parmer Instrument Co.) that were placed upstream and downstream of the construct. The flowmeter readings (± 1 ml/min accuracy) were recorded daily and represented time-

averaged values of the pulsatile flow, which was more pronounced at the construct inlet. Wall shear stress was calculated by assuming Hagen-Poiseuille flow through a rigid tube using the inner radius of the construct at the time of harvest and the lumen outlet time-averaged flow rate.

Harvested constructs were rinsed in PBS and construct wall thickness and inner diameter was measured with a digital micrometer (Mitutoyo Corp., Kanagawa, Japan). Separate construct rings approximately 5 mm long were sectioned from each harvested construct and used for biochemical, histological, and scanning electron microscopy analysis.

III.9 Dynamic Cell Seeding in the Bioreactor

Two SMC seeding protocols were explored in two-module bioreactors. In single (lumen only) seeding, SMC were perfused reciprocally through the scaffold lumen at a low flow rate by a dual syringe pump for 24 hours, and a fresh SMC suspension was seeded under the same conditions for an additional 24 hours. During these 48 hours, the external surface of the scaffolds was supplied with culture medium by a peristaltic pump. In dual (lumen and external surface) seeding, SMC were seeded (as previously described) for 24 hours, and then a fresh SMC suspension was perfused on the external surface of the scaffold for an additional 24 hours while culture medium was flown through the lumen by a peristaltic pump. During seeding in these two-module bioreactors, a separate syringe pump was used for each construct. After seeding, medium was delivered through both the lumen and the external surface of the scaffold at 1.5 Hz by a peristaltic pump (Figure 3.6).

Single- and dual-seeded constructs were endothelialized by flowing a EC suspension ($0.1x10^6$ cells/ml) through the construct lumen reciprocally by a dual syringe pump at 4 ml/min two days prior to harvest (late endothelialization) as described previously for SMC suspension. In a separate set of experiments with dual-seeded constructs, the endothelial cells were seeded after 10 days of culture (early endothelialization) to compare the effect of EC on SMC proliferation and matrix production.

Additionally, the nutrient composition in single- and dual-seeding experiments (early and late endothelialization) was modified compared to previous experiments by adding freshly prepared ascorbic acid to the bioreactor medium daily and removing externally added growth factors from the medium after 10 days of culture. Ascorbate has been shown to increase procollagen expression and collagen synthesis in human intestinal smooth muscle cells (Graham et al., 1995). This effect was more pronounced when heat-inactivated serum was used. However, approximately 88-98% of ascorbate undergoes auto-oxidation within 24 hours in culture medium (Chepda et al., 2001). Addition of freshly prepared ascorbic acid on a daily basis overcomes the ascorbate instability and supplies the cells with a constant concentration of ascorbic acid. Therefore, addition of ascorbic acid in combination with heat-inactivated serum to the bioreactor medium is hypothesized to increase collagen deposition leading to mechanically stronger arterial constructs.

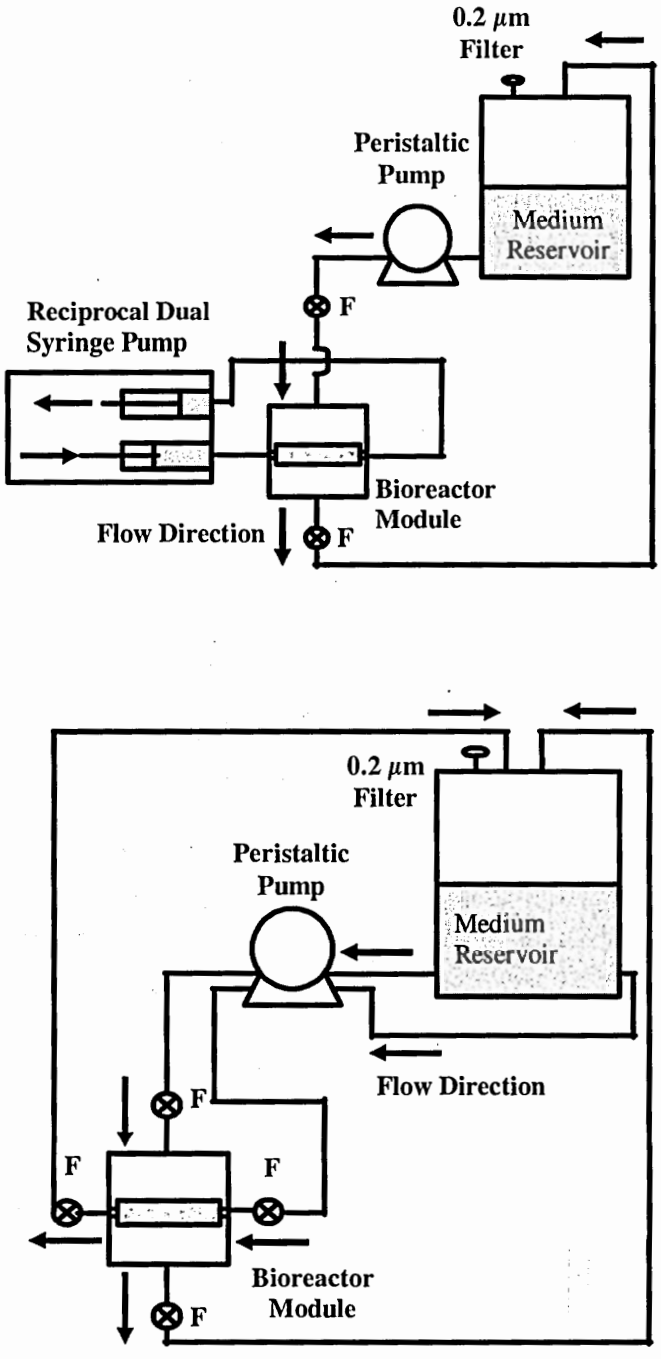

Figure 3.6 Bioreactor Assembly During Cell Seeding and Construct Growth.
Top: cell seeding bioreactor assembly and bottom: bioreactor assembly during construct growth (F indicates flowmeter).

The two growth factors that are added to the bioreactor medium in addition to the growth factors present in serum are human epidermal (EGF) and human basic fibroblast (bFGF) growth factor. Both growth factors are potent mitogens that stimulate smooth muscle and endothelial cell proliferation (Gospodarowicz et al., 1981). Basic FGF has been shown to decrease collagen type I, III, and V/XI production by bovine aortic smooth muscle cells in 2-D cultures (Kypreos and Sonenshein, 1998). Collagen types I and III are the main collagens expressed by smooth muscle cells in the medial layer of the arterial wall and contribute to the vessel's mechanical strength. Collagen V and XI are required for heterotypic collagen fibril assembly. Therefore, removing the externally-added growth factors after 10 days of culture is hypothesized to increase collagen synthesis.

III.10 Arterial Construct Analysis

III.10.1 Construct Digestion

Harvested constructs were frozen at -20°C, lyophilized, and the construct dry weight was measured. Extracellular matrix was digested by overnight incubation with proteinase K solution at 55°C (Kim and Mooney, 1998b). Digested (experimental) samples were stored at -20°C until used for biochemical assays.

III.10.2 DNA Content

Cell number was quantified by DNA measurement using Hoechst 33258 dye in a microplate spectrofluorometer (Spectra Max Gemini Dual-Scanning Microplate

Spectrofluorometer, Molecular Devices Corp., Sunnyvale, CA) (Kim and Mooney, 1998a). DNA standards were made by diluting the 10 μg/cc DNA working solution in PBS with EDTA (3.72g/L) (PBE) to give standards of 0.1-0.5 μg DNA. The dye solution was prepared by adding 5 μl of Hoechst 33258 dye to 50 ml of DNA solution in a beaker covered by aluminum foil and was mixed well with a stir bar. One liter of the DNA solution consisting of 990 ml DI water, 10 ml of 1M Tris-HCl, 0.372 g of EDTA, and 11.688 g of NaCl was prepared and stored at 4°C. A 10 μl sample of experimental samples/standards and 200 μl of the dye solution were added to duplicate wells of a black, flat-bottom 96-well plate, covered in aluminum foil, and optical density (OD) was read in a microplate spectrophotometer at ex/em 365/460. DNA content was calibrated with calf thymus DNA assuming 7.6 pg of DNA per SMC (Kim et al., 1998).

III.10.3 Collagen Content

Total collagen content was assessed by hydroxyproline measurement after acid hydrolysis in 6 N HCl for 3 hours at 120°C and reaction with chloramine-T and p-dimethylaminobenzaldehyde(DAB) (Woessner, 1961). Briefly, 500 μl of digested sample and 500 μl of 12N hydrochloric acid were pipetted into glass tubes, and heated at 120°C for 3 hours in a laboratory oven (Precision Scientific, Winchester, VA). The glass tubes were removed from the oven, cooled at room temperature, and 1000 μl of 12N hydrochloric acid was added to any of the tubes, in which the acid solution had evaporated (sample was a solid deposit at the bottom of the tubes). The contents of the tubes were transferred to 6 ml polystyrene round-bottom tubes using Pasteur pipettes and one sample was analyzed at a time until the end of the chloramine T step (see below). A

small stir bar was added to each tube and 1-2 drops of methyl red were pipetted in the solution over a stir plate. Drops of 5N NaOH were added until the solution turned yellow, then drops of 0.5N HCl until the solution turned pink, and 0.5N NaOH until it turned yellow again. Lower concentrations of HCl and NaOH were used to pinpoint the colorimetric reaction. Once all samples had been neutralized, 1 ml of each sample was transferred to 14 ml polystyrene round-bottom tubes. At this point, hydroxyproline standards of 1 through 5 μg were also prepared in 14 ml tubes and analyzed along with the experimental samples in a fume hood. Using glass pipettes, 0.5 ml of chloramine T solution was added to each tube to begin oxidation, mixed by shaking, and incubated for 20 min. The reaction was stopped by the addition of 0.5 ml of 70% perchloric acid (diluted in water) and 5 min incubation. The color reaction was initiated by adding 0.5 ml of DAB, capping the tubes, vortexing, and incubating the solution at 60°C for 20 min. The samples and standards were removed from the water bath, cooled down with tap water, poured into semi-frosted cuvettes, and OD was measured with a spectrophotometer at a wavelength of 557 nm. Collagen amount was quantified based on the calibration curve generated from the standards using a hydroxyproline to collagen ratio of 1:10.

Methyl red solution was prepared by adding 0.02 g of methyl red to 100 ml DI water and stirring for 20-30 min in a glass beaker covered with aluminum foil. Chloramine T solution was prepared by adding 1.41 g of chloramine T to 20 ml of DI water, 30 ml of ethylene glycol monomethyl ether (methyl cellosolve), and 50 ml of buffer. The buffer consisted of 50 g of citric acid, 12 ml glacial acetic acid, and 34 g sodium hydroxide in 1 L of DI water. The pH of the buffer was adjusted to 6 and the

solution was stored at 4°C. DAB solution was prepared during the chloramine T incubation step by adding 20 g of DAB to 100 ml of methyl cellosolve and warmed at 60°C in the water bath to facilitate solubilization. Hydroxyproline standards were prepared as follows: 25 mg of L-hydroxyproline were added to 250 ml of 0.001N HCl to make a 100 μg/ml stock solution; a 10 μg/ml working solution was diluted from the stock solution in DI water, and prepared fresh for each assay. Standards of 1 through 5 μg of hydroxyproline were prepared in DI water, and used to create calibration curve.

III.10.4 Glycosaminoglycan Content

Sulfated glycosaminoglycan (GAG) content was measured using the dimethylmethylene blue (DMMB) spectrophotometric assay (Farndale et al., 1982). Standards were made by diluting bovine chondroitin sulfate/PBE/cysteine stock solution to yield a 100 µg/ml working solution that was subsequently diluted with DI water to give standards of 1-5 µg chondroitin sulfate. The PBE/cysteine solution consisted of 0.105 g of cysteine in 60 ml of PBE and was filtered through a 0.2 μm filter. Chrondroitin sulfate/PBE/cysteine stock solution (50 mg/ml) was prepared by dissolving chondroitin sulfate in PBE/cysteine solution. The DMMB dye solution was made by adding 40.5 mM glycine, 40.5 mM NaCl, 9.5 mM HCl, and 8 mg DMMB in 500 ml of DI water, and adjusted to pH of 3. This solution could be stored wrapped in aluminum foil for 2-3 weeks. Samples concentrations were diluted in half; 8 μl of sample and standards were added to a well of a 96-well plate with 200 μl of dye solution and allowed to react for 2 min; and OD was measured in a spectrophotometer (PowerWaveX 340

Microplate spectrophotometer, Bio-Tek Instruments, Inc.) at 525 nm. Samples and standards were run in duplicates.

III.10.5 Construct Histological Analysis

Harvested construct rings approximately 5 mm in length were fixed in 10% formalin overnight at 4°C, paraffin embedded, cut in 5-μm thick cross sections, and mounted on glass slides. Slides were dried in an oven overnight at 37°C and subsequently stained with hematoxylin and eosin (H&E) (Electron Microscopy Sciences, Ft. Washington, PA) for cells and Masson's trichrome for collagen.

Slides were stained for hematoxylin and eosin as described in Table 3.1. Sections stained for collagen with Masson's trichrome were deparaffinized, rehydrated in distilled water, fixed in Bouin's solution for 1 hour at 56°C, cooled at room temperature, and washed in running tap water until yellow color was no longer visible (Carson, 1990). Slides were rinsed in distilled water, stained in Weigert's hematoxylin for 15 min, washed in running tap water for 10 min, and rinsed in distilled water. Sections were stained in Biebrich's scarlet-acid fuchsin for 1 min, rinsed in distilled water, immersed in phosphomolybdic-phosphotungstic acid for 20 min with agitation to remove the red color from collagen fibers, stained in aniline blue for 5-10 min, rinsed in 1% acetic acid for 3-5 min, and dehydrated in 95% and 100% ethanol twice each. Slides were cleared with 2-3 changes of xylene (Electron Microscopy Sciences) and coverslipped with synthetic resin (Richard Allan, Kalamazoo, MI).

Table 3.1 Hematoxylin and Eosin Staining Protocol for Paraffin-Embedded Tissues.

Step	Reagent	Time (min:sec)
1	Xylene substitute	3:00
2	Xylene substitute	3:00
3	Xylene substitute	3:00
4	100% Alcohol	2:00
5	100% Alcohol	2:00
6	100% Alcohol	2:00
7	95% Alcohol	2:00
8	Water	1:00
9	Hematoxylin	0:10
10	Water	1:00
11	0.5% Acid alcohol	0:01
12	Water	1:00
13	Bluing reagent	0:30
14	Water	1:00
15	80% Alcohol	1:00
16	Eosin	0:30
17	95% Alcohol	0:30
18	100% Alcohol	1:00
19	100% Alcohol	1:00
20	100% Alcohol	1:00
21	Xylene substitute	1:00
22	Xylene substitute	1:00
23	Xylene substitute	1:00

Elastin, smooth muscle α-actin, calponin and myosin heavy chain were visualized through immunohistochemical analysis by antibody binding (protocol provided by Vector Laboratories Inc., Burlingame, CA). Sections were deparaffinized and washed twice in PBS (Roche, Indianapolis, IN) for 5 min each. Sections for myosin heavy chain staining were proteolysed in 100 μg/ml pronase A for 10 min at room temperature to reveal the antigen and washed twice in PBS for 5 min each. Samples were blocked in 1% gelatin/PBS mixture (gelatin: JT Baker, Philipsburg, NJ) for 20 min and immunostained with mouse anti-elastin (1:5000), mouse smooth muscle α-actin (1:800), mouse anti-calponin (1:50), and myosin heavy chain (1:50) respectively, in 1% crystalline grade bovine serum albumin in PBS for 1 hour in a humid chamber. Excess antibody was then blotted off and the slides were rinsed in PBS twice for 5 min each. A biotinylated secondary antibody solution consisting of 1:400 antimouse IgG antibody (Vector Laboratories, Inc.) and 2% normal goat serum/1% bovine serum albumin in PBS (normal goat serum: Vector Laboratories, Inc.) was added to the slides and incubated for 30 min in a humid chamber. The excess solution was blotted off following incubation and slides were washed in PBS twice for 5 min each. The ABC-Vector Red complex (Vectastain ABC kit, Vector Laboratories Inc.) was applied on the slides and incubated for 1 hour in a humid chamber. Slides were then washed in PBS twice for 5 min each, followed by one wash in 100mM Tris solution (pH = 8.2) for 5 min.

The alkaline phosphatase substrate solution was then prepared immediately before use, applied on the slides, and incubated in the dark for 20-30 min checking color periodically up to 1 hour. Sections from native bovine thoracic aortas were used as positive controls and the incubation was complete when the protein of interest could be

clearly identified in the controls. Reaction was stopped by blotting off substrate and rinsing in tap water twice for 5 min each. Sections were then counterstained with Gill's hematoxylin (Electron Microscopy Sciences) for 10 sec, rinsed in tap water until clear, dipped once in 1% acid alcohol, rinsed in water, immersed in Scott's solution for 20 sec, rinsed in water, dehydrated through graded alcohols and xylene, and mounted in synthetic resin.

Immunohistochemical staining for von Willebrand factor (vWF) was by antibody binding using ABC-peroxidase (Vector Laboratories). Sections were deparaffinized and washed in PBS for 5 min. Endogenous peroxidase was blocked in samples using 0.3% hydrogen peroxide in methanol (Electron Microscopy Sciences) for 15 min. Slides were rehydrated in PBS twice for 5 min each, and antigen was retrieved by pretreatment with 100 μg/ml pronase A for 10 min. Slides were washed twice in PBS for 5 min each, blocked with 1% gelatin/PBS for 20 min and immunostained with rabbit anti-vWF in 1% crystalline grade bovine serum albumin in PBS for 1 hour in a humid chamber. Excess antibody was then blotted off and the slides were rinsed twice in PBS for 5 min each. A biotinylated secondary antibody solution consisting of 1:400 antimouse IgG antibody (Vector Laboratories, Inc.) and 2% normal goat serum/1% bovine serum albumin in PBS was added to the slides and incubated for 30 min in a humid chamber. Excess solution was blotted off with filter paper following incubation and slides were washed twice in PBS for 5 min each. The ABC-peroxidase complex (Elite Peroxidase ABC kit, Vector Laboratories Inc.) was applied to the slides and incubated for 1 hour in a humid chamber. Slides were then washed twice in PBS for 5 min each, followed by one wash in sterilized DI water for 5 min.

The diaminobenzidine substrate solution (Vector Laboratories Inc.) was then prepared by mixing components of the commercially-available kit and filtered immediately before use, applied on the slides, and incubated in the dark for up to 10 min checking color periodically. Reaction was stopped by blotting off substrate and rinsing in PBS three times for 5 min each. Sections were then lightly counterstained with Gill's hematoxylin as previously described and coverslipped.

Cell monolayers (SMC and EC) were occasionally plated on LAB-TEK® plastic chamber slides with walls, fixed and used as positive/negative controls for histological analyses. SMC were used as positive controls for SMC-specific markers, while EC were used as positive controls for vWF and negative controls for SMC-specific markers. Culture medium was removed from the wells; cells were rinsed in PBS twice for 1 min each, and fixed in 10% neutral buffered formalin for 10 min. The fixative was removed and cells were rinsed with PBS twice for 1 min each. The well walls were carefully removed leaving the gasket attached to the slide, slides were placed in 50 ml centrifuge tubes filled with 70% ethanol, and stored at 4°C until ready for use.

III.10.6 Scanning Electron Microscopy

Construct rings approximately 5 mm long were fixed overnight in 2.5% glutaraldehyde in 0.2 M cacodylate buffer (pH = 7.2) (Electron Microscopy Sciences) that was prepared immediately before use, rinsed in 0.2 M cacodylate buffer three times for 10 min each, and dehydrated in a graded series of ethanol/water solutions (25%, 50%, and 70% ethanol for 30 min each, and 90%, 100% twice for 30 min each) (Hayat, 2000). Samples were placed in 1.5 ml microcentrifuge tubes and dried with

hexamethyldisilazane (HMDS) (Electron Microscopy Sciences) gradually from 100% ethanol to 100% HMDS using the following gradations for 30 min each: 3:1, 1:1 and 1:3 ratio of ethanol to HMDS. Samples were then rinsed three times in 100% HMDS, surface covered with HMDS, and dried in a fume hood for 1-2 days with the microcentrifuge tube cap open. Dried samples were mounted on aluminum stubs (Structure Probe, Inc., West Chester, PA) using conductive, double-sided carbon adhesive tape (Structure Probe, Inc.), and sputter coated with gold at 20mA and 1-2kV for 4 min in a sputter coater (International Scientific Instruments). A scanning electron microscope (Hitachi S800 FEG scanning electron microscope, Hitachi Ltd., Tokyo, Japan) operating at 15 kV was used to visualize samples.

III.10.7 Confocal Microscopy

Cell viability was evaluated using the Live/Dead® Viability/Cytotoxicity kit (Molecular Probes Inc., Eugene, OR) and a Zeiss LSM 510 confocal microscope (Carl Zeiss Inc., Thornwood, NY). This kit is a two-color fluorescence cell viability assay that is based on the simultaneous determination of live and dead cells. Specifically, live cells were stained green with calcein AM dye (ex/em 495 nm/515 nm), and dead cells red with ethidium homodimer-1 (ex/em 495 nm/635 nm). Harvested constructs were rinsed in PBS 3 times for 10 min each, incubated in the calcein/ethidium solution wrapped in aluminum foil at 37°C for 30 min, rinsed in PBS three times for 10 min each, and stored in the dark until microscope viewing. The solution was prepared by adding 5 μl ethidium and 2.5 μl calcein to 1 ml PBS, mixing and centrifuging for 1 min at 9000 rpm in a Sorvall® RMC 14 centrifuge (Du Pont Medical Products).

III.10.8 Sirius Red Collagen Assay

Collagen fibril alignment was visualized using collagen's birefringence property under polarized light (Junqueira et al., 1979; Puchtler et al., 1973). Briefly, slides were deparaffinized, washed in DI water for 5 min, incubated with picro-sirius red for 90 min, washed in 0.01 N HCl for 1 min, washed in DI water for 5 min, dehydrated in alcohol, cleared in xylene, and mounted in synthetic resin. Fibrillar and highly aligned collagen appeared red on a black background under white light and polarized light.

III.10.9 Mechanical Testing

The uniaxial ring-tester apparatus used was developed in Dr. Robert M. Nerem's laboratory (Georgia Institute of Technology) by Dr. Dror Seliktar (Seliktar et al., 2000). The main components of the system are the testing chamber, the position controller, the strain imaging system, the load cell, and the data acquisition system. The force transducer was calibrated prior to testing with a set of calibrated weights, voltage was recorded, and the slope of a calibration curve of weight vs. volts was used in the data analysis. Harvested constructs were rinsed in PBS and 5 mm long rings were sectioned using a scalpel blade and a ruler. Four small black beads with 300 μm average diameters were glued with SuperGlue™ using a 21-gauge syringe needle on one cross-section, two on each wall across from each other. These beads were used to measure the true local strain of the material during the tensile test. The samples were then placed between the two hooks in the test chamber with the beaded cross-section facing a CCD camera; the bottom computer-controlled hook was lowered at a constant rate of 0.2 mm/sec to failure while LabView™ software (National Instruments, Austin, TX) was recording the

force/displacement data and Inspector™ software (Matrox Electronic Systems Ltd., Montreal, Canada) taking digital images. The data was then analyzed and the ultimate tensile strength and Young's modulus were calculated for each construct sample (Seliktar et al., 2000).

III.11 Medium Analysis

Medium samples were collected from the medium reservoir before every bioreactor feeding, frozen at -20°C, and analyzed for glucose and lactate using commercially available kits.

Glucose levels were measured using Trinder reagent that was prepared by reconstituting one vial of reagent with 100 ml DI water. One ml of reagent and 5 μl of sample were added in each semi-frosted cuvette (Fisher Scientific, Suwannee, GA); the cuvette was capped, mixed by inversion, and allowed to incubate for 18 min at room temperature. After incubation, samples were read in a spectrophotometer and the OD was measured at 505 nm. A calibration curve was generated with three glucose standards, 100 mg/dl, 300 mg/dl and 800 mg/dl. Standard samples were run in triplicate and experimental samples in duplicate. Time zero glucose concentration was measured from control medium solution.

Lactate levels in the bioreactor medium were measured using the Lactate reagent that was prepared by reconstituting one vial of reagent with 10 ml of DI water. One ml of reagent and 10 μl of sample were added to each semi-frosted cuvette that was capped, mixed by inversion, and incubated for 10 min at room temperature. Time zero lactate

concentration was measured from control medium solution. Additional medium samples were used to monitor pH during the experiments.

III.12 Statistical Analysis

In this thesis, N indicates number of independent experiments performed and n number of constructs per data point. For example, single and dual seeding bioreactor experiments were run in triplicate with two constructs in each bioreactor. Therefore, for these experiments N = 3 and n = 2. For each data set representing 3 or more samples, values are presented as mean ± standard deviation. Comparisons were made using Student's t test and one factor ANOVA (Hayter, 1996).

CHAPTER IV

RESULTS

IV.1 Static Seeding

Static seeding experiments of aortic smooth muscle cells in various biodegradable polymer matrices helped reveal a cell-matrix combination with potential for use as a small caliber blood vessel substitute based on important parameters, such as cell attachment efficiency, distribution, and proliferation. Growth of human, bovine and rat aortic smooth muscle cells in poly-L-lactic acid (PLLA), poly-ε-caprolactone (PCL), and polyglycolic acid (PGA) was compared (Table 4.1). Additionally, different polymer surface modifications with NaOH and extracellular matrix protein coatings were investigated to improve cell attachment and proliferation, and the chosen cell-scaffold combination was used to validate the bioreactor system. An exhaustive search of all possible combinations of cell types, polymers and surface modifications was not performed. Rather, the goal here was to select a biodegradable polymer scaffold that supports cell attachment and proliferation for use in bioreactor experiments. The criteria for selecting SMC species were ability to proliferate in the polymer scaffold and availability of primary cells. In all the static seeding experiments, cell number on day 0 represents the initial cell number that each scaffold was seeded with. Therefore, 100% cell seeding efficiency is assumed for all the experiments and cell number with culture time is compared to the initial cell number that each construct was seeded with.

Table 4.1 Static Seeding Experimental Design.
PCL and PLLA scaffold diameter was 1 cm. Asterisk (*) indicates that PGA scaffold diameter was 2.4 cm and that PGA scaffolds were seeded with 2.14×10^6 and 5.14×10^6 cells (corresponding to approximately 0.5×10^6 and 1×10^6 cells per cm^2).

Cell Passage Number	Cell Species Polymer	Polymer Surface Modification	Cell Seeding Number ($x10^6$)	Culture Time (Days)	Proliferation
10	Human PCL, PLLA	None	0.075, 0.15, 0.5	7	Cell death to modest proliferation
6	Human PLLA	None	1	7	Constant cell number
7	Human PCL, PLLA	None	0.9	14	Modest cell proliferation followed by cell death
7	Human PLLA	Prewetting	1	30	Constant cell number
7	Human PCL	Prewetting	1	30	High cell proliferation followed by cell death
7	Human PGA*	None	0.5* and 1*	6	High cell proliferation
2	Bovine PCL	NaOH, Fn, NaOH+Fn	1	14	Modest cell proliferation
2	Bovine PCL, PLLA	NaOH, Fn, NaOH+Fn	1	28	Low to modest cell proliferation
2	Bovine PCL	Various	1	30	Modest cell proliferation

IV.1.1 Human Aortic Smooth Muscle Cells

Cylindrical discs of PLLA and PCL polymer scaffolds with 92% porosity were used in a series of static seeding experiments to assess their ability to support human smooth muscle cell (HASMC) attachment and proliferation. Initial experiments explored the use of three different initial cell densities. HASMC were seeded on PLLA and PCL scaffolds with 75,000, 150,000 and 500,000 cells per scaffold (Figure 4.1). For all seeding densities, cell seeding efficiency was lower than 43%. After 1 and 4 days of culture both polymers seeded with 500,000 HASMC contained significantly more cells than scaffolds seeded with 75,000 and 150,000 cells. The same was true for PCL scaffolds after 7 days. Additionally, PCL scaffolds seeded with 75,000 HASMC contained significantly less cells than those seeded 150,000 after 1 day of culture. Even though PLLA constructs seeded with 500,000 HASMC showed significantly higher cell number after 4 days compared to day 1, PCL construct cell number did not change significantly under the same conditions. In PCL scaffolds seeded with 150,000 cells, cell number decreased significantly from day 1 to 7. In summary, PCL and PLLA scaffolds seeded with 500,000 HASMC had a significantly higher cell number compared to scaffolds with lower initial cell densities at all the time points studied, and PCL and PLLA constructs of a given initial cell density showed either modest cell proliferation or cell number decrease over the course of 7 days.

Since cells appeared to proliferate modestly in PLLA constructs seeded with 500,000 HASMC, a higher initial cell density of 1 million cells per scaffold was used. When PLLA scaffolds were seeded with HASMC, approximately 100% seeding

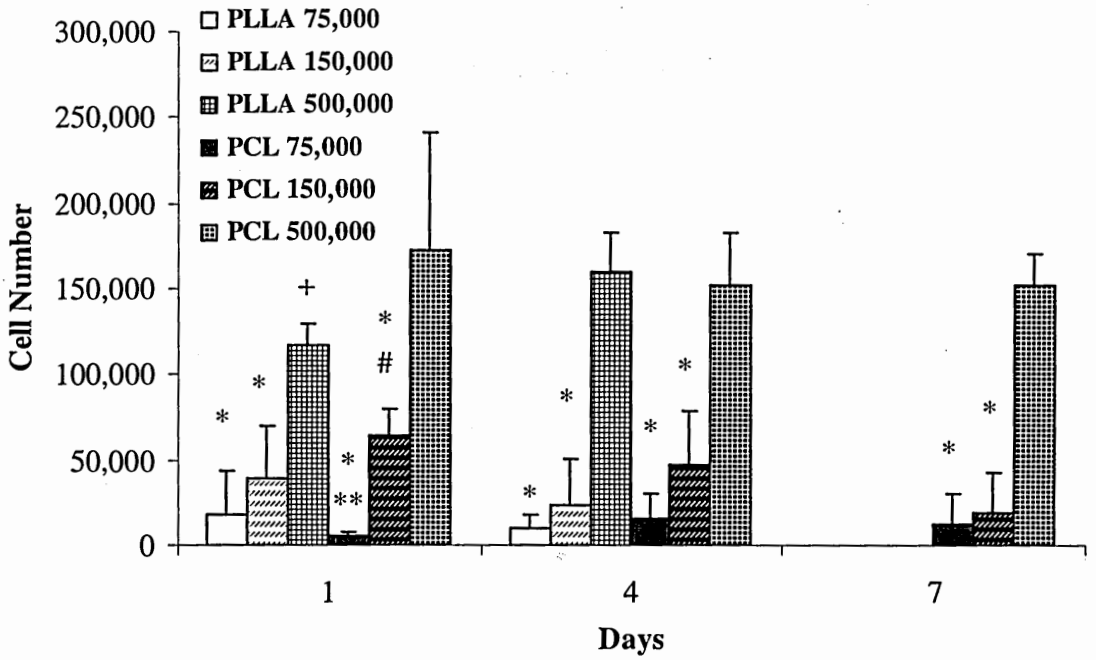

Figure 4.1 Human Aortic SMC Proliferation in PCL and PLLA Scaffolds.
PLLA and PCL scaffolds were seeded with HASMC at three different initial cell densities: 75,000, 150,000, and 500,000 cells per scaffold. On days 1 and 4, PCL and PLLA scaffolds seeded with 500,000 cells contained significantly more cells (*) than PCL and PLLA scaffolds seeded with 75,000 and 150,000 ($p<0.05$). The same was true for PCL at 7 days ($p<0.05$). On day 1, PCL scaffolds seeded with 75,000 cells contained significantly less (**) cells than PCL scaffolds seeded with 150,000 ($p<0.05$). PLLA scaffolds seeded with 500,000 contained significantly more (+) cells on day 4 than day 1 ($p<0.05$). PCL scaffolds seeded with 150,000 had significantly higher (#) cell number on day 1 than day 7 ($p<0.05$). Data are mean ± standard deviation for N = 1 independent experiments with n = 3-4 constructs per experiment.

efficiency was achieved and the cell number remained the same for up to 7 days (Figure 4.2). Under these conditions cell number did not decrease with time so a longer term experiment was performed using both PCL and PLLA scaffolds at an initial cell density close to $1x10^6$ cells.

In this experiment, PCL and PLLA scaffolds were seeded with HASMC at an initial density of 900,000 cells per scaffold and cultured for 14 days with samples harvested after 1, 7, and 14 days. Cell number increased in 24 hours, remained the same at day 7, and significantly decreased at day 14 compared to days 1 and 7 for both polymers (Figure 4.3).

Since high proliferation rates were not observed with PLLA or PCL at the initial cell densities studied, the polymer surface was modified by prewetting the polymers in culture medium. To determine whether prewetting scaffolds would increase cell attachment and proliferation compared to previous experiments, prewetted and dry PLLA scaffolds were each seeded with $1x10^6$ HASMC (Figure 4.4). It was found that dry scaffolds had significantly higher cell number than prewetted scaffolds after 1 and 3 days of culture. However, when this experiment was run with PCL scaffolds, cell number in prewetted scaffolds was higher at every time point studied and was significantly higher after 30 days of culture compared to dry scaffolds (Figure 4.5).

Other key parameters that were studied in these longer term (30-day) static seeding experiments were cell viability and distribution and total collagen production. Cell viability was studied using live/dead assay and SMC were found to be uniformly distributed on the surface and across the larger part of the cross-section of the scaffolds within 30 days (Figure 4.6).

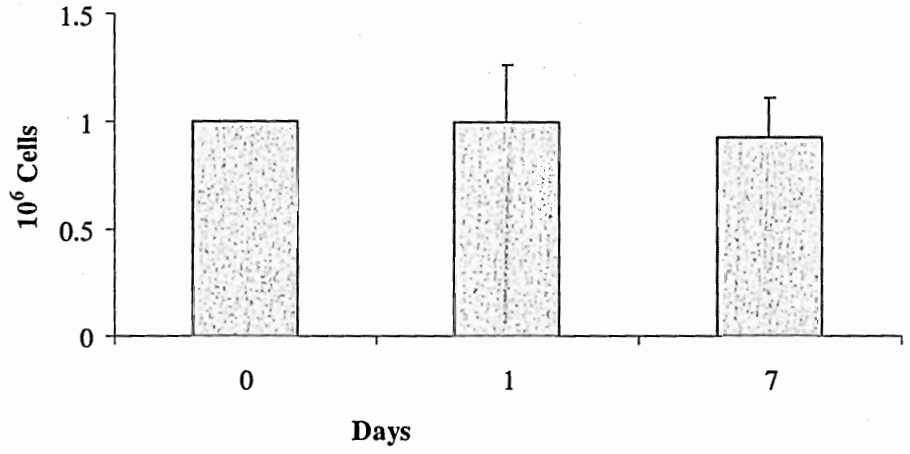

Figure 4.2 Human Aortic SMC Proliferation in PLLA Scaffolds.
Data are mean ± standard deviation for N = 1 independent experiments with n = 3 constructs per experiment.

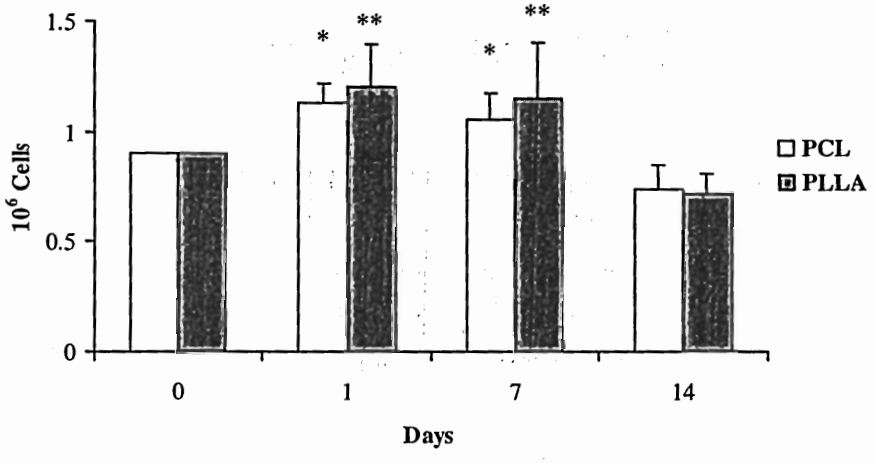

Figure 4.3 Human Aortic SMC Proliferation in PCL and PLLA Scaffolds.
Cell number in PCL constructs significantly decreased (*) from days 1 and 7 to day 14 ($p<0.05$). The same was observed with PLLA (**) ($p<0.05$). Data are mean ± standard deviation for N = 1 independent experiments with n = 4-6 constructs per experiment.

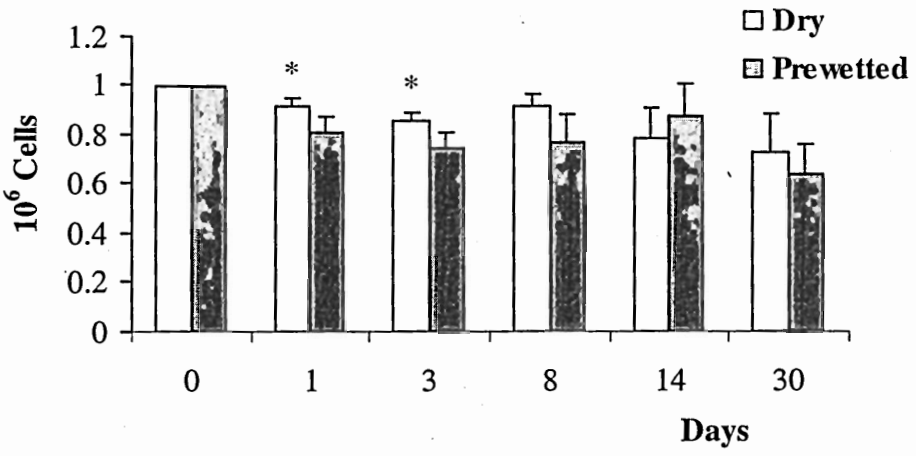

Figure 4.4 Effect of PLLA Prewetting on Cell Proliferation.
On days 1 and 3 dry PLLA constructs contained significantly more cells (*) than prewetted constructs ($p<0.05$). Data are mean ± standard deviation for N = 1 independent experiments with n = 3-4 constructs per experiment.

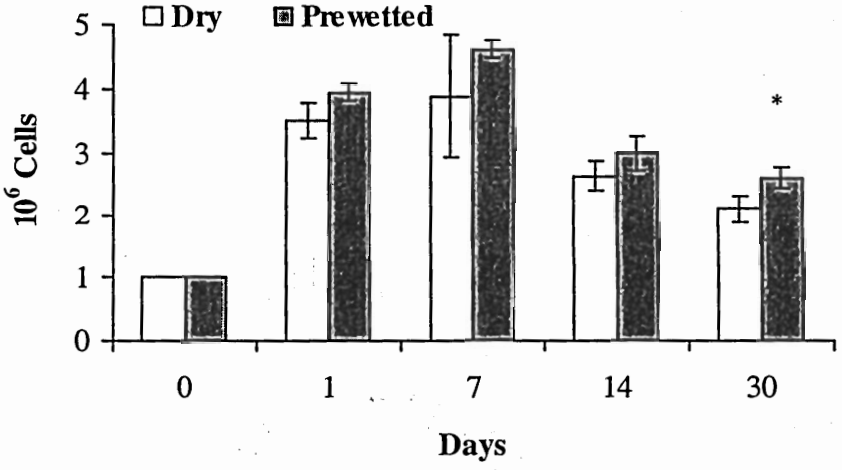

Figure 4.5 Effect of PCL Prewetting on Cell Proliferation.
On day 30, cell number in prewetted scaffolds was significantly higher (*) than cell number in dry scaffolds ($p<0.05$). Data are mean ± standard deviation for N = 1 independent experiments with n = 3-4 constructs per experiment.

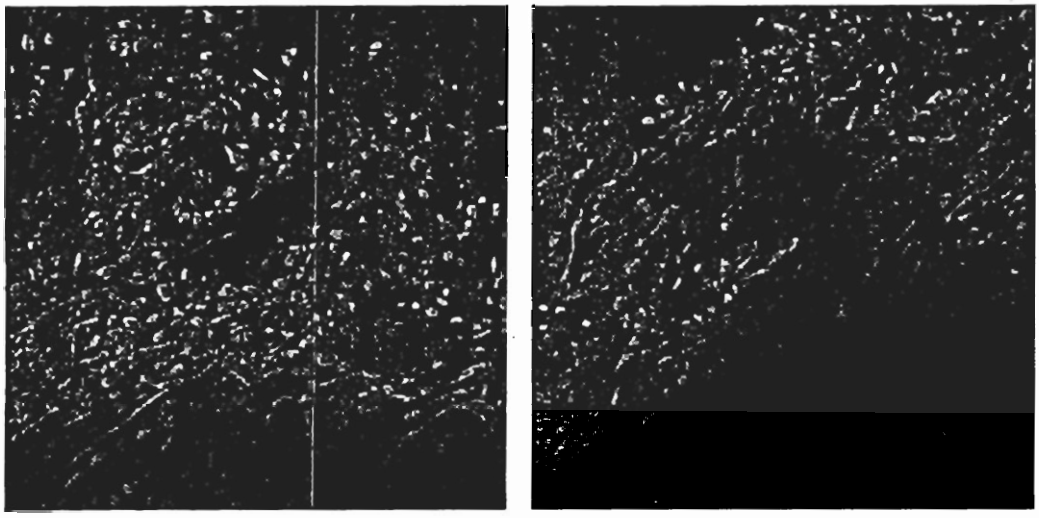

Figure 4.6 Human Aortic Smooth Muscle Cell Viability on PCL Scaffolds.
These scaffolds were seeded with $1x10^6$ cells and cultured for 30 days. Viable cells are stained green and dead cells' nuclei red.

Total collagen production was measured with the hydroxyproline assay for the last two experiments and for the two final time points (14 and 30 days). Although collagen production was higher in the prewetted PLLA constructs after 14 days and lower after 30 days compared to dry constructs (Figure 4.7), the amount of collagen per cell was lower in prewetted constructs compared to dry PLLA constructs after 14 days (Figure 4.8). In contrast, collagen and collagen per cell contents of prewetted PCL constructs were significantly higher than dry constructs after 14 days but lower after 30 days (Figures 4.9 and 4.10). Although cell number slightly decreased from day 14 to 30 in dry PCL and dry and prewetted PLLA constructs, the amount of collagen produced per cell increased. This finding could mean that cells decreased their proliferation rate and are laying down extracellular matrix.

Since only moderate proliferation rates were observed with HASMC on PLLA and PCL, non-woven felts of PGA, another biodegradable polymer, were also considered. This material has been used extensively for the development of vascular grafts and has

been shown to support cell proliferation, and extracellular matrix production. Two limitations of PGA use are its high cost and availability only as sheets of non-woven meshes. Initial experiments with PGA compared HASMC proliferation under two initial cell densities. PGA discs of 2.4 cm diameter and 6 mm thickness were seeded at two initial cell densities: 2.57 and 5.14 million cells per scaffold, which correspond to approximately $0.5x10^6$ and $1x10^6$ cells per 1 cm^2 scaffold surface area (so that comparisons with the seeding densities of previous experiments could be made). PGA scaffolds were able to support cell attachment and proliferation of HASMC, with cells reaching four times their initial density (2,570,000 initial density) within 6 days (Figure 4.11).

In contrast, PLLA scaffolds seeded with $1x10^6$ HASMC for 7 days did not show any proliferation (Figure 4.2). The same was observed with PCL and PLLA scaffolds in Figure 4.3 over 14 days. Prewetting of PLLA scaffolds did not increase cell proliferation (Figure 4.4), but a similar experiment with PCL scaffolds showed increased proliferation up to day 7 for both dry and prewetted scaffolds and cell number decrease between days 7 and 30 (Figure 4.5). Therefore, HASMC are able to proliferate in PGA at higher rates compared to PCL and PLLA scaffolds.

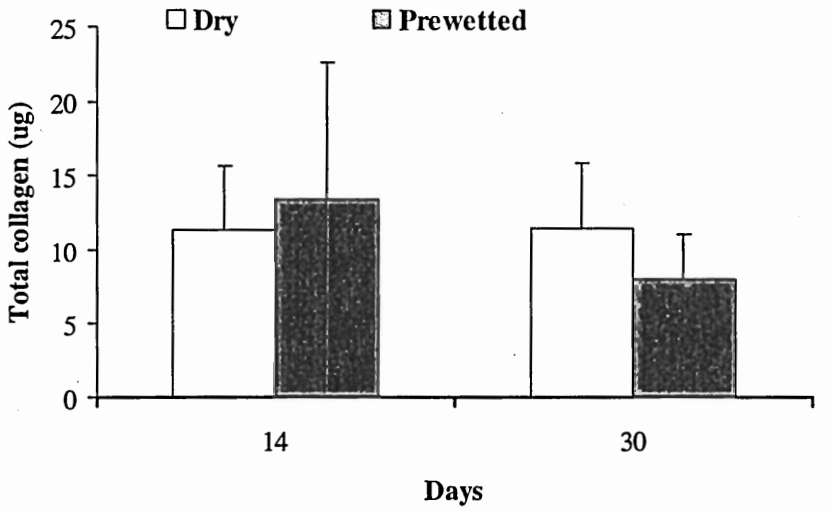

Figure 4.7 Total Collagen Deposition in Dry and Prewetted PLLA Constructs. Data are mean ± standard deviation for N = 1 independent experiments with n = 3-4 constructs per experiment.

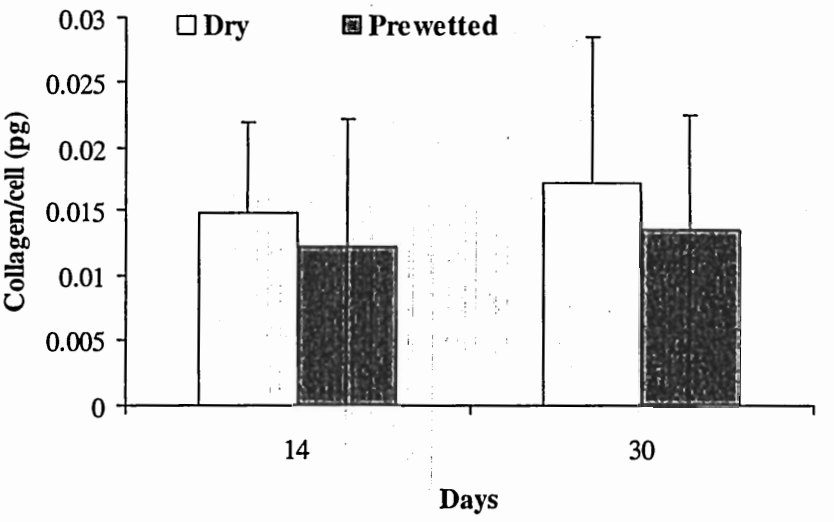

Figure 4.8 Collagen per Cell Content in Dry and Prewetted PLLA Constructs. Data are mean ± standard deviation for N = 1 independent experiments with n = 3-4 constructs per experiment.

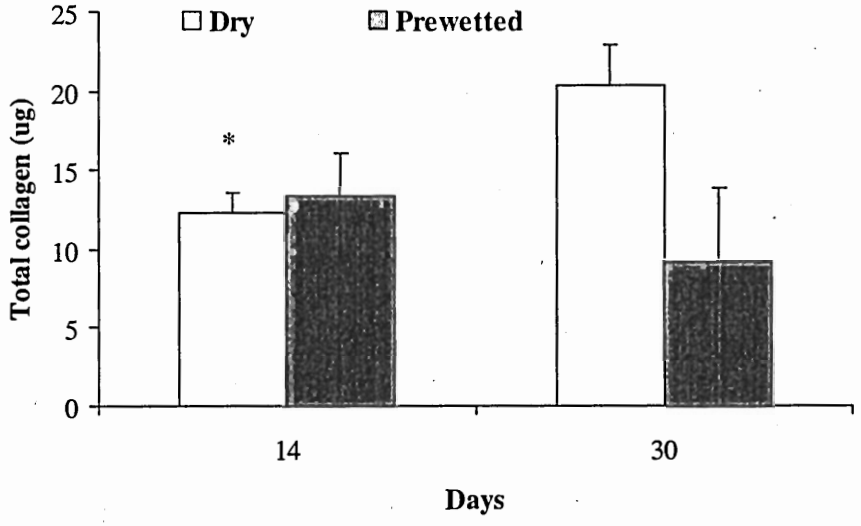

Figure 4.9 Total Collagen Deposition in Dry and Prewetted PCL Constructs.
Collagen was significantly higher (*) in prewetted compared to dry PCL scaffolds after 14 days ($p<0.05$). Data are mean ± standard deviation for N = 1 independent experiments with n = 3-4 constructs per experiment.

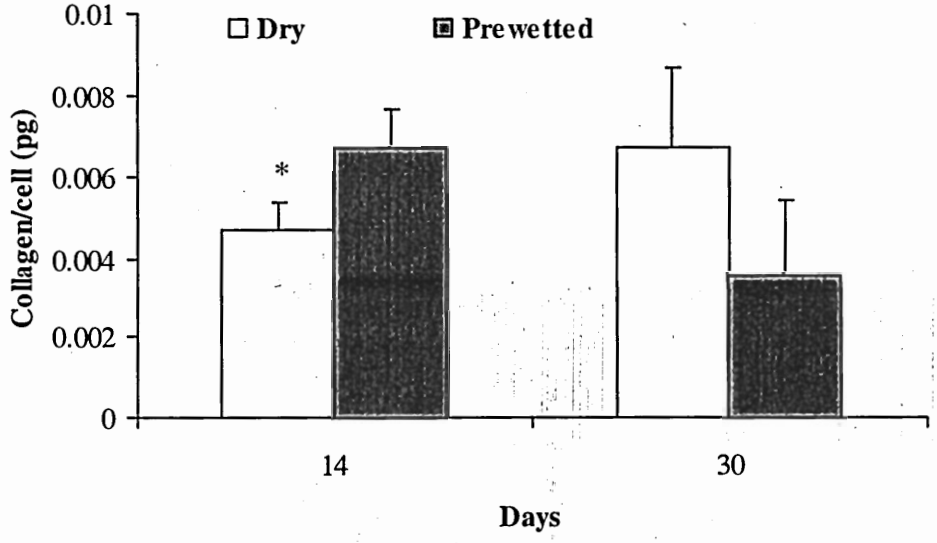

Figure 4.10 Collagen per Cell Content in Dry and Prewetted PCL Constructs.
Collagen per cell was significantly higher (*) in prewetted compared to dry PCL constructs on day 14 ($p<0.05$). Data are mean ± standard deviation for N = 1 independent experiments with n = 3-4 constructs per experiment.

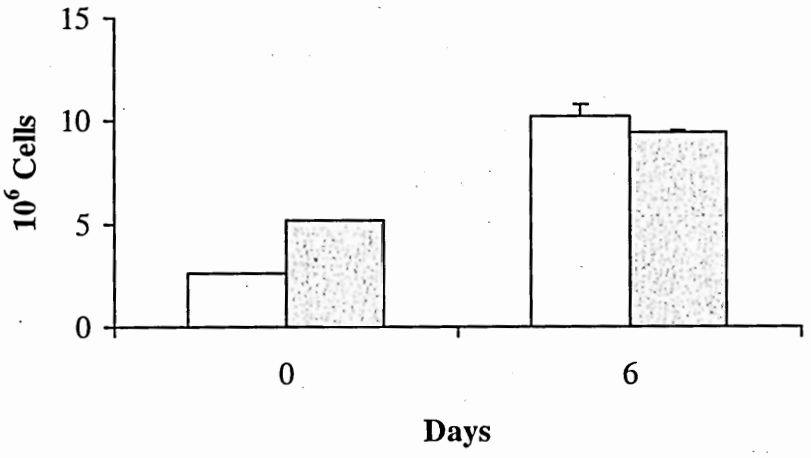

Figure 4.11 Human Aortic Smooth Muscle Cell Proliferation in PGA Scaffolds. Data are mean ± standard deviation for N = 1 independent experiments with n = 3-5 constructs per experiment.

IV.1.2 Bovine Aortic Smooth Muscle Cells

Animal cell sourcing offers the possibility of using primary cells, which is important for SMC since they tend to switch phenotype and dedifferentiate in vitro (Campbell, 1985). In addition, larger numbers of animal cells compared to human cells can be obtained in culture at a much lower cost. A clear disadvantage is that animal cell behavior does not always predict that of human cells.

A readily available source of primary animal aortic smooth muscle cells is cells isolated from bovine thoracic aortas. These cells are well-characterized and have been used in fluid flow experiments (Benbrahim et al., 1996; Kanda et al., 1993; Sterpetti et al., 1993). In addition, previous work in vascular tissue engineering has shown that SMC can be successfully used to develop small diameter vascular grafts (Niklason et al., 1999). For these reasons, SMC proliferation was studied in PCL and PLLA scaffolds.

SMC ($1x10^6$) were seeded on PCL scaffolds that were pretreated with NaOH, fibronectin (Fn), and NaOH in combination with Fn, and were cultured for 14 days. NaOH has been shown to increase the hydrophilicity of PGA scaffolds by hydrolyzing their surface (Gao et al., 1998). Fibronectin is a ubiquitous extracellular matrix protein that facilitates cell attachment and migration and is involved in various cellular processes (Bhat et al., 1998; Clyman et al., 1990). Cell number increased with time and pretreated constructs had higher cell number compared to the controls after 1 and 14 days (Figure 4.12). Cell number was significantly higher in NaOH, NaOH+Fn treated and in control scaffolds on day 14 compared to day 1 ($p<0.05$). However, no statistically significant differences were observed between treatments and cells proliferated moderately within 14 days (less than two-fold increase in cell number). NaOH+Fn treated scaffolds had a significantly higher cell number after 14 days compared to control scaffolds ($p<0.05$).

Cell proliferation was studied further in a 28-day experiment where PCL and PLLA scaffolds were seeded with $1x10^6$ SMC. PCL and PLLA constructs pretreated with NaOH and Fn had higher cell number after 28 days of culture compared to PCL control constructs (Figure 4.13). In contrast to previous seeding experiments with untreated PCL and PLLA scaffolds that showed a low cell seeding efficiency after 1 day, pretreated constructs showed high cell seeding efficiency and proliferation within 1 day of culture (Figures 4.12 and 4.13). However, cells did not proliferate significantly within 28 days of culture.

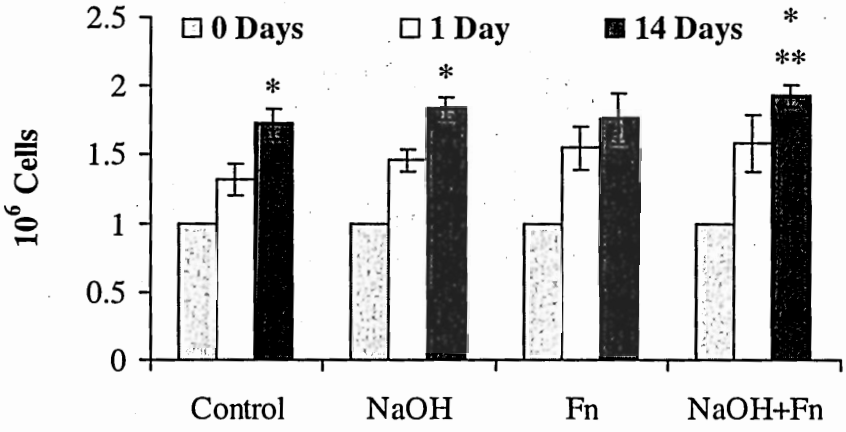

Figure 4.12 Bovine Aortic SMC Proliferation in PCL Scaffolds.
Scaffolds were pretreated with sodium hydroxide (NaOH), fibronectin (Fn), or both. On day 14, cell number in NaOH-treated, NaOH+Fn treated and control scaffolds was significantly higher (*) than cell number on day 1 ($p<0.05$). Cell number in NaOH+Fn treated scaffolds was significantly higher compared to control scaffolds on day 14 ($p<0.05$). Data are mean ± standard deviation for N = 1 independent experiments with n = 3-5 constructs per experiment.

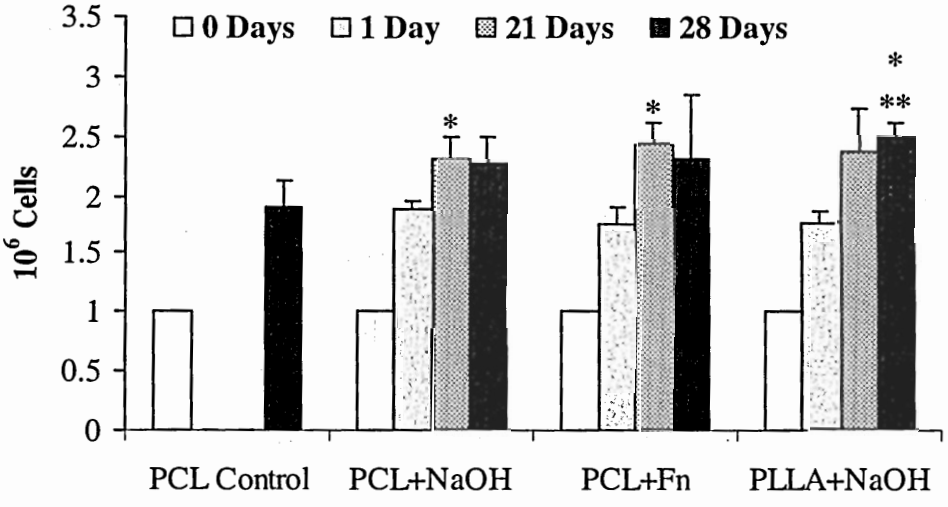

Figure 4.13 Bovine Aortic SMC Proliferation in PCL and PLLA Scaffolds.
NaOH- and Fn-treated PCL scaffolds had a significantly higher cell number on day 21 compared to day 1 ($p<0.05$). NaOH-treated PLLA scaffolds had significantly higher cell number on day 28 compared to day 1 and compared to PCL control after 28 days ($p<0.05$). Data are mean ± standard deviation for N = 1 independent experiments with n = 3-4 constructs per experiment.

Collagen deposition, measured after 21 and 28 days of culture, showed that PCL constructs treated with NaOH contained more collagen compared to PLLA constructs pretreated with NaOH after 21 days ($p<0.06$), but the opposite trend was observed after 28 days ($p<0.08$) (Figure 4.14). In addition, PCL constructs treated with Fn had significantly more collagen than PLLA constructs pretreated with NaOH after 21 days ($p<0.05$).

SMC populated mostly the top surface areas of the constructs (Figure 4.15) and deposited small amounts of collagen (Figure 4.16). SMC in NaOH-treated PCL scaffolds were distributed across a larger part of the construct's cross-section compared to Fn-treated constructs and contained more collagen. Histological analysis of constructs cultured under static conditions even for 28 days was cumbersome because tissue sections would not fully adhere to the slides and sections were partially washed off during the staining process. Therefore, only constructs cultured for 28 or 30 days were analyzed with histology.

These results indicate that surface modifications have an effect not only on cell seeding efficiency but also on cell proliferation and collagen deposition. Since PCL porous scaffolds are less brittle than PLLA scaffolds, a set of three 30-day experiments was run to compare the effects of different surface modifications on SMC proliferation in PCL. In addition to NaOH and Fn pretreatments, collagen and gelatin, two other extracellular matrix proteins were used to coat the surface of PCL scaffolds, as well as combinations of NaOH with Fn, gelatin, and collagen. Cell number increased in all cases between days 14 and 30, except in constructs treated with collagen (Figure 4.17).

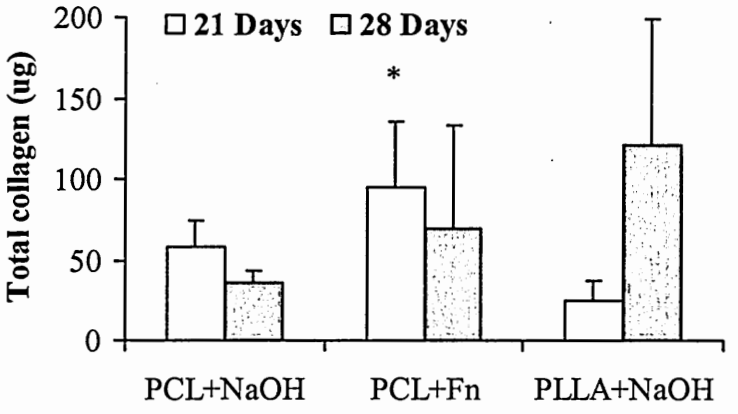

Figure 4.14 Total Collagen Deposition in Pretreated PCL and PLLA Constructs.
PCL was pretreated with NaOH and Fibronectin (Fn), and PLLA with NaOH. On day 21, PCL scaffolds pretreated with Fn contained significantly more cells (*) than PLLA scaffolds treated with NaOH. Data are mean ± standard deviation for N = 1 independent experiments with n = 3-4 constructs per experiment.

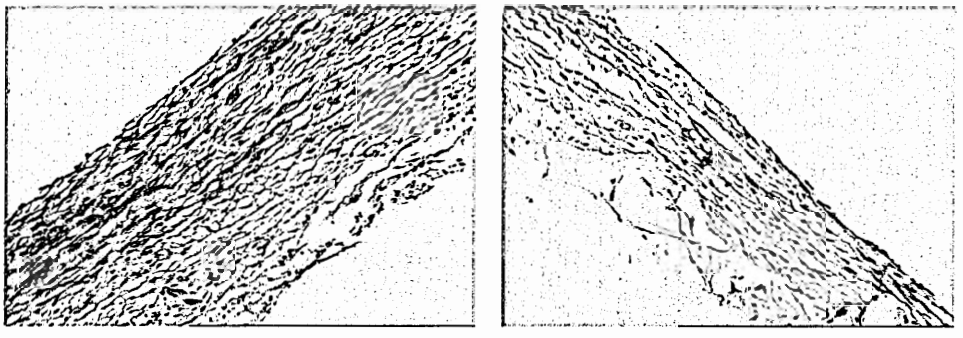

Figure 4.15 Bovine Aortic SMC Distribution in Pretreated PCL Constructs.
Left: pretreated with NaOH and right: with fibronectin after 28 days of culture. Cell nuclei are stained dark blue and cytoplasm is stained purple (20X).

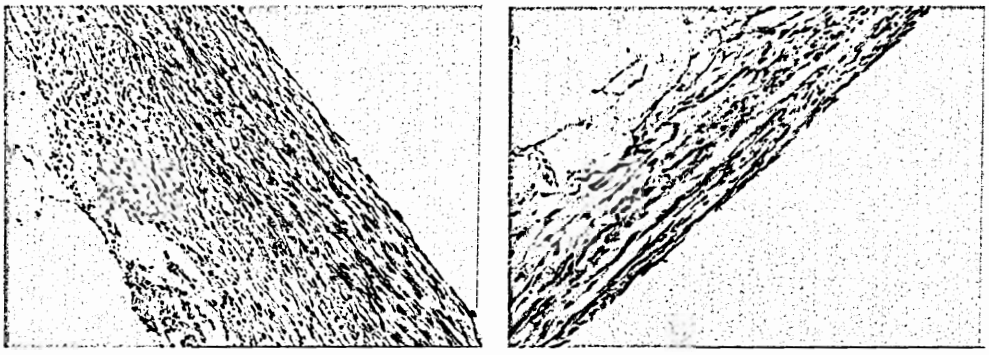

Figure 4.16 Collagen Deposition in Pretreated PCL Constructs.
PCL scaffolds were pretreated with NaOH (Left) and Fibronectin (Right), seeded with SMC and cultured for 28 days. Cell nuclei are stained dark blue and collagen is stained blue (20X).

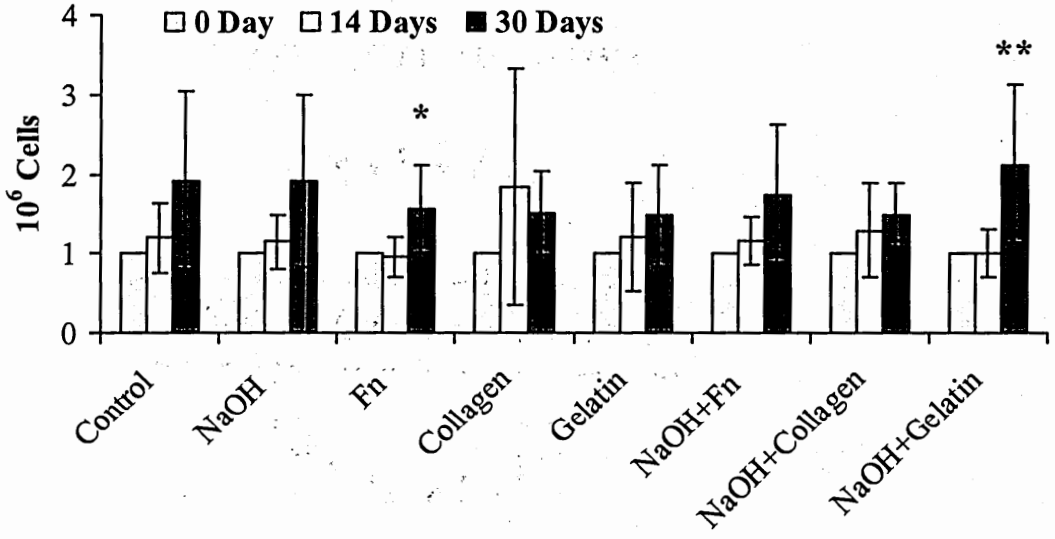

Figure 4.17 Thirty-Day SMC Proliferation in Pretreated PCL Scaffolds.
Scaffolds were pretreated with NaOH, fibronectin (Fn), collagen, gelatin, NaOH and Fn, NaOH and collagen, and NaOH and gelatin. Cell number increased significantly between days 14 and 30 in Fn-treated (*) and NaOH and gelatin treated scaffolds (**) ($p<0.05$). Data are mean ± standard deviation for N = 3 independent experiments with n = 3-5 constructs per experiment.

Specifically, cell number increased less than two-fold in control, NaOH treated ($p<0.06$), Fn treated ($p<0.005$), and NaOH with collagen treated constructs ($p<0.06$), and two-fold in NaOH with gelatin treated constructs ($p<0.005$). After 4 weeks of culture, constructs treated with NaOH and gelatin had higher cell number compared to Fn treated, collagen treated ($p<0.06$), and gelatin treatedconstructs. Overall, there was no significant difference in cell number between the various surface treatments and the control after 4 weeks of culture. Histological analysis of 4-week constructs showed that SMC were distributed throughout the cross-section but had a higher cell density near the top surface (Figure 4.18). PCL constructs that were pretreated with NaOH and gelatin had a thin tissue-dense periphery with cells populating areas of high nutrient concentration.
The static seeding experiments described here showed that human and bovine aortic smooth muscle cells proliferate moderately in PCL and PLLA scaffolds and that prewetting and modifying the polymers' surface did not result in high proliferation rates. In contrast, HASMC number increased four-fold in PGA scaffolds in 6 days. Therefore, PGA scaffolds were selected for bioreactor experiments in combination with bovine aortic cells that can be harvested from native tissue and used at low passages.

IV.1.3 Effect of Pore Size on Cell Proliferation

This experiment tested the hypothesis that scaffolds with smaller pore sizes may retain more cells and result in higher cell numbers. PLLA scaffolds with different pore sizes have been previously investigated (Saini, 2001). In those studies, no significant differences were observed in chondrocyte attachment, proliferation and matrix production

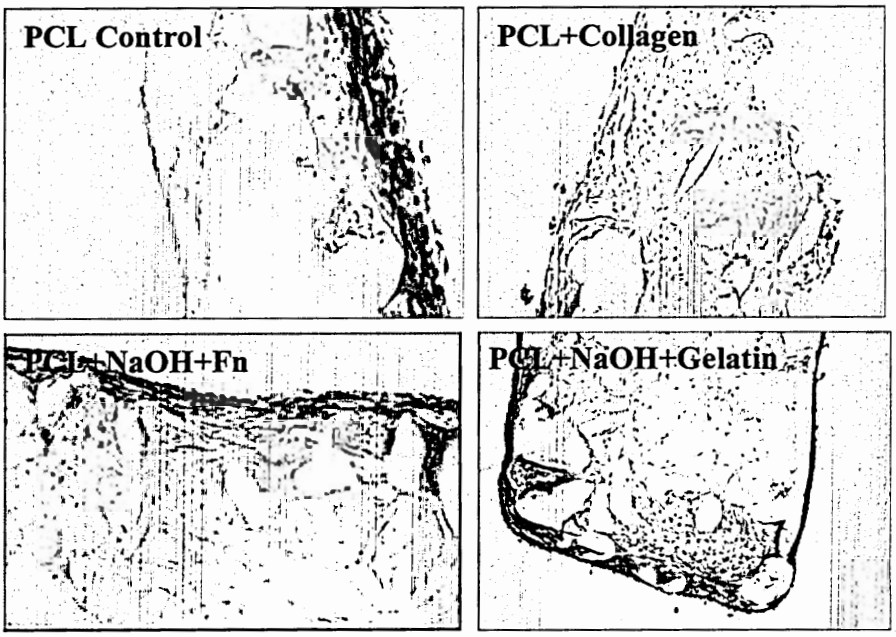

Figure 4.18 Bovine Aortic Smooth Muscle Cell Distribution in PCL Scaffolds. Original magnification: 10X.

between 106-150 μm and 150-250 μm pore size scaffolds. However, histological analysis showed that the smaller pore size may keep cells in closer proximity.

For arterial constructs, the scaffold pore size is determined by the size of sodium chloride crystals used and in all previous experiments 150-250 μm crystals were used. The experiment described here compared cell proliferation in PLLA scaffolds of two different pore sizes for three different initial cell densities. Rat aortic smooth muscle cells (RASMC) were used in these experiments because the experiments took place during the transition from human to bovine cells, and bovine cells were not available. PLLA scaffolds were seeded with passage 5 RASMC at three different initial cell densities ($0.5x10^6$, $1x10^6$ and $2x10^6$ cells per scaffold) as shown in Figure 4.19. Constructs with two ranges of pore size, 106-150 μm and 150-250 μm, were also studied to determine the effect of pore size on cell proliferation.

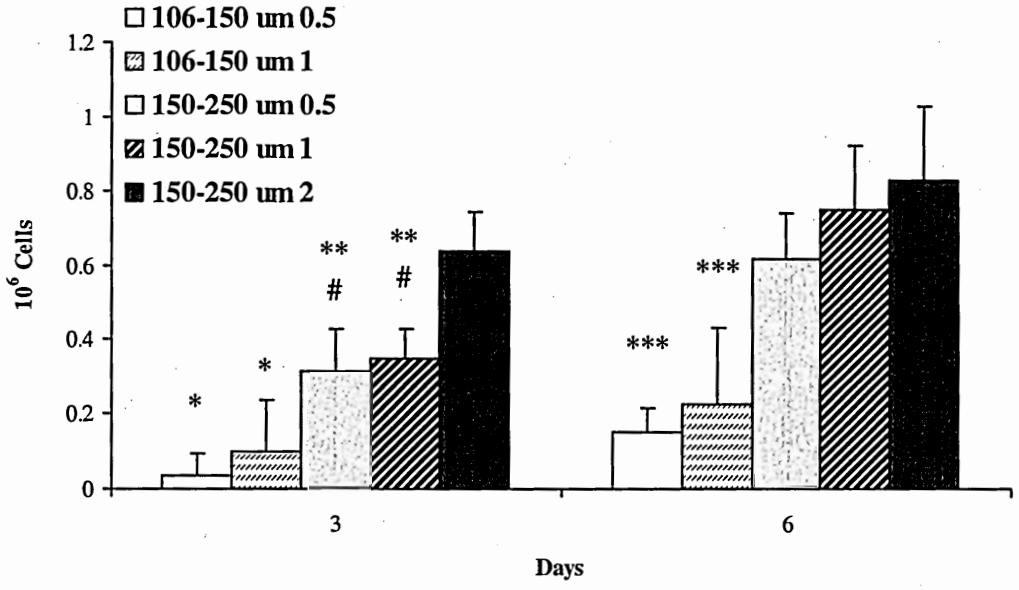

Figure 4.19 Rat Aortic SMC Proliferation on PLLA Scaffolds of Different Porosities. PLLA scaffolds were seeded with $0.5x10^6$, $1x10^6$, and $2x10^6$ cells and cultured for 6 days. Scaffolds with 106-150 μm pore size and seeded with $0.5x10^6$ and $1x10^6$ had significantly lower cell number than scaffolds seeded with the same cell number but with 150-250 μm pore size on day 3 (*) and 6 (***) ($p<0.05$). Scaffolds with 150-250 μm pore size and seeded with $0.5x10^6$ and $1x10^6$ had significantly lower cell number than same pore size scaffolds seeded with $2x10^6$ cells (**) on day 3 and compared to same pore size scaffolds seeded with $0.5x10^6$ and $1x10^6$ on day 6 (#). Data are mean ± standard deviation for N = 1 independent experiments with n = 3-5 constructs per experiment.

Significant differences were observed between the two pore sizes at day 3 and 6. Larger pore size constructs (150-250 μm) seeded with $0.5x10^6$ and $1x10^6$ cells had a higher cell number compared to smaller pore size constructs (106-150 μm) at day 3 (greater than 9- and 3-fold for each seeding density) and 6 (greater than 4- and 3-fold for each seeding density), respectively. In addition, larger pore size constructs seeded with $2x10^6$ cells had significantly higher cell number compared to the lower initial cell densities after 3 days of culture (less than 2-fold compared to $1x10^6$ seeding density and greater than 2-fold compared to $0.5x10^6$ seeding density). Finally, larger pore size constructs seeded with $0.5x10^6$ and $1x10^6$ cells increased in cell number significantly between days 3 and 6. These data indicate that 150-250 μm pore size constructs support RASMC proliferation to a greater extent than 106-150 μm pore size, and higher initial cell densities result in higher cell numbers after 3 days of culture. Therefore, 150-250 μm pore size constructs retain more cells than 106-150 μm pore size constructs.

IV.2 Tubular Scaffolds

While the static seeding experiments provided information on cell proliferation in PLLA and PCL scaffolds, bioreactor experiments require tubular scaffolds. Since both PLLA and PCL were prepared with the salt leaching technique, two different methods were used to develop tubular PLLA scaffolds that could also be employed with PCL. Tubular PLLA scaffolds were manufactured in a die under the following conditions: Temperature (T) = 338 °F, Force = 0.7 tons, Time (t) = 5 min. Since these conditions resulted in only partial melting of PLLA, the following experiments were run at higher temperature and pressure and for longer time (Temperature (T) = 350 °F, Force = 2 tons,

Time (t) = 10 min). PLLA scaffolds fabricated in initial experiments would adhere to the metal rods and aluminum slots and could not be removed from the die. To prevent this phenomenon, Teflon® tubing was inserted into the slots of the bottom plate.

However, instead of coating all metal surfaces with Teflon® to prevent adherence, another mold design was made that can be used for polymer casting and is made entirely out of Teflon®. No adherence problems were encountered with this design, but uniform distribution of salt crystals in the small 2 mm gap was difficult. The Teflon® mold was heated at 210°C and used successfully to prepare tubular PLLA scaffolds as shown in Figure 4.20.

Since static seeding experiments favored the use of PGA for bioreactor experiments, tubular PLLA and PCL scaffolds were not used in bioreactor experiments. Instead, PGA non-woven felts that were made into tubular form by suturing across the length of the scaffolds with Dexon sutures (Figure 4.20) (Niklason et al., 1999).

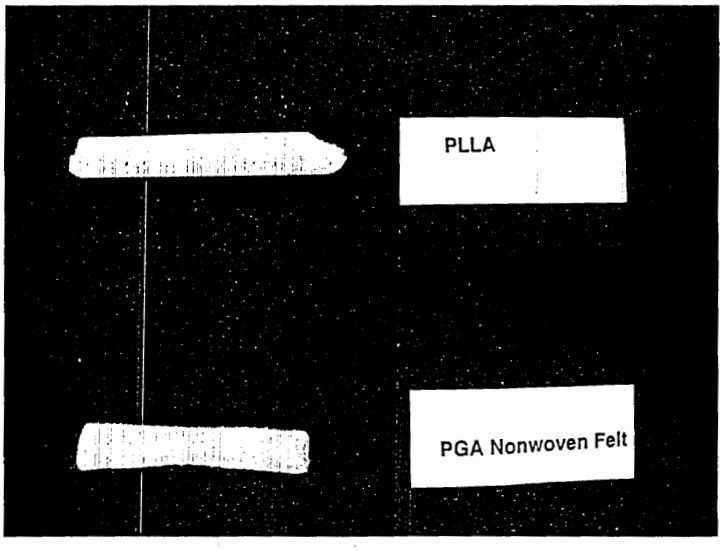

Figure 4.20 Tubular Cast PLLA and Sutured PGA Scaffolds.

IV.3 Bioreactor Experiments

All bioreactor experiments were run using EC and/or SMC seeded on PGA polymer scaffolds.

IV.3.1 Arterial Construct Development in Dual Perfusion Bioreactor

Initial experiments were run for 4-16 days to assess smooth muscle cell seeding, proliferation, and distribution in 3D scaffolds cultured in one-module bioreactors. These experiments demonstrated robust cell proliferation during the first few days of bioreactor culture leading to an over three-fold increase in cell number in 4- and 9-day experiments, and an over two-fold increase in a 16-day experiment (Figure 4.21). In Figure 4.21, initial cell number in the construct is assumed equal to the cell seeding number (100% cell seeding efficiency) since no living cells were observed in the bioreactor culture medium. Histological examination of the constructs showed uniform seeding throughout the cross-section after 4 and 9 days of growth (Figure 4.22) and collagen deposition within 9 days, mostly around the lumen. Construct cell density and matrix production were increased after 16 days of culture with cells populating the construct near the lumen and the external flow areas (Figure 4.23). These areas also contained the smallest amounts of polymer compared to the middle parts of the cross-section. Smooth muscle cells were circumferentially aligned in the external areas but were randomly oriented near the construct lumen and in the middle parts of the construct. Masson's trichrome stain for collagen was positive in the construct near the lumen and the external surfaces. Immunohistochemical staining for elastin was marginally positive in the lumen area in these short-term growth constructs (Figure 4.23). Smooth muscle cells close to the free surfaces stained positively for smooth muscle α-actin (Figure 4.23).

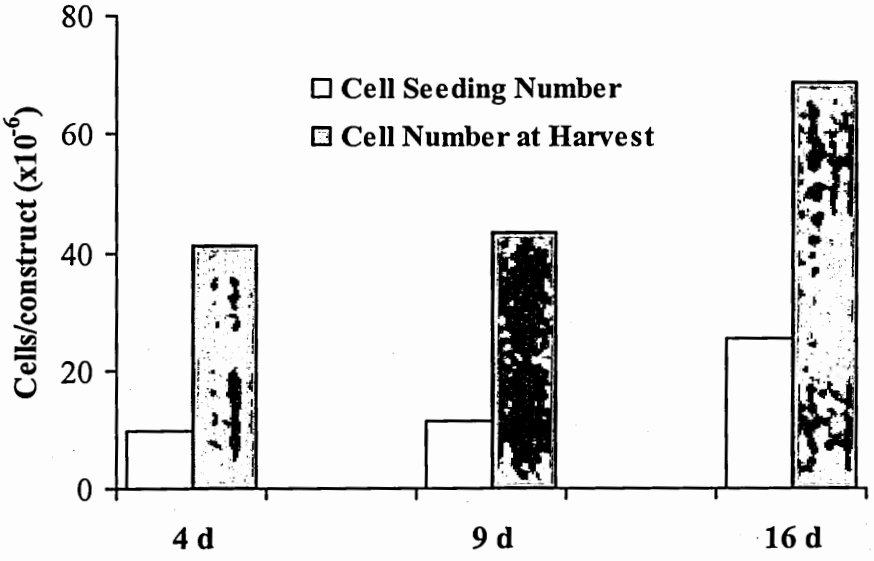

Figure 4.21 SMC Proliferation in Single-Module Bioreactors.
Number of cells/construct following seeding and growth for 4, 9 and 16 days in three separate single module bioreactors. The unshaded bar represents cell seeding number per construct assuming 100% cell seeding efficiency.

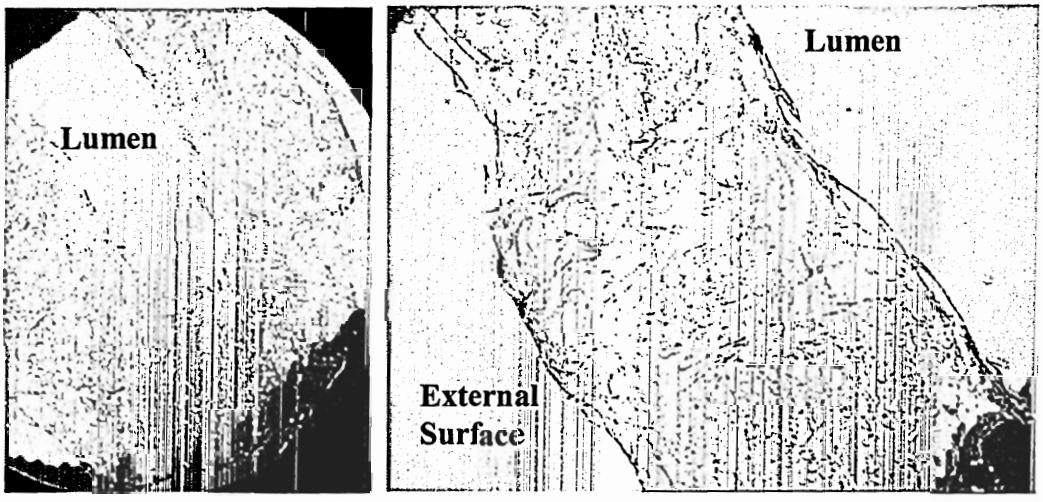

Figure 4.22 SMC Distribution in 4-Day and 9-Day Constructs.
SMC distribution across the wall of a 4-day (left) and a 9-day construct (right). Cells are stained purple (hematoxylin and eosin stain) and polymer fragments appear white. Original magnification: 4X.

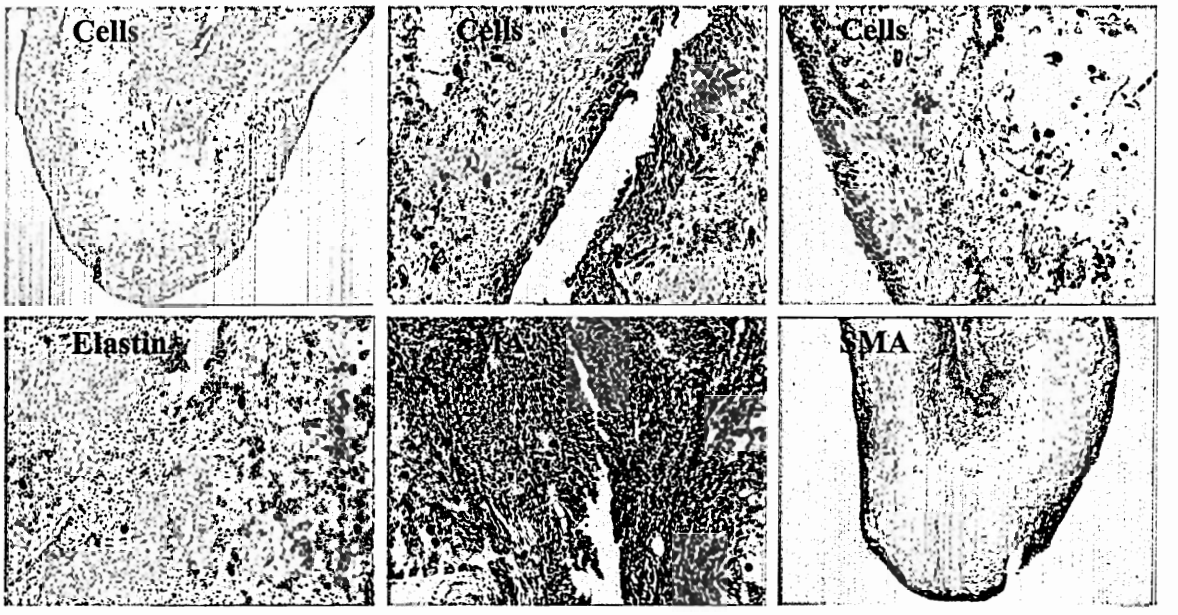

Figure 4.23 Histology of 16-Day Construct Seeded with SMC.
SMC distribution across the cross-section (top left), lumen (top middle), and external surface (top right). Tissue is stained pink (hematoxylin and eosin) and polymer fragments appear white. Immunohistochemistry for elastin (bottom left) shows staining around the lumen surface (red). Immunohistochemistry for smooth muscle α-actin (SMA) showing intense staining (red) near the lumen (bottom middle) and close to the external surface (bottom right). Original magnification: 4X (top left and bottom right), 10X (remaining panels).

Therefore, short term bioreactor experiments showed that SMC adhere to PGA during dynamic seeding, proliferate, deposit small amounts of extracellular matrix, and express differentiated function.

A three-module bioreactor experiment was performed to establish whether three constructs could be seeded simultaneously under dynamic conditions. In this experiment, all constructs were seeded with SMC through the lumen and grown for 8 days under flow. Similar smooth muscle cell proliferation was observed among all three constructs and cell number increased over two-fold as shown in Figure 4.24. Histological analysis of all three constructs showed uniform cell distribution across the wall thickness (Figure 4.25), minimal collagen production and smooth muscle α-actin expression (Figure 4.25) and no detectable elastin deposition. Therefore, reproducible results can be obtained in multi-module bioreactor experiments.

Longer-term (25-day) experiments were designed to assess bioreactor suitability for the development of functional small diameter arterial constructs in single module bioreactors. After 25 days of growth, smooth muscle cells populated the construct cross-section with higher cell density observed close to the free surfaces (Figure 4.26). High cell density regions also contained the smallest amounts of polymer fragments (Figure 4.26). Smooth muscle cells close to the external surface were circumferentially aligned and had an elongated morphology (Figure 4.26). Elastin staining and collagen deposition were most abundant in areas with high cell density such as the external surface areas of the cross-section (Figure 4.26). Elastin appeared to be deposited around polymer fibers very close to the free surfaces but not in the middle regions of the cross-sections (Figure 4.26).

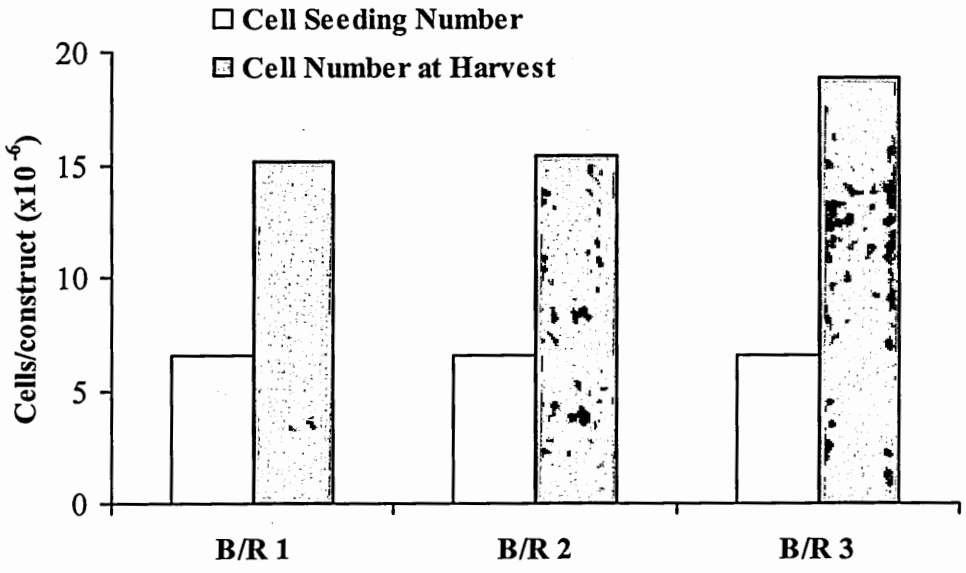

Figure 4.24 SMC Proliferation in a Three-Module Bioreactor.
Number of cells/construct in 3 separate constructs seeded in a 3-module bioreactor following 8-day culture. The unshaded bar represents cell seeding number per construct assuming 100% cell seeding efficiency.

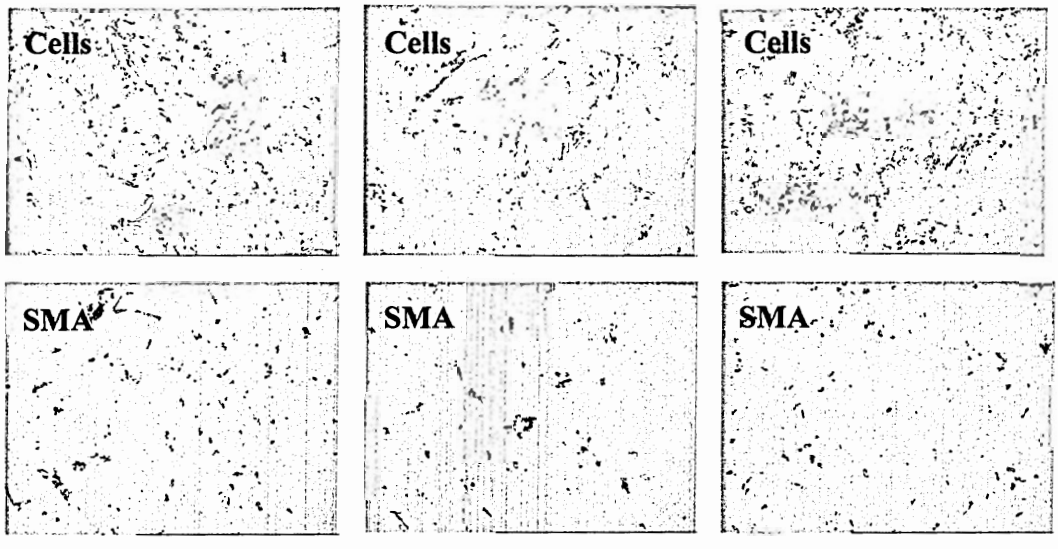

Figure 4.25 SMC Distribution and Smooth Muscle α-Actin Expression in Constructs Cultured in a Three-Module Bioreactor.
SMC distribution in three constructs cultured in a 3-module bioreactor for 8 days (top panels) and smooth muscle α-actin (SMA) expression (bottom panels). Construct 1 (left), construct 2 (middle), and construct 3 (right). Original magnification: 10X.

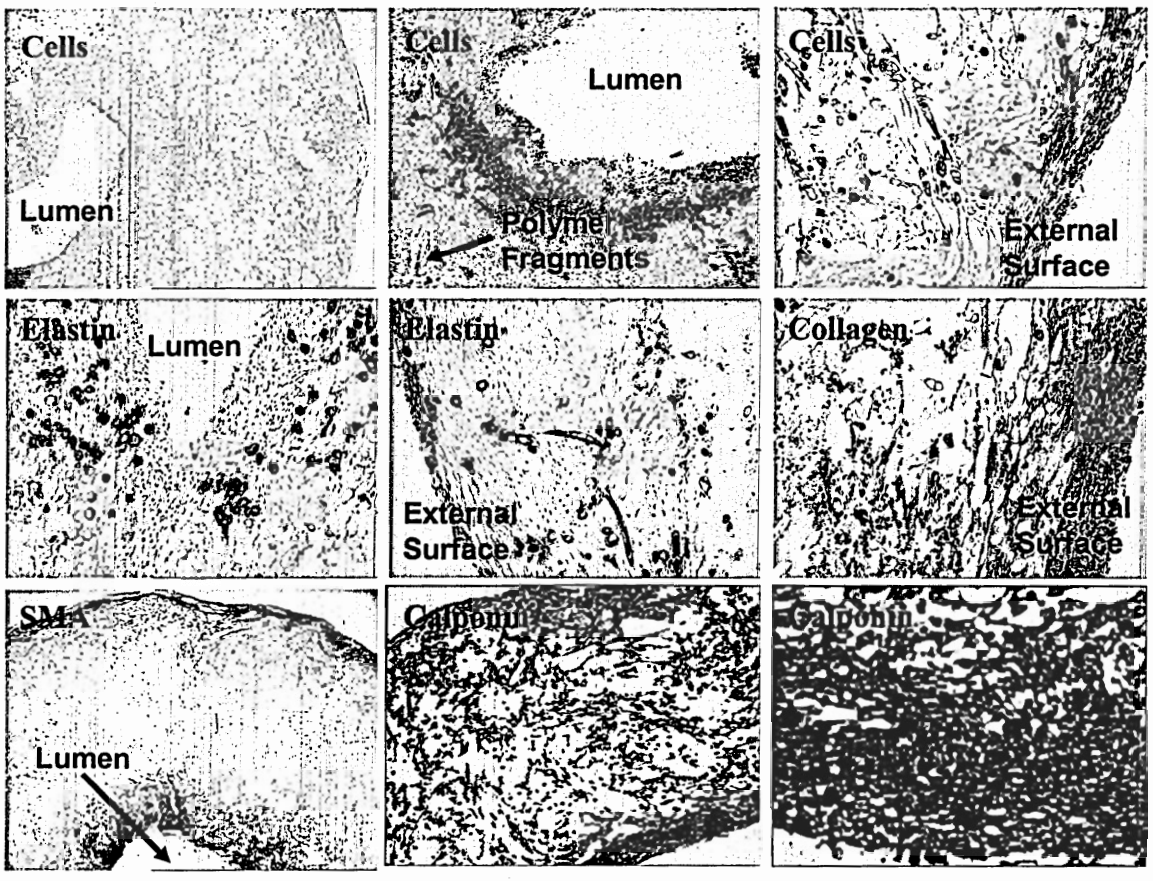

Figure 4.26 Histology of 25-Day Constructs Seeded with SMC.
SMC distribution (hematoxylin and eosin stain, H&E) of construct cross-section, lumen and external surface. Cell nuclei are stained dark blue and cytoplasm is stained pink. Polymer fragments appear white. Immunohistochemistry for elastin (red) in the lumen and external surface of the constructs. Collagen distribution (trichrome AB stain) of the construct external surface (blue). Immunohistochemistry for smooth muscle α-actin (SMA) of the construct cross-section (red), and immunohistochemistry for calponin of the construct cross-section and external surface (red). Original magnification: 4X (H&E, SMA, and calponin cross-sections), 20X (H&E external surface, elastin lumen and external surface, and collagen), and 10X (remaining panels).

Similarly, smooth muscle α-actin expression was mostly localized near the lumen and external areas of the construct wall and gradually decreased towards the middle of the sections (Figure 4.26). Smooth muscle cells populating the middle part of the construct wall stained weakly for smooth muscle α-actin (Figure 4.26).

Biochemical analysis of constructs from three separate 25-day experiments showed an over two-fold increase in cell number (assuming 100% cell seeding efficiency). Collagen and glycosaminoglycan compositions were 2% and 19% of the dry weight, respectively (Table 4.2).

Table 4.2 Biochemical Analysis of 25-Day Constructs.
Data are mean ± standard deviation for N = 3 independent experiments with n = 1 construct per experiment.

	25-day
Smooth muscle cell seeding number	47×10^6
Cell number at harvest	$(102 \pm 17) \times 10^6$
Cell number at harvest per g dry weight	$(1{,}018 \pm 48) \times 10^6$
Collagen (mg)	2 ± 1
Collagen per dry weight (%)	2 ± 1
Collagen per cell (pg)	19 ± 8
Glycosaminoglycans (GAG) (mg)	19 ± 1
GAG per dry weight (%)	19 ± 3
GAG per cell (pg)	190 ± 30

Therefore, 25-day experiments showed that SMC dynamic seeding and growth in PGA constructs in the bioreactor results in cell proliferation, SMC distribution across the construct wall, collagen, elastin, and GAG deposition, and SMC expression of contractile markers.

Culture medium samples were assayed for pH, lactate and glucose. Bioreactor medium pH varied between 6.6 and 7.4, glucose between 0.9 and 5.5 mmol/L, and lactate between 1.3 and 8.1 mmol/L, indicating that cells were metabolically active over the course of the experiments. Based on these measurements, feeding frequency was every 7 days early in culture and was increased to every 4-5 days as nutrient demand increased with cell number to maintain cell metabolic activity.

Polymer degradation was determined by scanning electron microscopy of polymer scaffolds as purchased and 25-day construct sections. Long, intact fibers were observed in the polymer scaffolds, whereas the 25-day constructs contained short and degrading polymer fragments (Figure 4.27). Polyglycolic acid cell-free scaffold initial fiber diameter was 19.1 ± 2.0 μm and it decreased to 15.7 ± 2.1 μm in smooth muscle-seeded constructs after 25 days of bioreactor culture. Smooth muscle cells were spread on the polymer fibers and had deposited extracellular matrix proteins that interconnected the individual polymer fragments (Figure 4.27). Therefore, scanning electron microscopy confirmed the biochemical data that showed cell proliferation and matrix deposition across the construct wall.

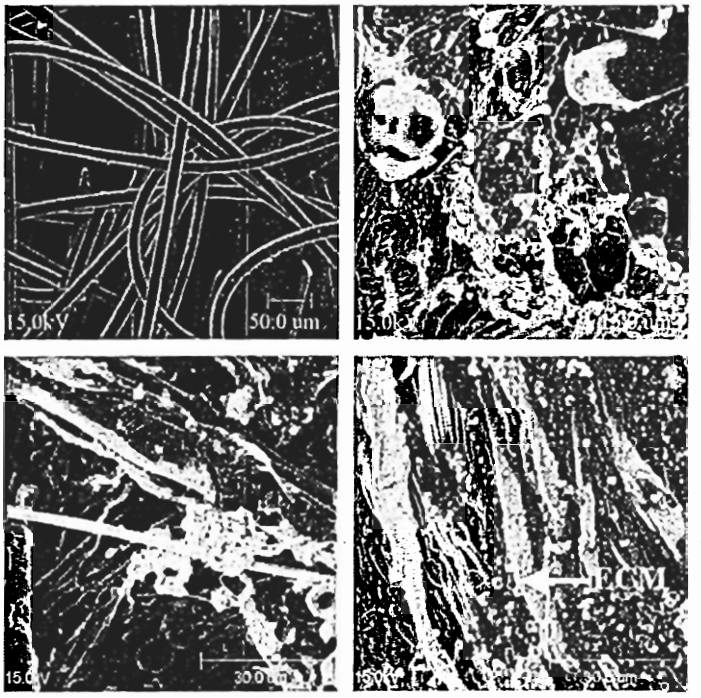

Figure 4.27 Ultrastructural Analysis of PGA Fibers and 25-Day Constructs.
PGA only fibers (top left), 25-day construct external surface (top right), 25-day construct cross-section (bottom left), extracellular matrix proteins (ECM) in 25-day cross-section (bottom right).

Inlet and outlet flow rates were monitored throughout the experiments to characterize the fluid mechanical environment in the construct lumen (Figure 4.28). Figure 4.28 shows the flow rate through the lumen and around the external surface of the constructs over the course of a 25-day experiment. Initially, lumen flow rate fluctuations were observed indicating a significant amount of cross-flow through the construct wall during the first few days of culture. These flow variations between the lumen and external flows decreased as smooth muscle cells populated the construct so that by day 10, the two flow loops were independent and flow through the construct wall appeared to be minimized. Based on these observations, wall shear stress was only calculated past day 10, when wall permeability was decreased and lumen inlet and outlet flow rates converged (Figure 4.28). Pulsatile flow values were time-averaged and used to calculate

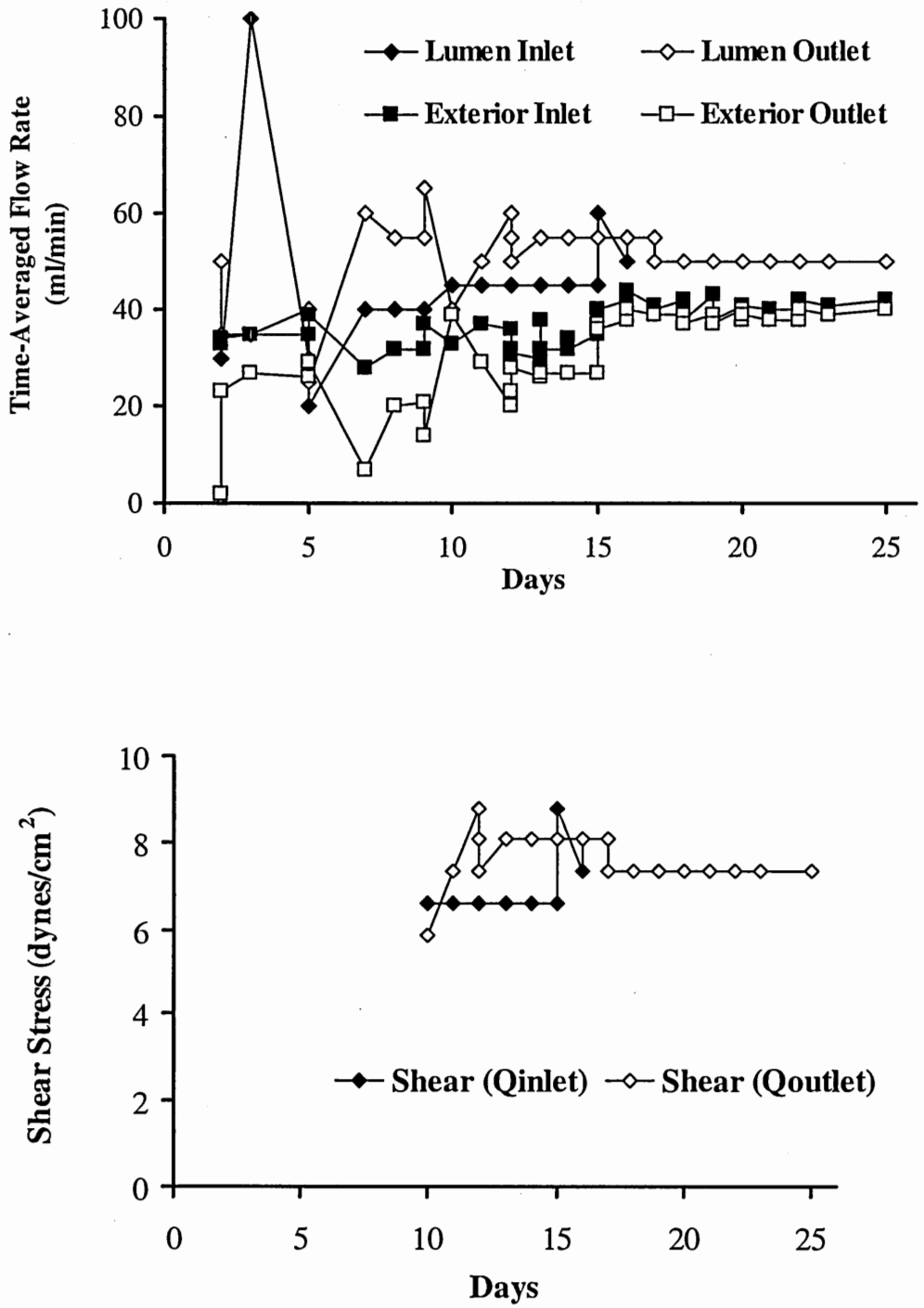

Figure 4.28 Time-Averaged Flow Rate and Wall Shear Stress in a 25-Day Construct. Time-averaged flow rate through the construct lumen and on the external surface (top), and construct wall shear stress (bottom) from a 25-day experiment. Wall shear stress is calculated past day 10, when cross-flow through the construct wall is decreased.

wall shear stress assuming Hagen-Poiseuille flow. Wall shear stress ranged from 2.2 to 8.8 dynes/cm^2 among the three experiments (Table 4.3).

Table 4.3 Lumen Diameter, Time-Averaged Flow Rate and Shear Stress in 25-Day Experiments.
Data are mean ± standard deviation for N = 3 independent experiments with n = 1 construct per experiment.

	Lumen Diameter (mm)	**Lumen Inlet Flow Rate ($\dot{Q}_{in}$) (ml/min)**	**Lumen Outlet Flow Rate ($\dot{Q}_{out}$) (ml/min)**	**Shear Stress based on $\dot{Q}_{out}$ (dynes/cm^2)**
25 days (N = 3)	2.2 ± 0.6	46.2 ± 6.3	37.1 ± 13.3	5.5 ± 3.3

IV.3.2 Dynamic Seeding of Endothelial Cells in Co-Culture Experiments

The ability of the bioreactor to support sequential seeding of smooth muscle and endothelial cells was tested in an experiment in which smooth muscle cells were grown for 13 days and endothelial cells were subsequently seeded for 24 hours to create an endothelialized arterial construct. Cell counts performed on culture medium samples using a hemocytometer following endothelialization showed 100% EC seeding efficiency. After 15 days of bioreactor culture, collagen and glycosaminoglycan content were 1% and 17% of the construct's dry weight, respectively (Table 4.4). A small number of cells with large nuclei and rounded morphology resembling endothelial cells were seen around the lumen and appeared to uniformly populate the construct lumen (Figure 4.29). Smooth muscle cells were predominantly localized near the lumen and external flow areas of the construct wall, collagen deposition was predominantly

co-localized with high cell density, but no elastin deposition was detected. Smooth muscle cells expressing smooth muscle α-actin were observed both near the lumen and in the external areas of the construct wall (Figure 4.29). Finally, lumen inlet and outlet flow rates were monitored throughout the experiment and the time-averaged outlet flow rate beyond day 10 was used to calculate wall shear stress (Table 4.5).

Scanning electron microscopy of the cross-section showed that smooth muscle cells adhered to the polymer fibers and deposited extracellular matrix proteins (Figure 4.29). The average fiber diameter was 14.6 ± 1.9 μm, which was a 23.6% decrease compared to the polymer's initial fiber diameter. Polymer fibers were not visible near the construct lumen, which was covered by a sheet of confluent cells (Figure 4.29) that resembled the appearance of native endothelium.

Table 4.4 Biochemical Analysis of 15-Day Construct.
Data are mean ± standard deviation for N = 1 independent experiments with n = 1 construct per experiment.

	15-day
Smooth muscle cell seeding number	$40x10^6$
Endothelial cell seeding number	$7x10^6$
Cell number at harvest	$129x10^6$
Cell number at harvest per g dry weight	$221x10^6$
Collagen (mg)	1
Collagen per dry weight (%)	1
Collagen per cell (pg)	35
Glycosaminoglycans (GAG) (mg)	24
GAG per dry weight (%)	17
GAG per cell (pg)	760

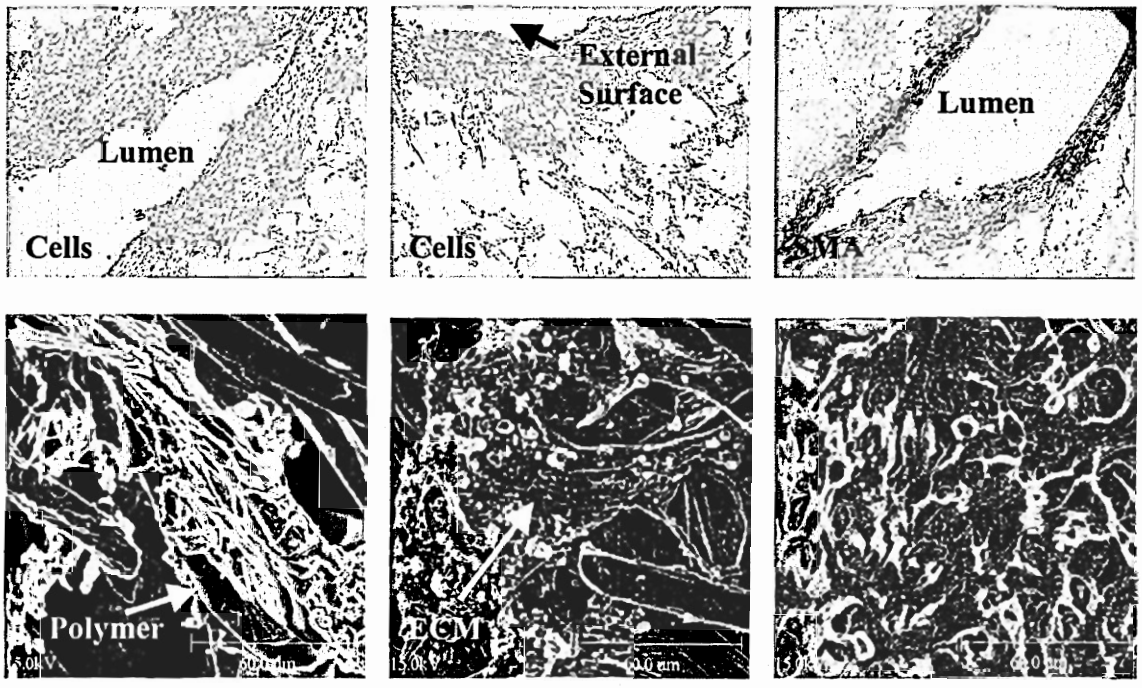

Figure 4.29 Histology and Ultrastructure of 15-Day Co-Culture Construct.
Cell distribution near the construct lumen and the external surface (hematoxylin and eosin stain) lumen. Immunohistochemistry for smooth muscle α-actin (SMA) near the construct lumen surface (red). Scanning electron microscopy of the cross-section (bottom left and middle) and the lumen (bottom right) showing cells and extracellular matrix proteins (ECM) around polymer fibers. Original magnification (top panels): 10X.

Table 4.5 Time-Averaged Flow Rate and Shear in a 15-Day Construct.

	Lumen Diameter (mm)	**Lumen Inlet Flow Rate ($\dot{Q}_{in}$) (ml/min)**	**Lumen Outlet Flow Rate ($\dot{Q}_{out}$) (ml/min)**	**Shear Stress based on $\dot{Q}_{out}$ (dynes/cm^2)**
15 days (N = 1)	2.6	36.7	31.3	2.3

IV.3.3 Single vs. Dual Seeding

This perfusion bioreactor design allows for nutrient delivery inside the constructs from the lumen and external surfaces (dual perfusion), thereby reducing nutrient diffusion distance. The same concept was used for SMC delivery to the polymer scaffold: the cell suspension was introduced through the lumen for 24 hours and a fresh cell suspension on the external surface for another 24 hours (dual seeding). This experiment was designed to test the hypothesis that dual seeding of SMC will result in uniform cell distribution across the thickness of arterial constructs compared to cell seeding only through the lumen (single seeding).

The concept of dual seeding was tested initially in a 35-day experiment. A PGA construct was seeded in a single module bioreactor through the lumen with 35.6×10^6 SMC for 24 hours and 35.3×10^6 cells on the external surface for another 24 hours. Following seeding, the construct was cultured for 35 days and medium was replaced every 5-7 days. The harvested construct had an inner diameter of 1.44 mm and very good handling ability, i.e. structural integrity (Figure 4.30). Assuming 100% cell seeding efficiency, cell number increased from 71×10^6 to 99×10^6 within 35 days (Table 4.6). Cell distribution across the construct wall was uniform and very few polymer fragments were observed (Figure 4.30). Collagen was 3% and GAG 57% of the construct's dry weight. Collagen deposition was prominent close to the lumen and external surfaces (Figure 4.31). Collagen fibrils appeared assembled and organized by the SMC around the PGA fibers. Sirius red staining showed aligned collagen fibers mostly close to the lumen surface (Figure 4.32). Amorphous elastin deposition was evident close to the lumen surface and did not appear organized by the cells after 35 days of culture (Figure 4.31).

Table 4.6 Biochemical Analysis of a 35-Day Construct.

	35-day
Smooth muscle cell seeding number	$71x10^6$
Cell number at harvest	$99x10^6$
Cell number at harvest per g dry weight	$930x10^6$
Collagen (mg)	1
Collagen per dry weight (%)	3
Collagen per cell (pg)	30
Glycosaminoglycans (GAG) (mg)	12
GAG per dry weight (%)	57
GAG per cell (pg)	610

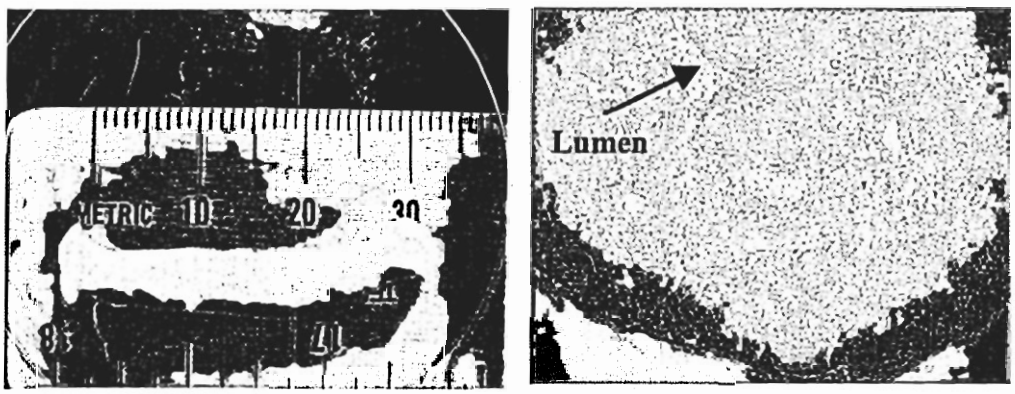

Figure 4.30 Morphology and SMC Distribution in a 35-Day Construct.
Harvested construct morphology (left) and SMC distribution across the construct's wall (hematoxylin and eosin) (right). Original magnification: 4X (right).

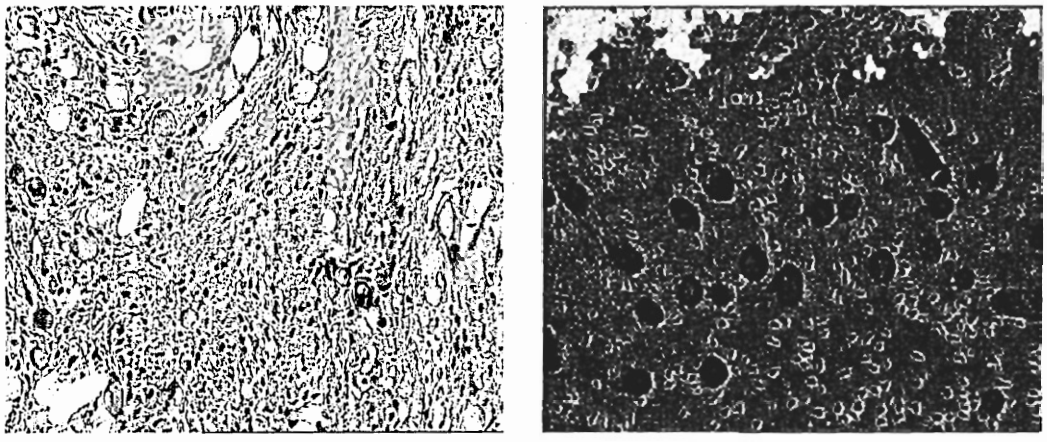

Figure 4.31 Collagen and Elastin Deposition in a 35-Day Construct.
Left: Collagen fibers are stained blue and polymer fragment appear white. Right: Elastin and polymer fragments are stained red. Cell nuclei are stained dark blue in both panels. Original magnification: 20X.

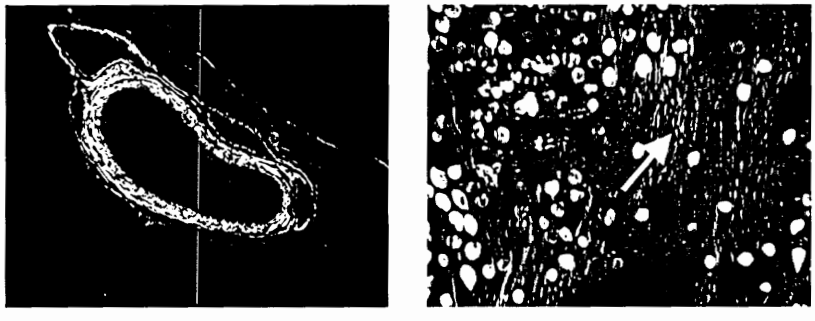

Figure 4.32 Sirius Red Stain for Aligned Collagen Fibers.
Rat kidney control sample (left) and 35-day dual-seeded construct (right). Right: Polymer fragments are bright white and aligned collagen fibers are also shown in white (white arrow). Original magnification: 4X (left) and 20X (right).

SMC were in a highly differentiated state. SMC stained positively for smooth muscle α-actin and calponin mostly close to the lumen and external surfaces of the construct (Figure 4.33). SMC monolayer cultures of the same cell population that was used to seed the polymer scaffold stained positively but weakly for smooth muscle α-actin (Figure 4.33). However, when the cells were seeded on PGA and cultured under dynamic flow conditions in the bioreactor, smooth muscle α-actin expression was upregulated and was most intense close to the lumen and external surfaces of the construct (Figure 4.33). This indicates that bioreactor culture increases smooth muscle α-actin expression by SMC compared to static culture.

Table 4.7 and Figure 4.34 summarize the cellular metabolic activity. Cells were metabolically active particularly during the first 20 days of culture. The highest metabolic activity was observed on day 20. At this time, lactate values were especially high, glucose levels were low and the lactate to glucose ratio was 18.5. The lactate to glucose ratio was greater than one at multiple time points indicating anaerobic cell culture conditions and oxygen depletion.

Table 4.8 shows the time-averaged lumen inlet and outlet flow rates and wall shear stress based on the lumen outlet flow rate. Cell proliferation appeared to occur toward the lumen resulting in significantly reduced lumen diameter, 1.44 mm, compared to the initial scaffold lumen diameter of approximately 4.5 mm.

In summary, dual seeding of SMC under the conditions described here results in uniform cell distribution across the construct wall, high metabolic activity, high tissue density, greater extracellular matrix production compared to previous experiments (Tables 4.2 and 4.4), and tissue differentiation.

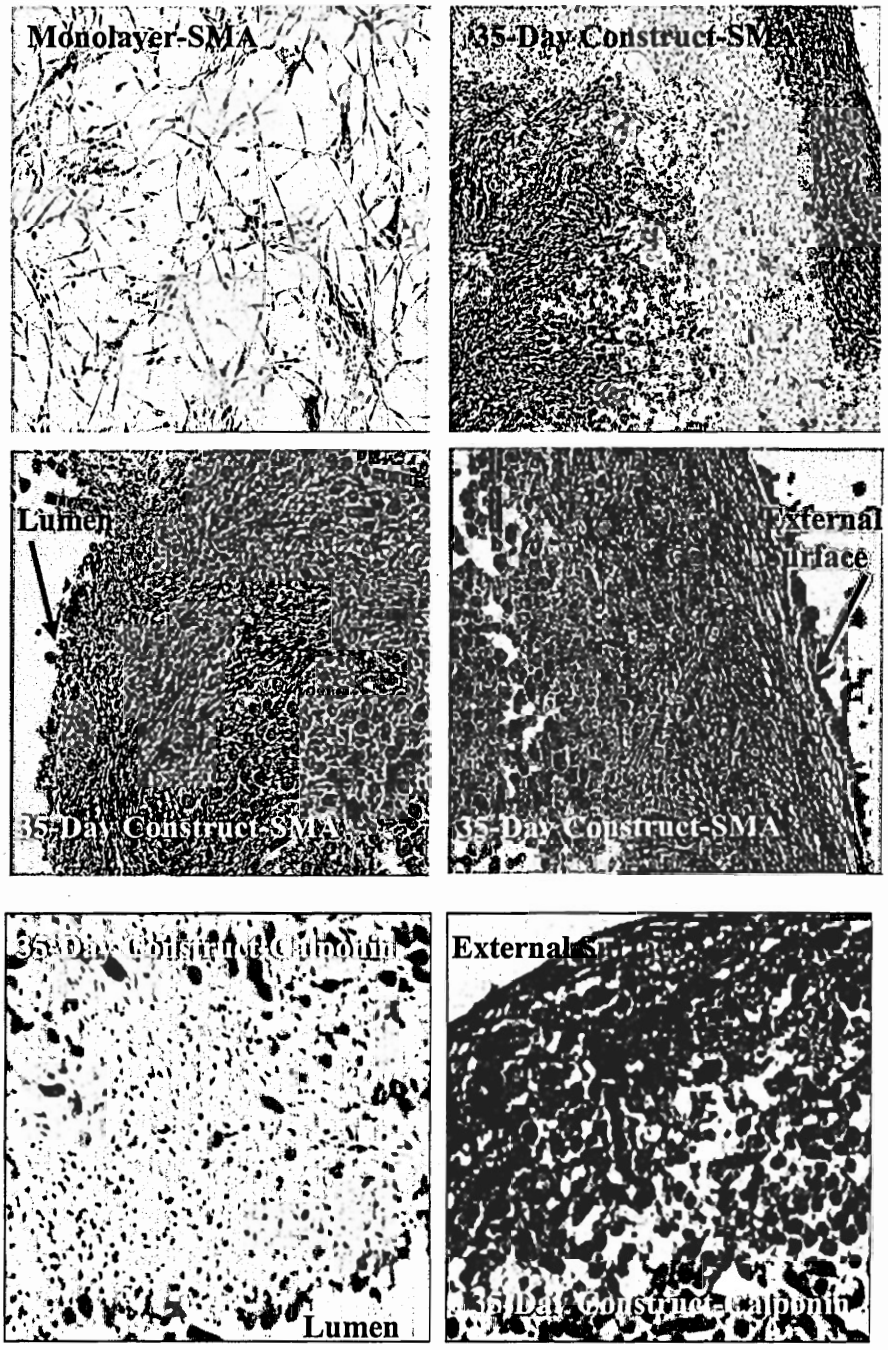

Figure 4.33 Smooth Muscle α-Actin Expression in SMC Monolayer and in a 35-Day Construct and Calponin Expression in a 35-Day Construct.
Smooth Muscle α-actin (SMA) and calponin assayed by immunohistochemistry are shown in red. SMC monolayer cultures stained positive for SMA. Cells stained positive for smooth muscle α-actin across the construct's wall, near the lumen and the external surface of a 35-day construct. Cells also stained positive for calponin near the lumen and the external surface of a 35-day construct. Original magnification: 10X.

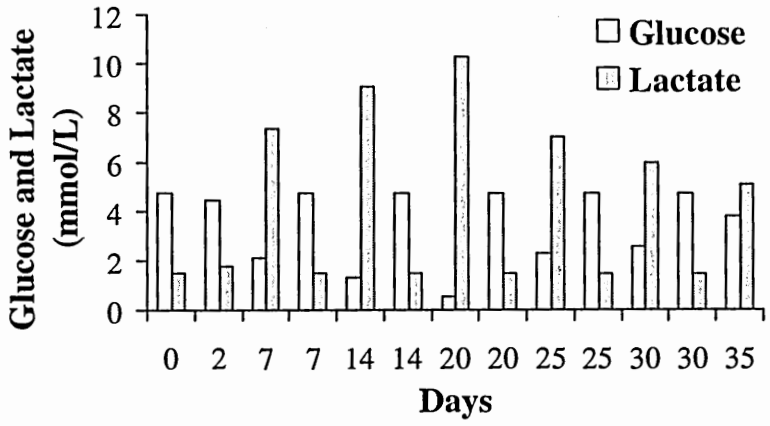

Figure 4.34 Glucose Uptake and Lactate Production in a 35-Day Construct.

Table 4.7 pH and Lactate/Glucose Ratio in a 35-Day Experiment.
pH and Lactate/Glucose values in spent medium are in bold.

Days	pH	Lactate/Glucose
0	7.40	0.3
2	**7.03**	**0.4**
7	**6.74**	**3.5**
7	7.40	0.3
14	**6.84**	**7.1**
14	7.40	0.3
20	**6.76**	**18.5**
20	7.40	0.3
25	**6.84**	**3.0**
25	7.40	0.3
30	**6.85**	**2.3**
30	7.40	0.3
35	**6.93**	**1.3**

Table 4.8 Time-Averaged Flow Rate and Wall Shear Stress in a 35-Day Experiment. Data are shown as mean ± standard deviation and are averaged for the course of 35 days.

	Lumen Diameter (mm)	**Lumen Inlet Flow Rate ($\dot{Q}_{in}$) (ml/min)**	**Lumen Outlet Flow Rate ($\dot{Q}_{out}$) (ml/min)**	**Shear Stress based on $\dot{Q}_{out}$ (dynes/cm^2)**
35 days (N = 1)	1.44	40.6 ± 6.5	41.3 ± 11.1	16.4

Based on the uniform cell distribution of the dual-seeded 35-day construct, a set of 25-day experiments was designed to directly compare the effect of SMC dual seeding on cell proliferation, distribution and extracellular matrix production. The reason for choosing 25-day experiments instead of 35 days is two-fold. First, twenty-five instead of 35-day experiments were chosen due to rapid polymer degradation within 25 days of bioreactor culture. Specifically, it was found using scanning electron microscopy that PGA fiber diameter decreased from 19.1 ± 2.0 μm to 15.7 ± 2.1 μm after 25 days and to 11.8 ± 0.7 μm after 35 days (Figures 4.27 and 4.35).

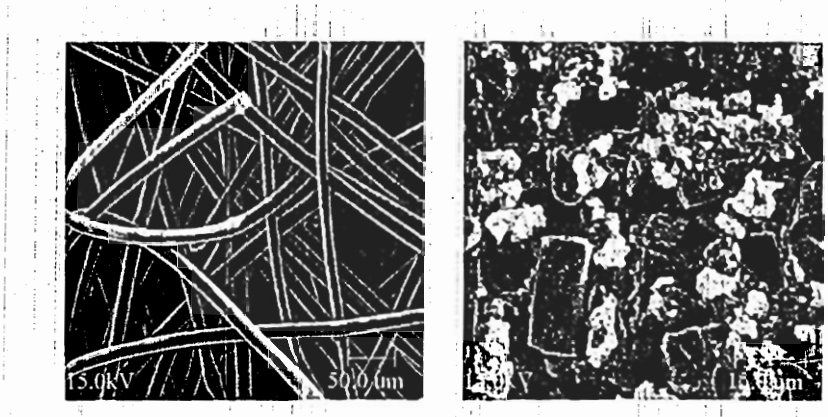

Figure 4.35 Ultrastructure of PGA and 35-Day Dual-Seeded Construct.
Left: Intact, long PGA fibers. Right: Fragmented PGA fibers surrounded by cells and extracellular matrix components in a 35-day construct.

Second, in previous 25-day experiments, SMC express contractile phenotype and contract the constructs both in the longitudinal and radial direction. As a result, constructs containing low amounts of collagen and elastin begin pulling off the bioreactor holders after approximately 24 days of culture leading to early termination of the experiments. Therefore, three 25-day experiments were run in two-module bioreactors, in which SMC suspension was introduced through the lumen only (single seeding) for 24 hours and through the lumen and the external surface (dual seeding) for another 24 hours. In both protocols, EC were seeded through the lumen after 23 days of SMC culture (late EC).

Additionally, the nutrient composition was modified compared to previous experiments by adding freshly prepared ascorbic acid to the bioreactor medium daily to increase collagen deposition and removing externally added growth factors from the medium after 10 days of culture. Short-term bioreactor experiments have demonstrated that SMC proliferation occurs within 4 to 9 days of culture with uniform cell distribution across the constructs' wall. Therefore, addition of growth factors during the first 10 days in culture is hypothesized to result in high cell number and uniform distribution across the wall, and subsequent externally added growth factor removal is aimed at stimulating extracellular matrix synthesis.

Harvested constructs had a tissue-like appearance (Figure 4.36) and dual-seeded constructs had better handling ability compared to single-seeded constructs. The lumen of harvested constructs had a teardrop shape, which is most likely due to the suture line, although the suture line cannot be detected (Figure 4.37). Cell number was $18x10^6$ in single-seeded and $16x10^6$ in dual-seeded constructs and cells per g of dry weight were

$739x10^6$ and $776x10^6$, respectively (Figure 4.38). Total collagen and GAG production were higher in dual seeding compared to single seeding: 4% versus 2% for collagen, and 44% versus 34% for GAG, respectively (Figure 4.38). However, differences in cell, collagen and GAG content were not statistically significant.

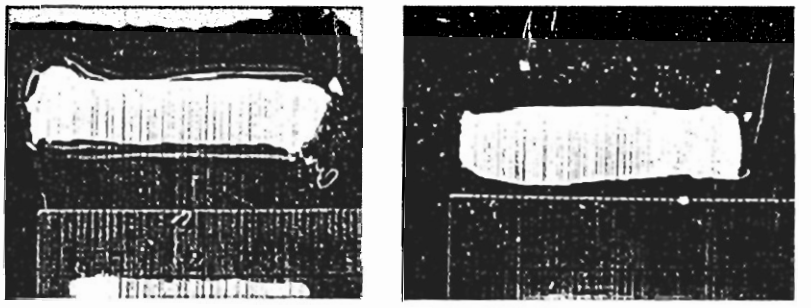

Figure 4.36 Morphology of 25-Day Single- and Dual-Seeded Constructs.
25-day single-seeded (left) and dual-seeded (right) late EC constructs. Ruler shown in cm.

These results were consistent with histological analysis that showed more collagen (Figure 4.39) and elastin deposition in dual-seeded compared to single-seeded constructs but similar cellularity (Figure 4.40). Higher tissue density and matrix content were observed near the lumen and the external surfaces of both single- and dual-seeded constructs.

Expression of SMC- and EC-specific markers was similar in constructs seeded under both protocols. SMC stained intensely for smooth muscle α-actin (Figure 4.41), calponin (Figure 4.42) and myosin heavy chain (Figure 4.43) indicating highly differentiated cell population expressing contractile phenotype. Von Willebrand factor (vWF) immunohistochemistry appeared non-specific in tissue-engineered constructs and stained polymer fibers throughout the cross-sections (Figure 4.44).

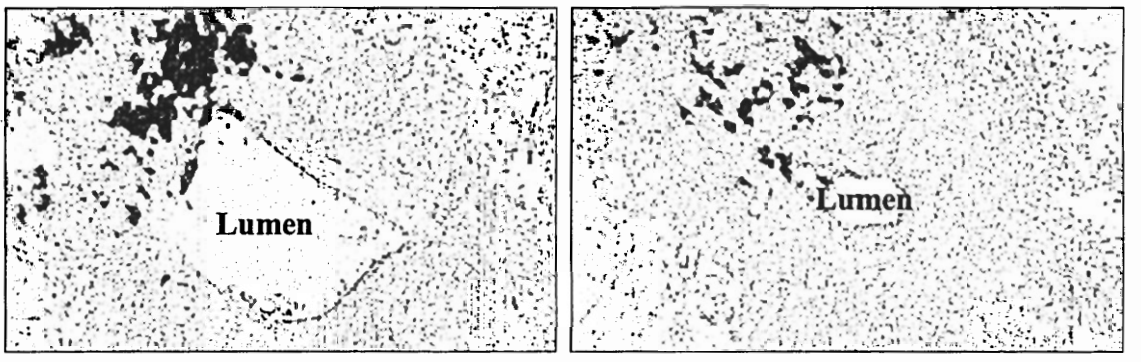

Figure 4.37 SMC and EC Distribution and Lumen Morphology in Dual-Seeded Late EC 25-Day Constructs.
Lumen is tear-shaped but cells are distributed uniformly in the circumferential direction and the suture line cannot be seen after 25-days of bioreactor culture. Original magnification: 10X (left) and 4X (right).

The vWF antibody specificity and dilution were tested by staining endothelial cell monolayers (Figure 4.44) and bovine thoracic aortas that were positive. However, staining of constructs appeared non-specific and extracellular matrix components stained positively in areas near the lumen of dual-seeded late EC constructs (Figure 4.44).

Cellular metabolic activity was monitored by measuring pH, glucose and lactate levels in the culture medium. Glucose levels were higher at all time points studied in single seeding late EC compared to dual seeding late EC experiments and lactate was lower except at 5 days (Figure 4.45). This suggests that cells in dual-seeded constructs were metabolically more active compared to single-seeded constructs. Levels of pH were similar except after 25 days, when pH in single-seeded constructs was significantly higher than that of dual-seeded constructs ($p<0.02$) (Table 4.9). Finally, lactate/glucose (L/G) ratio was higher in dual seeding late EC experiments compared to single seeding, and cells were in anaerobic conditions after 10 days of culture in both seeding protocols ($L/G > 2$).

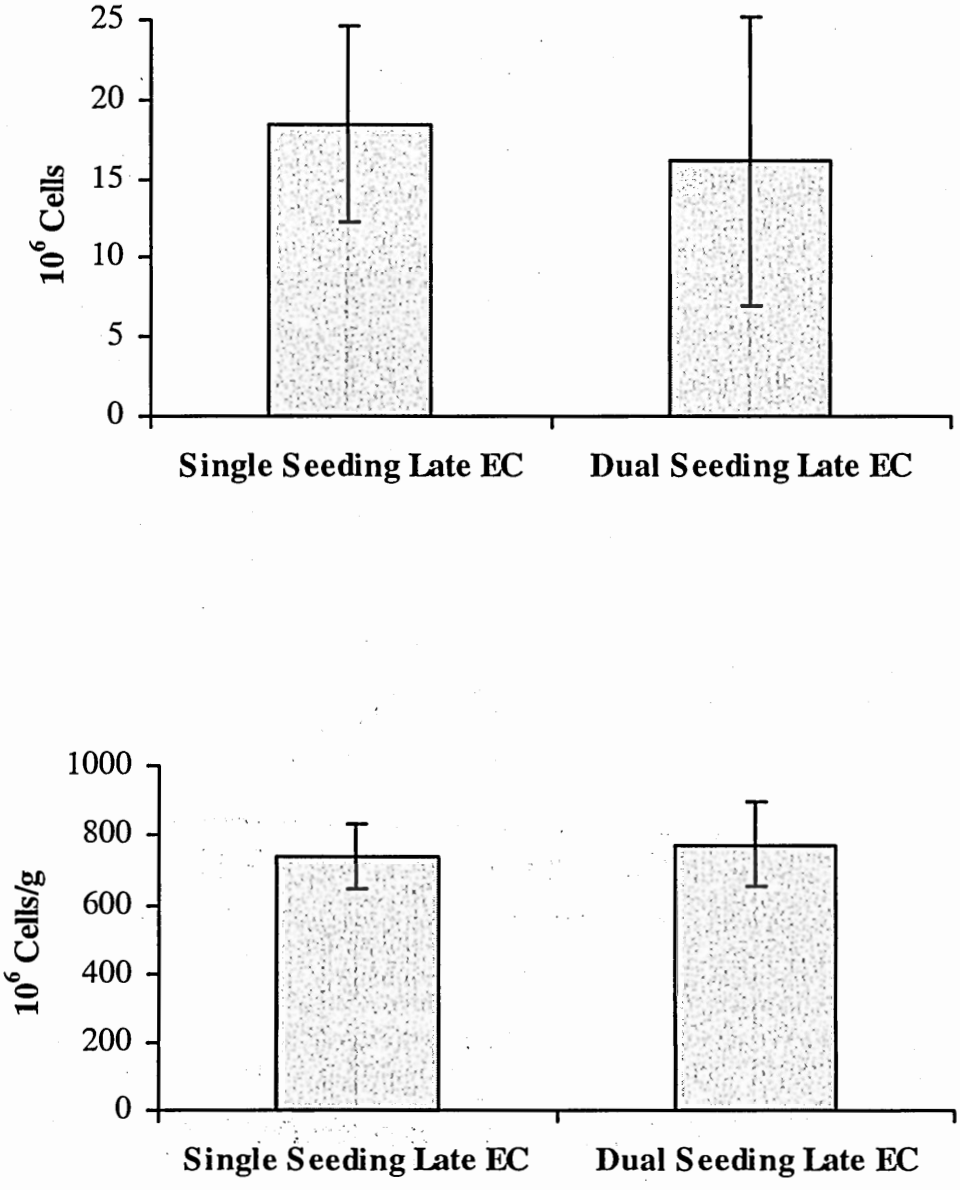

Figure 4.38 Biochemical Analysis of 25-Day Constructs Seeded with SMC Through the Lumen Only (Single Seeding) and Through the Lumen and the External Surface (Dual Seeding).
These constructs were cultured for 25 days and seeded with EC through the lumen at day 23. Data are collected from a 5 mm construct ring. Data are mean ± standard deviation for N = 3 independent experiments with n = 1-2* constructs per experiment. (*) In one single seeding experiment, one of the constructs was harvested after 15 days. In all other experiments, two constructs were cultured for 25 days in each bioreactor.

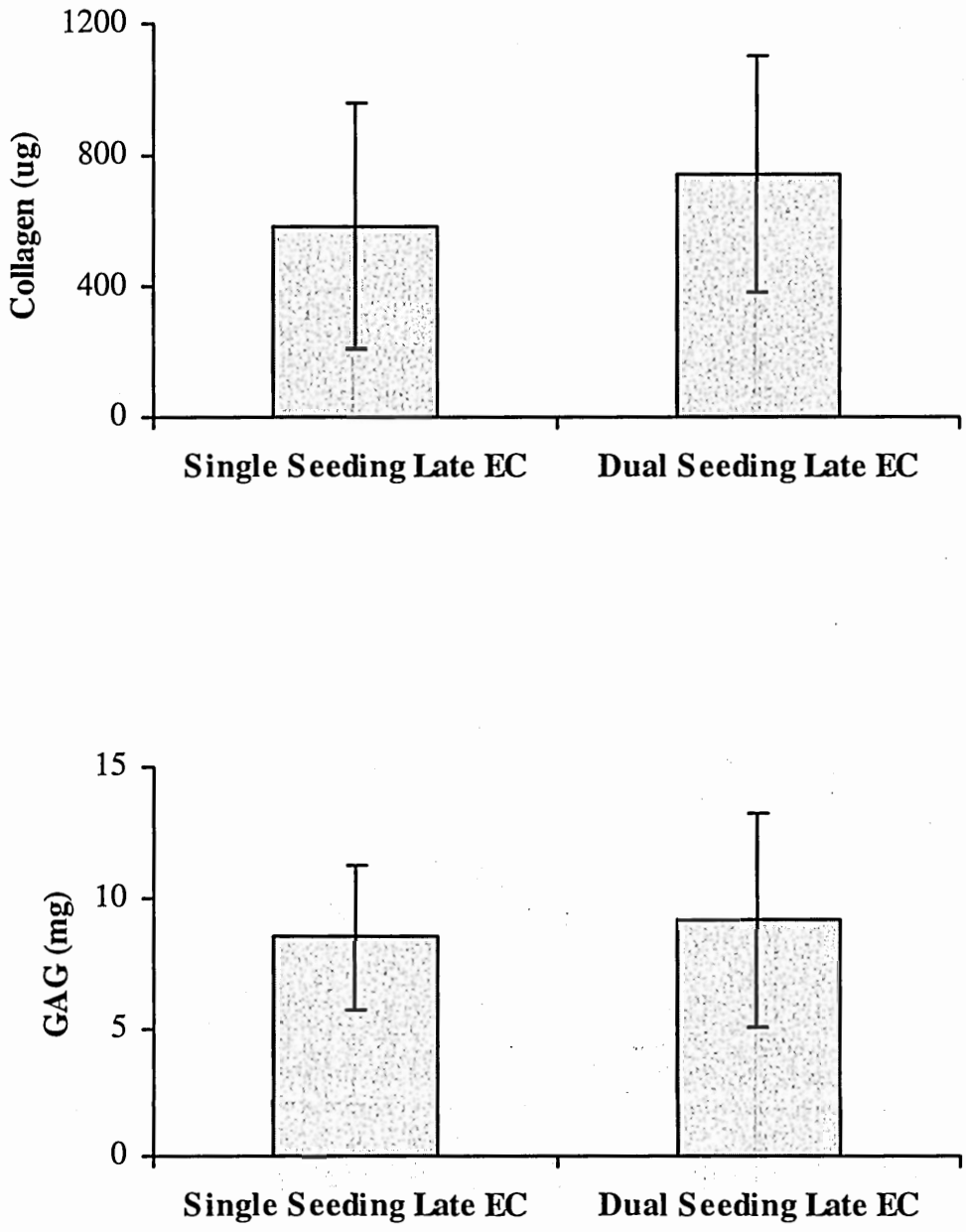

Figure 4.38 Biochemical Analysis of 25-Day Constructs Seeded with SMC Through the Lumen Only (Single Seeding) and Through the Lumen and the External Surface (Dual Seeding).
These constructs were cultured for 25 days and seeded with EC through the lumen at day 23. Data are collected from a 5 mm construct ring. Data are mean ± standard deviation for N = 3 independent experiments with n = 1-2* constructs per experiment. (*) In one single seeding experiment, one of the constructs was harvested after 15 days. In all other experiments, two constructs were cultured for 25 days in each bioreactor.

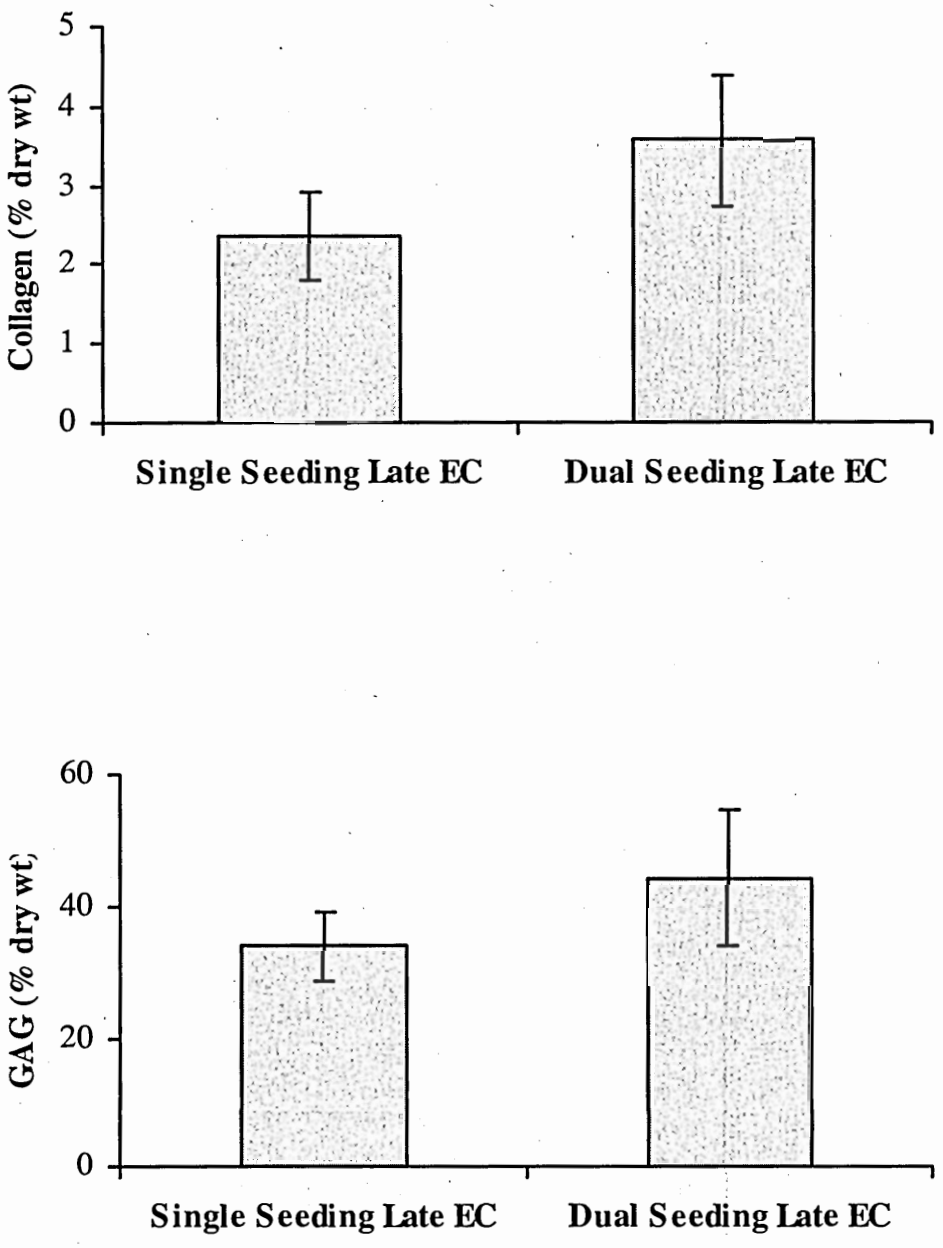

Figure 4.38 Biochemical Analysis of 25-Day Constructs Seeded with SMC Through the Lumen Only (Single Seeding) and Through the Lumen and the External Surface (Dual Seeding).
These constructs were cultured for 25 days and seeded with EC through the lumen at day 23. Data are collected from a 5 mm construct ring. Data are mean ± standard deviation for N = 3 independent experiments with n = 1-2* constructs per experiment. (*) In one single seeding experiment, one of the constructs was harvested after 15 days. In all other experiments, two constructs were cultured for 25 days in each bioreactor.

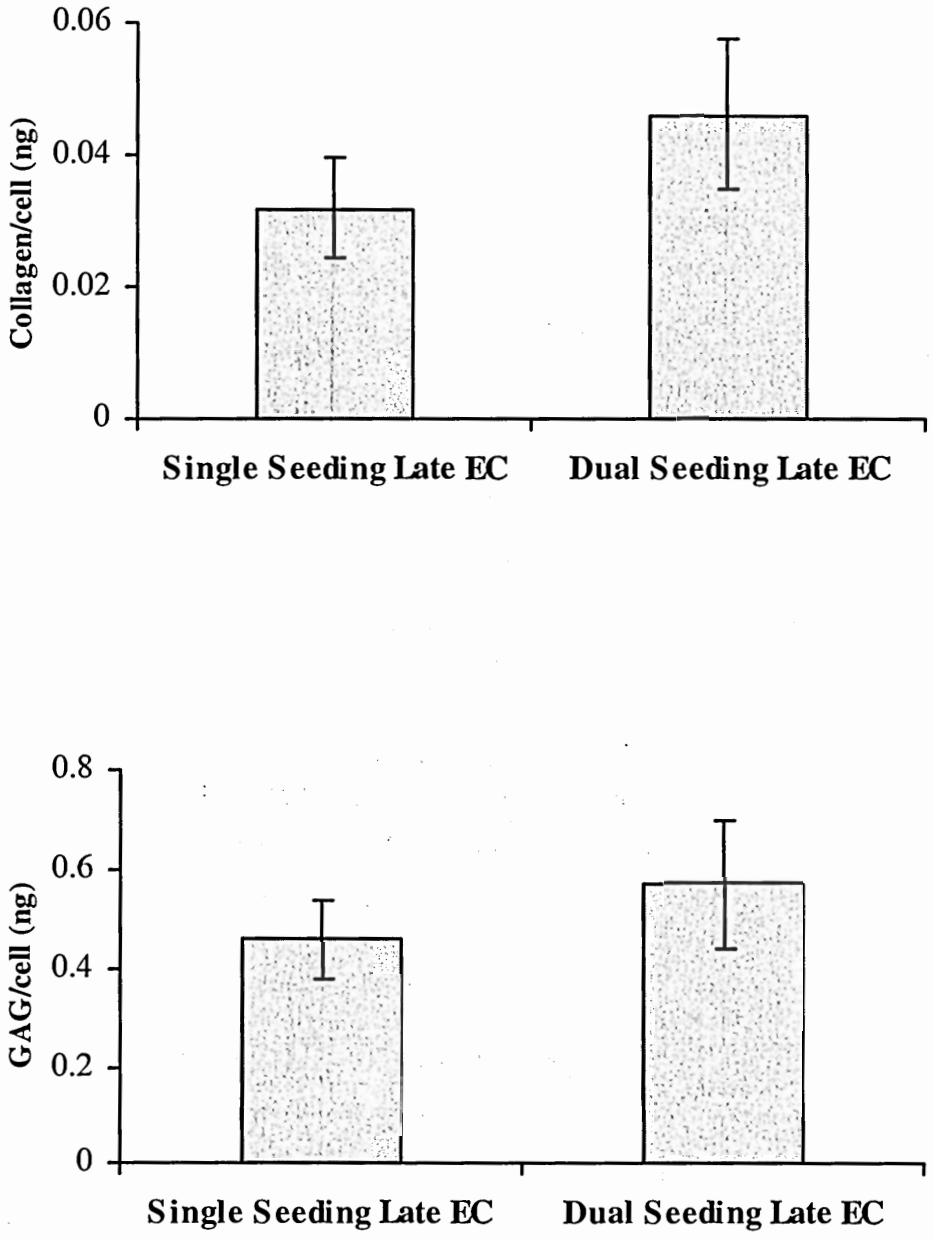

Figure 4.38 Biochemical Analysis of 25-Day Constructs Seeded with SMC Through the Lumen Only (Single Seeding) and Through the Lumen and the External Surface (Dual Seeding).
These constructs were cultured for 25 days and seeded with EC through the lumen at day 23. Data are collected from a 5 mm construct ring. Data are mean ± standard deviation for N = 3 independent experiments with n = 1-2* constructs per experiment. (*) In one single seeding experiment, one of the constructs was harvested after 15 days. In all other experiments, two constructs were cultured for 25 days in each bioreactor.

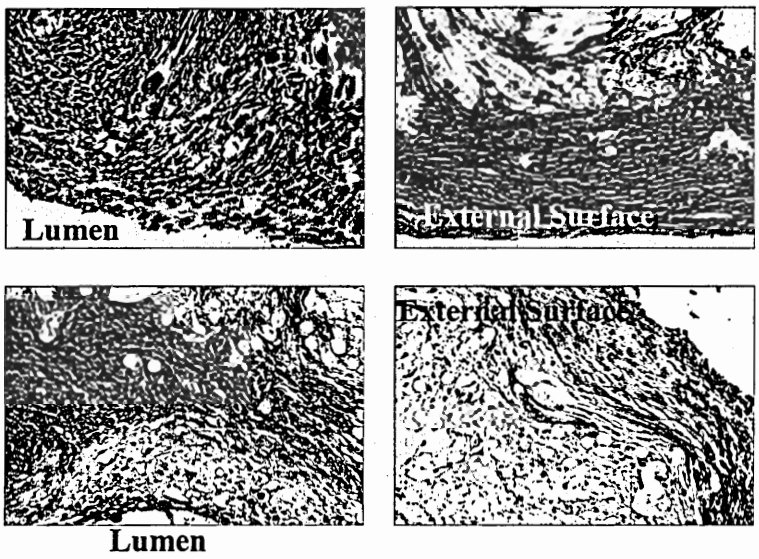

Figure 4.39 Collagen Deposition in Single-Seeded and Dual-Seeded Late EC Constructs. Collagen deposition in the lumen and external surface of 25-day single-seeded (top) and dual-seeded (bottom) constructs. Collagen is stained blue. Original magnification: 20X.

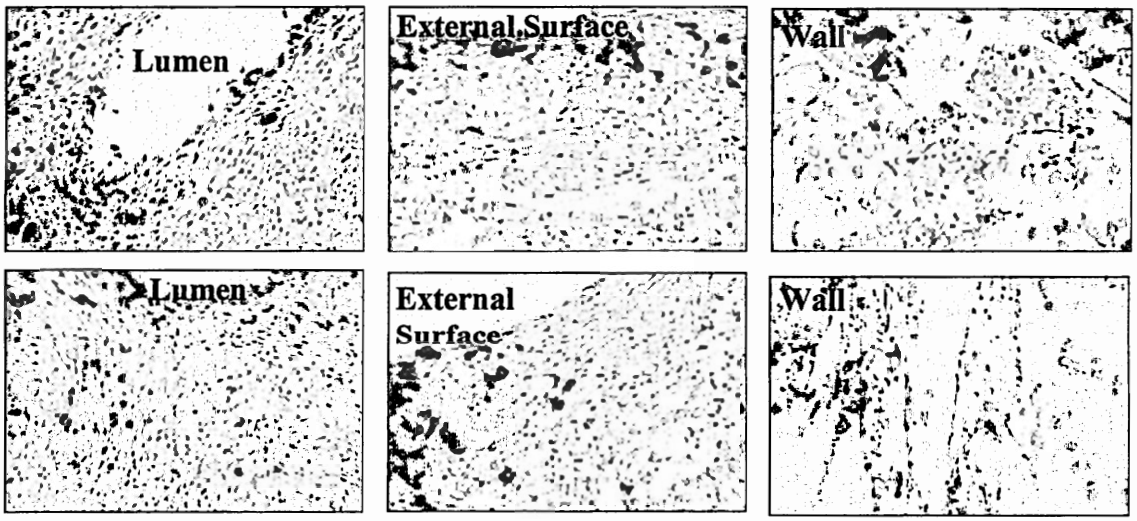

Figure 4.40 SMC and EC Distribution in Single-Seeded and Dual-Seeded Late EC 25-Day Constructs.
Cell distribution (hematoxylin and eosin stain) near the lumen, the external surface and the wall of single-seeded (top) and dual-seeded (bottom) 25-day constructs. Original magnification: 10X.

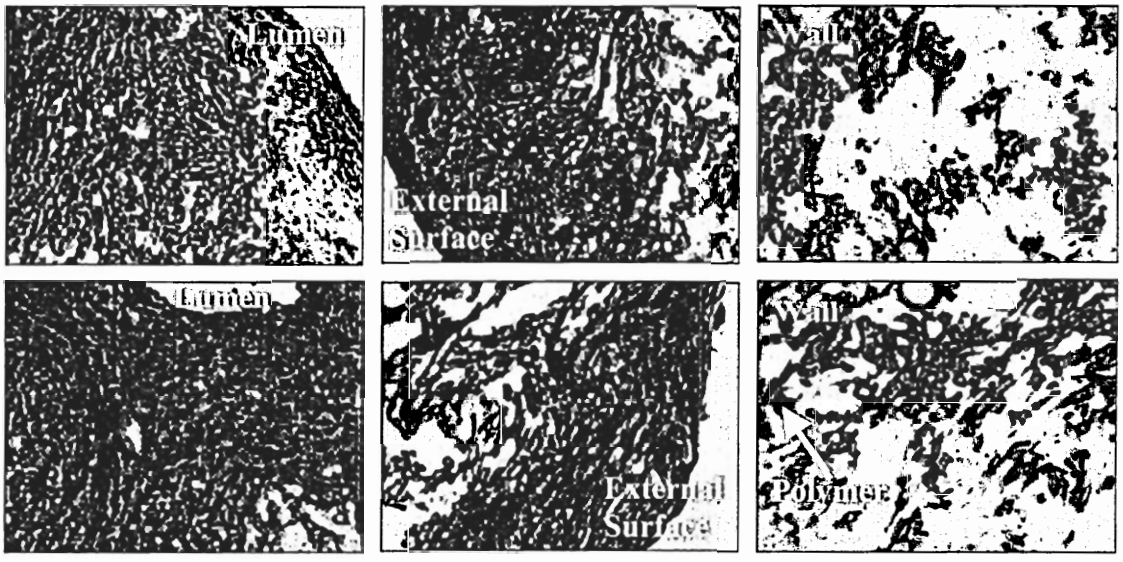

Figure 4.41 Smooth Muscle α-Actin Expression in Single-Seeded and Dual-Seeded Late EC Constructs.
Positive staining (red) is observed near the lumen, external surface and in the wall of single-seeded (top) and dual-seeded (bottom) 25-day constructs. White arrow shows residual polymer fragments. Original magnification: 10X.

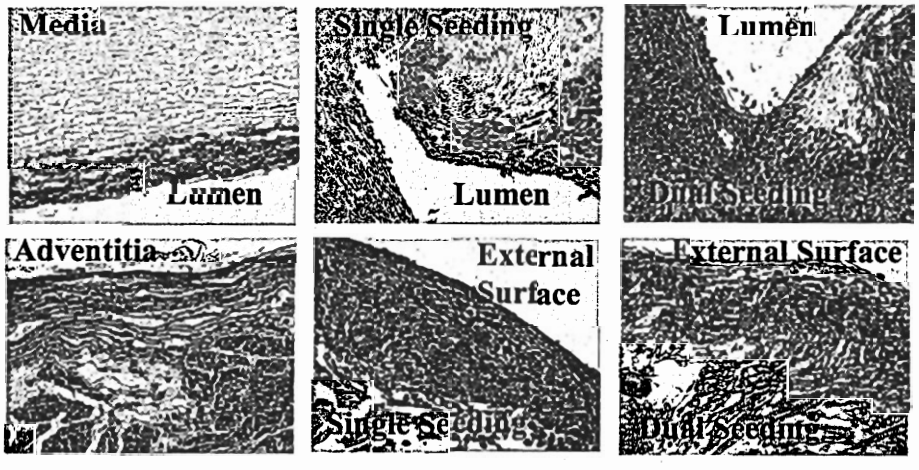

Figure 4.42 Calponin Expression in Bovine Thoracic Aorta, Single-Seeded and Dual-Seeded Late EC 25-Day Constructs.
Calponin expression (red) in media layer and adventitia of a bovine thoracic aorta and near the lumen and external surface of single-seeded and dual-seeded 25-day constructs. Original magnification: 10X.

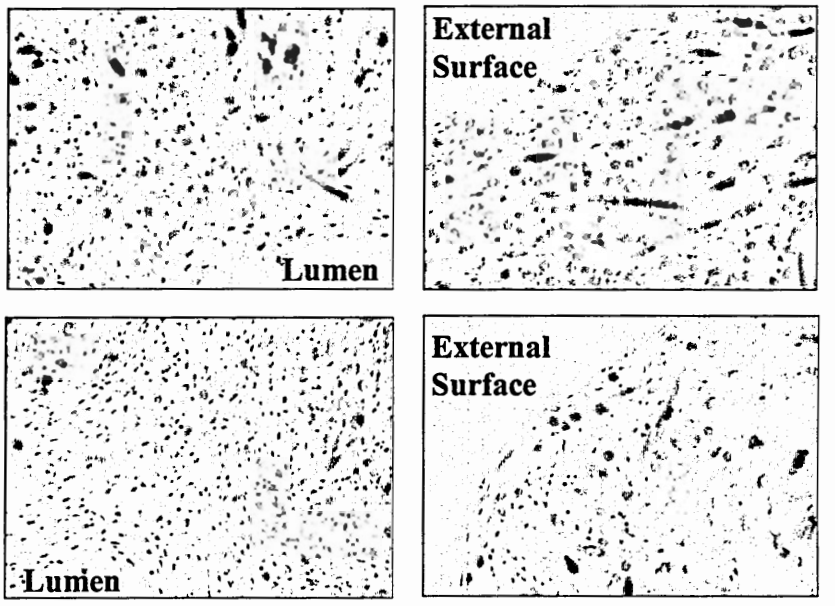

Figure 4.43 Myosin Heavy Chain Expression in Single- and Dual-Seeded Late EC 25-Day Constructs.
Myosin heavy chain is expressed by cells (red) near the lumen and the external surface of single-seeded (top) and dual-seeded (bottom) 25-day constructs. Polymer fragments near the free surfaces are also stained red. Original magnification: 10X.

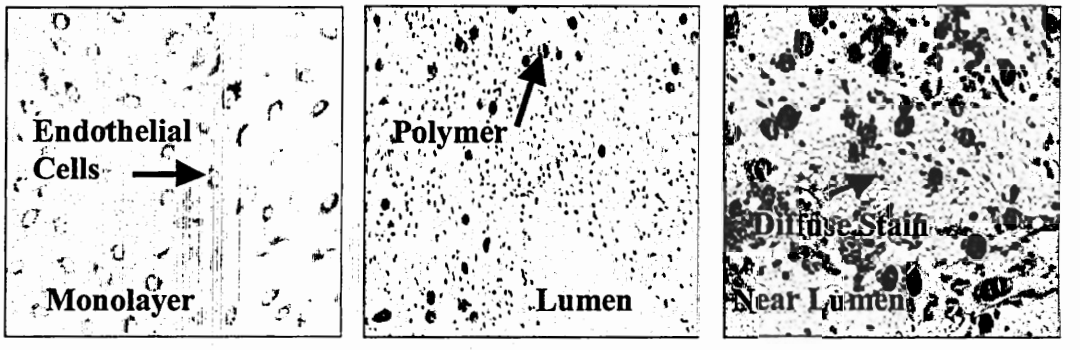

Figure 4.44 Von Willebrand Factor Expression in Microvascular Dermal Endothelial Cells and Single- and Dual-Seeded Late EC 25-Day Constructs.
Von Willebrand factor is expressed (brown color) by endothelial cells. However, polymer fragments also stained positive throughout the cross-section of both single- (middle panel) and dual-seeded constructs. A diffuse stain pattern was observed near the lumen surface of dual-seeded constructs (right). Original magnification: 10X (left and middle) and 20X (right).

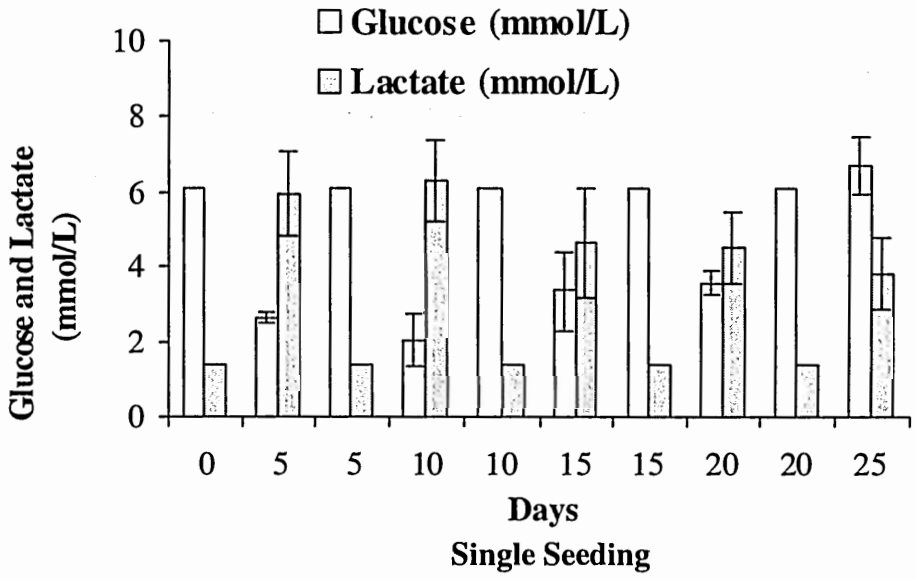

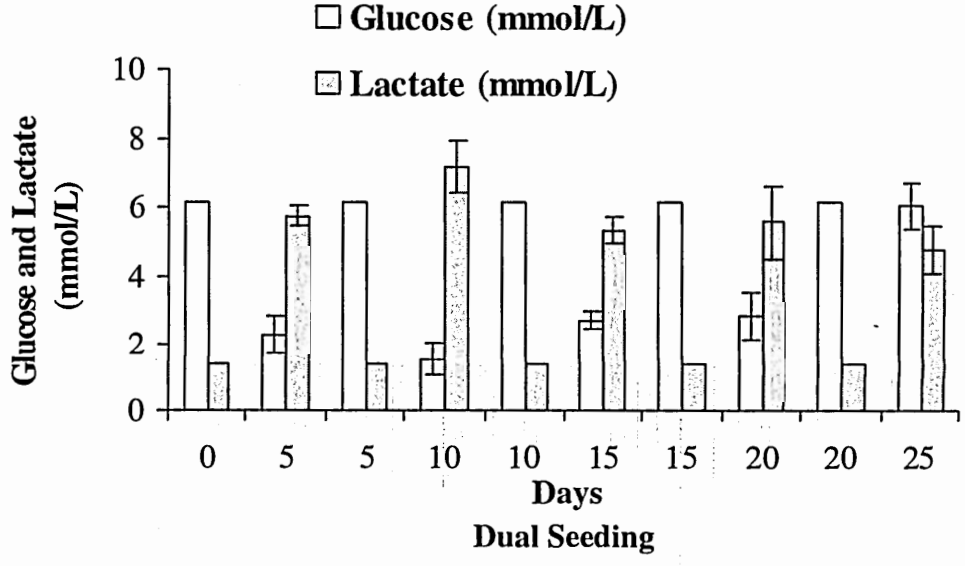

Figure 4.45 Glucose Uptake and Lactate Production in Single Seeding and Dual Seeding Late EC Experiments.
Data are mean ± standard deviation for N = 3 independent experiments with n = 1-2* constructs per experiment. (*) In one single seeding experiment, one of the constructs was harvested after 15 days. In all other experiments, two constructs were cultured for 25 days in each bioreactor.

Scanning electron micrographs showed that the lumen surface of single-seeded constructs was not fully populated with cells as PGA fibers were exposed on the surface (Figure 4.46). In contrast, the lumen of dual-seeded late EC constructs was covered with cells (Figure 4.46), and the cross-section was dense with extracellular matrix proteins (Figure 4.47).

Flow rates through the construct lumen and on the external surface were monitored throughout the experiments and used to calculate wall shear stress (Table 4.10). Lumen diameter of single-seeded constructs was smaller than the diameter of dual-seeded constructs. This could be because SMC are seeded through the construct lumen for 48 hours resulting in higher cell density near the lumen surface. Figure 4.48 shows a representative time-averaged flow rate distribution of the inlet and outlet flows of a two-module bioreactor that was run under the dual seeding late EC protocol. The external outlet flow rate was initially high due to the constructs' high porosity, and was subsequently decreased as constructs became less porous. As a result, lumen inlet and outlet flow rates do not match initially because medium flows through the construct wall to the external space, but there is much closer agreement with time.

However, in some experiments, another flow rate pattern was observed (Figure 4.49), in which lumen outlet flow rate of one or both constructs decreased towards the end of the experiment and external outlet flow rate was increased. These results were observed in constructs with smaller (< 2 mm) lumen diameter, indicating that flow resistance was increased to the point of creating another flow outlet through the construct wall and into the external space of the bioreactor.

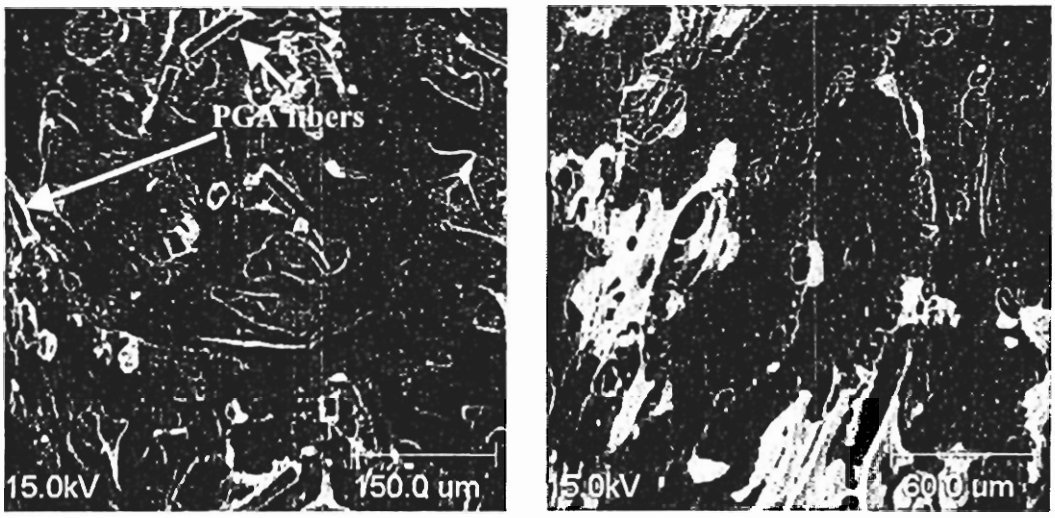

Figure 4.46 Ultrastructure of Single-Seeded and Dual-Seeded Late EC Constructs. Few PGA fibers are exposed on the lumen surface of single-seeded constructs (left), whereas no PGA fibers can be seen in the lumen surface of dual-seeded constructs (right).

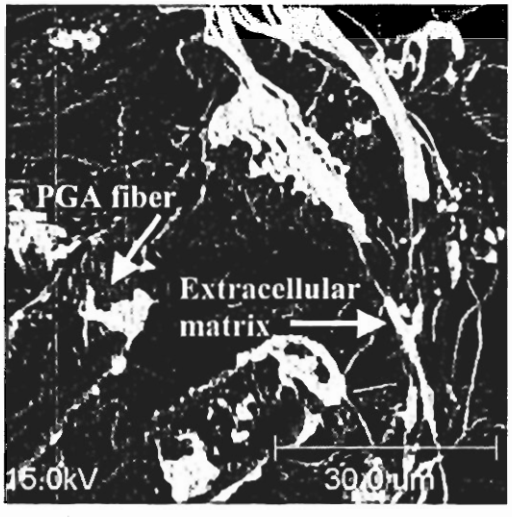

Figure 4.47 Ultrastructure of the Cross-Section of Dual-Seeded Late EC Constructs. White arrows show PGA polymer fragments and extracellular matrix fibers across the polymer scaffold.

Table 4.9 pH and Lactate/Glucose Ratio in Single and Dual Seeding Late EC Experiments.
Lactate/Glucose and pH values in spent medium are shown in bold. Data are mean ± standard deviation for N = 3 independent experiments with n = 1-2* constructs per experiment. (*) In one single seeding experiment, one of the constructs was harvested after 15 days. In all other experiments, two constructs were cultured for 25 days in each bioreactor.

	pH		Lactate/Glucose	
Days	**Single Seeding Late EC**	**Dual Seeding Late EC**	**Single Seeding Late EC**	**Dual Seeding Late EC**
0	7.40	7.40	0.2	0.2
5	**6.72 ± 0.04**	**6.75 ± 0.05**	**2.3 ± 0.2**	**2.5 ± 0.3**
5	7.40	7.40	0.2	0.2
10	**6.70 ± 0.04**	**6.64 ± 0.02**	**3.4 ± 0.8**	**4.7 ± 1.1**
10	7.40	7.40	0.2	0.2
15	**6.73 ± 0.08**	**6.73 ± 0.02**	**1.5 ± 0.4**	**2.0 ± 0.1**
15	7.40	7.40	0.2	0.2
20	**6.70 ± 0.05**	**6.67 ± 0.08**	**1.3 ±0.2**	**2.0 ± 0.5**
20	7.40	7.40	0.2	0.2
25	**6.88 ± 0.04**	**6.78 ± 0.01**	**0.6 ± 0.1**	**0.8 ± 0.1**

In summary, dual-seeded constructs contained more extracellular matrix proteins as shown in biochemical and histological analysis and more metabolically active cells compared to single-seeded constructs. However, SMC distribution was similar in both protocols and was not affected by seeding the external surface of the scaffolds.

Table 4.10 Time-Averaged Flow Rate and Wall Shear Stress in Single and Dual Seeding Late EC 25-Day Experiments.
Data are mean ± standard deviation for N = 3 independent experiments with n = 1-2* constructs per experiment. (*) In one single seeding experiment, one of the constructs was harvested after 15 days. In all other experiments, two constructs were cultured for 25 days in each bioreactor.

	Lumen Diameter (mm)	**Lumen Inlet Flow Rate ($\dot{Q}_{in}$) (ml/min)**	**Lumen Outlet Flow Rate ($\dot{Q}_{out}$) (ml/min)**	**Shear Stress based on $\dot{Q}_{out}$ (dynes/cm^2)**
Single Seeding Late EC (N = 3 and n = 2*)	2.3 ± 0.5	35.5 ± 7.9	31.1 ± 11.4	3.1
Dual Seeding Late EC (N = 3 and n = 2)	3.0 ± 0.7	44.0 ± 11.6	34.8 ± 11.8	1.6

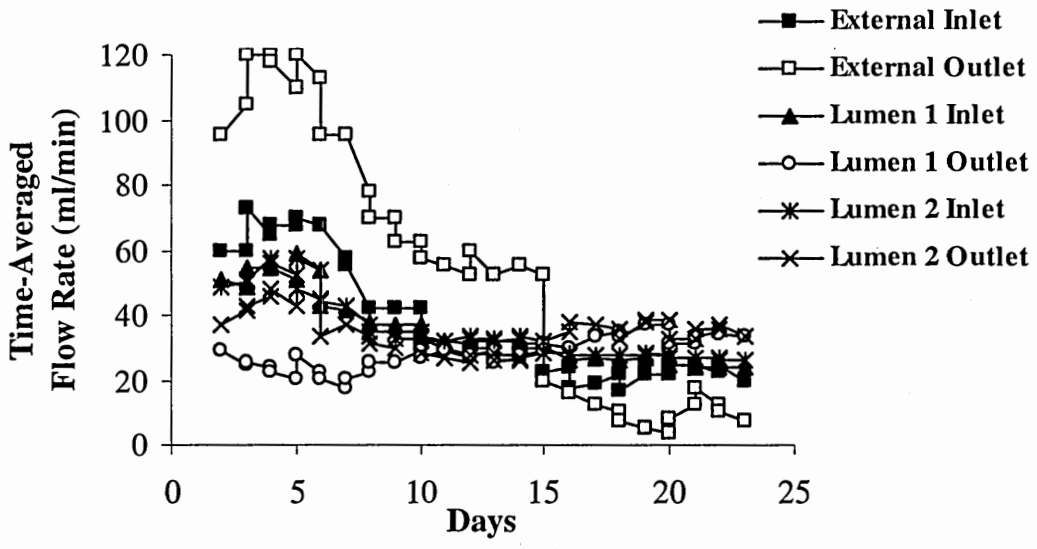

Figure 4.48 Time-Averaged Flow Rate of a Dual Seeding Late EC Experiment.
Flow rates were monitored at the lumen inlet and outlet of each construct and at the inlet and outlet of the bioreactor external space flow loop.

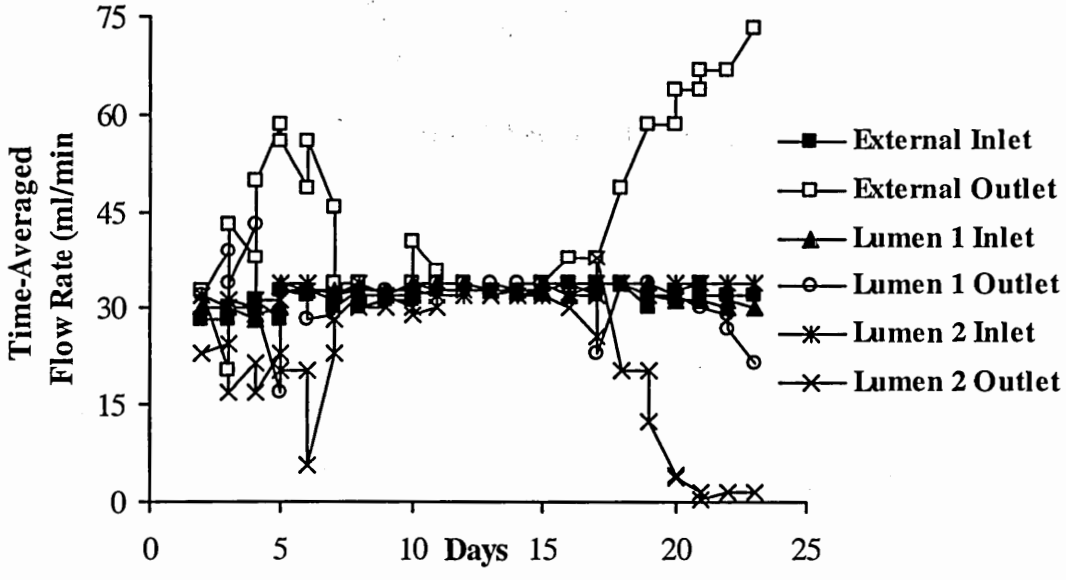

Figure 4.49 Time-Averaged Flow Rate of a Single Seeding Late EC Experiment.
Flow rates were monitored at the lumen inlet and outlet of each construct and at the inlet and outlet of the bioreactor external space flow loop.

IV.3.4 Seeding Efficiency

The seeding efficiency of the two different SMC seeding protocols was measured in two-module bioreactor experiments. SMC were seeded according to single seeding and dual seeding protocol as previously described in Chapter III, medium cell counts were done after 24 and 48 hrs and the constructs were harvested after 48 hrs and analyzed for DNA content. It was found that based on the syringe medium (50 ml volume per construct) cell counts, high cell seeding efficiencies were observed for both protocols (Figure 4.50). However, the seeding efficiency based on cells present in the constructs was 13% in single seeding and 12% in dual seeding (Figure 4.50).

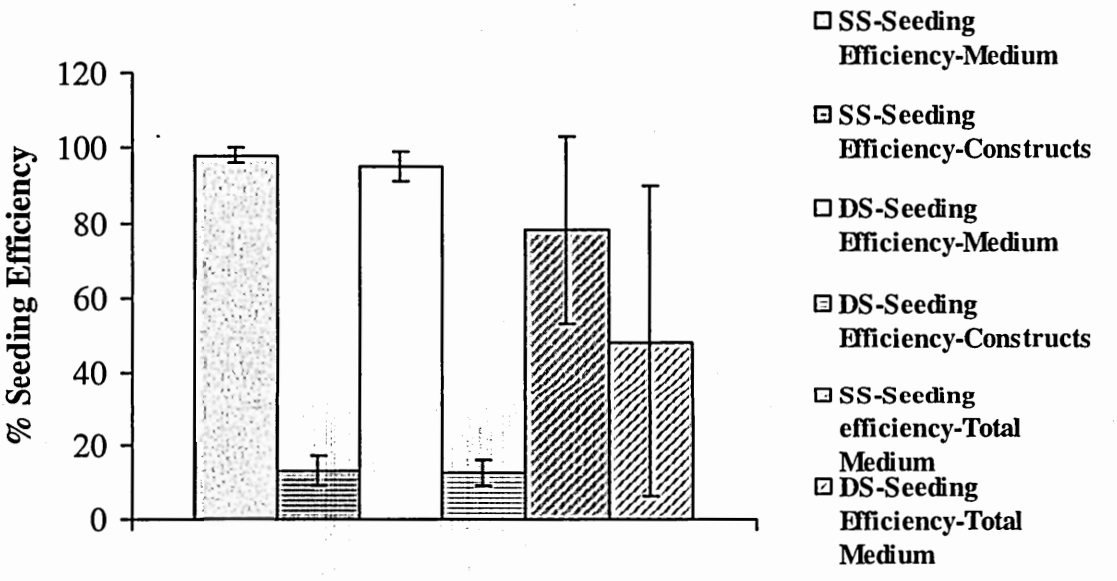

Figure 4.50 SMC Seeding Efficiency under Single Seeding (SS) and Dual Seeding (DS) Protocols.
Cells were counted in the medium volume used for seeding (Medium) or the total medium volume in the flow loop (Total Medium). Cells were also counted in the constructs. Data are mean ± standard deviation for N = 3 independent experiments with n = 2 constructs per experiment.

If it is assumed that cells were equally distributed in the total flow loop medium volume, i.e. 1100 ml (lumen seeding) or 1050 ml (external seeding), then single seeding efficiency is 78 ± 25% and dual seeding efficiency is 48 ± 42% (Figure 4.50). These numbers are in closer agreement with the number of cells present in the constructs after 48 hours of seeding and show that a small cell number is lysed or otherwise unaccounted for. These data indicate that dynamic cell seeding in the bioreactor through the construct lumen and/or the external surface result in low cell seeding efficiency.

IV.3.5 Late vs. Early Endothelialization

Single- and dual-seeded constructs were endothelialized late in culture, i.e. on day 23. To test the hypothesis that EC affect SMC proliferation and matrix deposition, a set of early endothelialization experiments was designed where EC were seeded after 10 days. Culture conditions were identical to previous single and dual seeding experiments (freshly prepared ascorbic acid was added to the bioreactor medium daily and externally-added growth factors were removed from the medium after 10 days). The 10-day time point was chosen for the endothelialization for two reasons. First, externally added growth factors have been removed from the culture medium and the EC effect on SMC proliferation is independent of externally-added growth factors. Second, wall permeability has decreased after 10 days (Figure 4.48). Therefore, EC seeded through the lumen are more likely to adhere on the lumen surface and not inside the construct wall. This early EC seeding protocol was compared to late EC seeding, in which EC were seeded after 23 days of SMC seeding. In both cases, constructs were harvested in 25 days.

Harvested dual-seeded early EC constructs had very good handling ability and tissue-like appearance (Figure 4.51). The cross-section of both late and early EC constructs had a non-homogeneous architecture. Denser tissue was observed near the lumen and the external surface compared to the middle parts of the cross-section (Figure 4.51). Early EC construct cell number ($27x10^6$ cells) was significantly higher than cell number in late EC constructs ($16x10^6$ cells) as shown in Figure 4.52 ($p<0.002$). The percentage of collagen per g of dry weight (2%) and amount of collagen produced per cell (0.02 ng) was significantly lower in early EC constructs compared to late EC (4% and 0.05 ng, respectively) with $p<0.05$ for both. In addition, the percentage of GAG in late EC constructs (44%) was higher than that of early EC constructs (37%) and the amount of GAG produced per cell in early EC constructs (0.4 ng) was significantly lower than that of late EC constructs (0.6 ng) with $p<0.03$. These results indicate that even though higher cell number is present in early EC constructs, matrix production is lower than the matrix produced by late EC constructs.

Differences between the two endothelialization protocols were further investigated by histological and immunohistochemical analyses. Cell distribution in early EC constructs was more uniform than in late EC constructs, but the lumen and external areas did not have as high cellularity as late EC constructs (Figure 4.53). One early EC construct appeared to have a second lumen formed next to the lumen surface (Figure 4.53). This second lumen formation did not appear to be a tear in the wall but was well structured with smooth walls. It could be hypothesized that EC present on the lumen surface assembled to form this second lumen. Collagen deposition in early EC constructs was primarily near the lumen and external surfaces and was not as pronounced

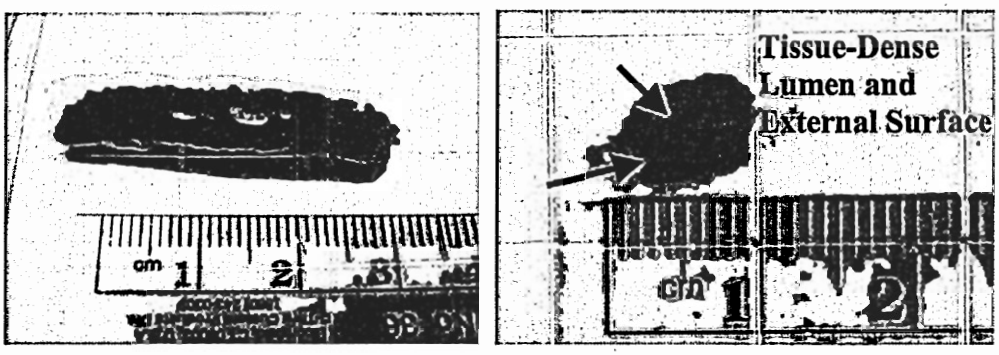

Figure 4.51 Harvested Dual-Seeded Early EC Construct Morphology.
Morphology of harvested construct (left) and construct cross-section (right). Higher tissue density is observed near the lumen and on the external surface compared to the wall in the construct cross-section.

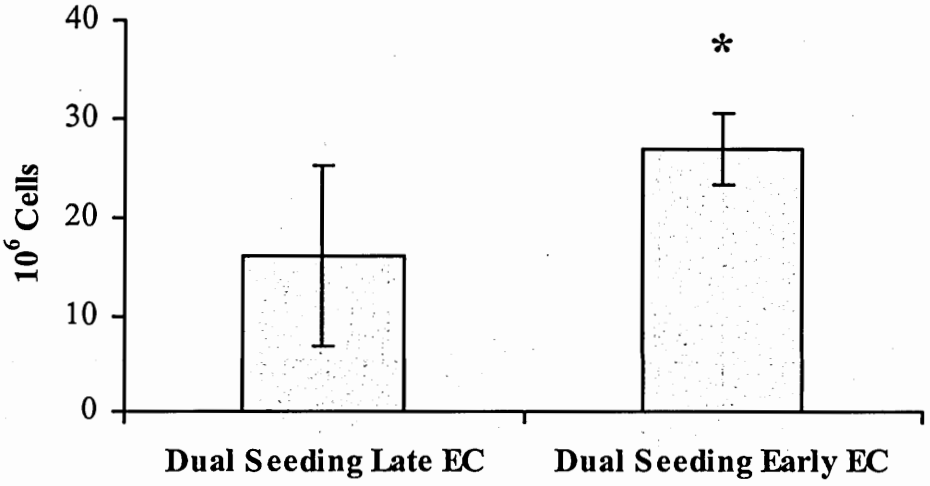

Figure 4.52 Biochemical Analysis of 25-Day Constructs Seeded with EC after 23 Days (Late Endothelialization) and after 10 Days (Early Endothelialization) of SMC Culture. These constructs were seeded with SMC through the lumen and on the external surface (dual seeding). Data are collected from a 5 mm construct ring. Data are mean ± standard deviation for N = 3 independent experiments with n = 2 constructs per experiment.

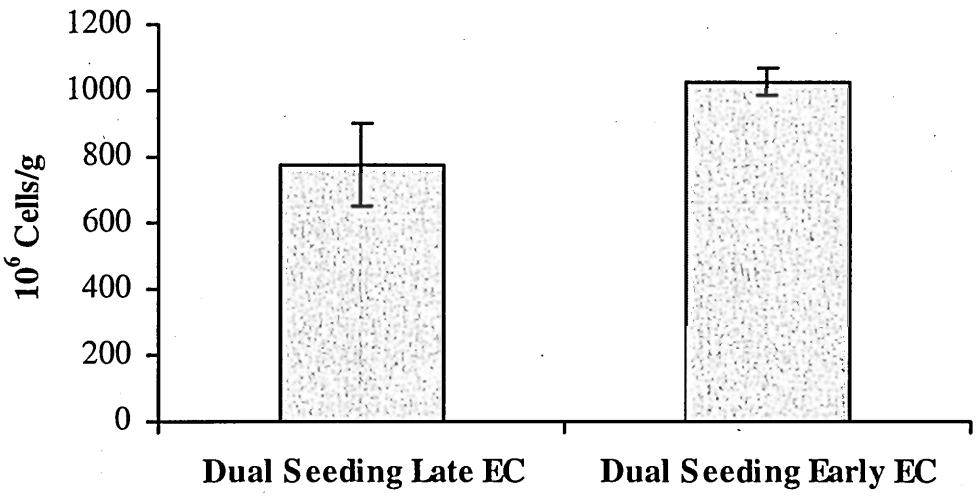

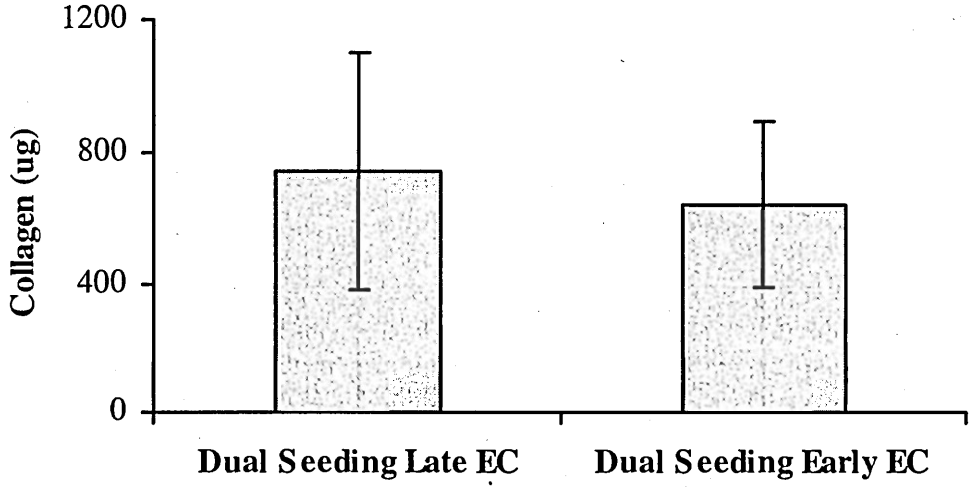

Figure 4.52 Biochemical Analysis of 25-Day Constructs Seeded with EC after 23 Days (Late Endothelialization) and after 10 Days (Early Endothelialization) of SMC Culture. These constructs were seeded with SMC through the lumen and on the external surface (dual seeding). Data are collected from a 5 mm construct ring. Data are mean ± standard deviation for N = 3 independent experiments with n = 2 constructs per experiment.

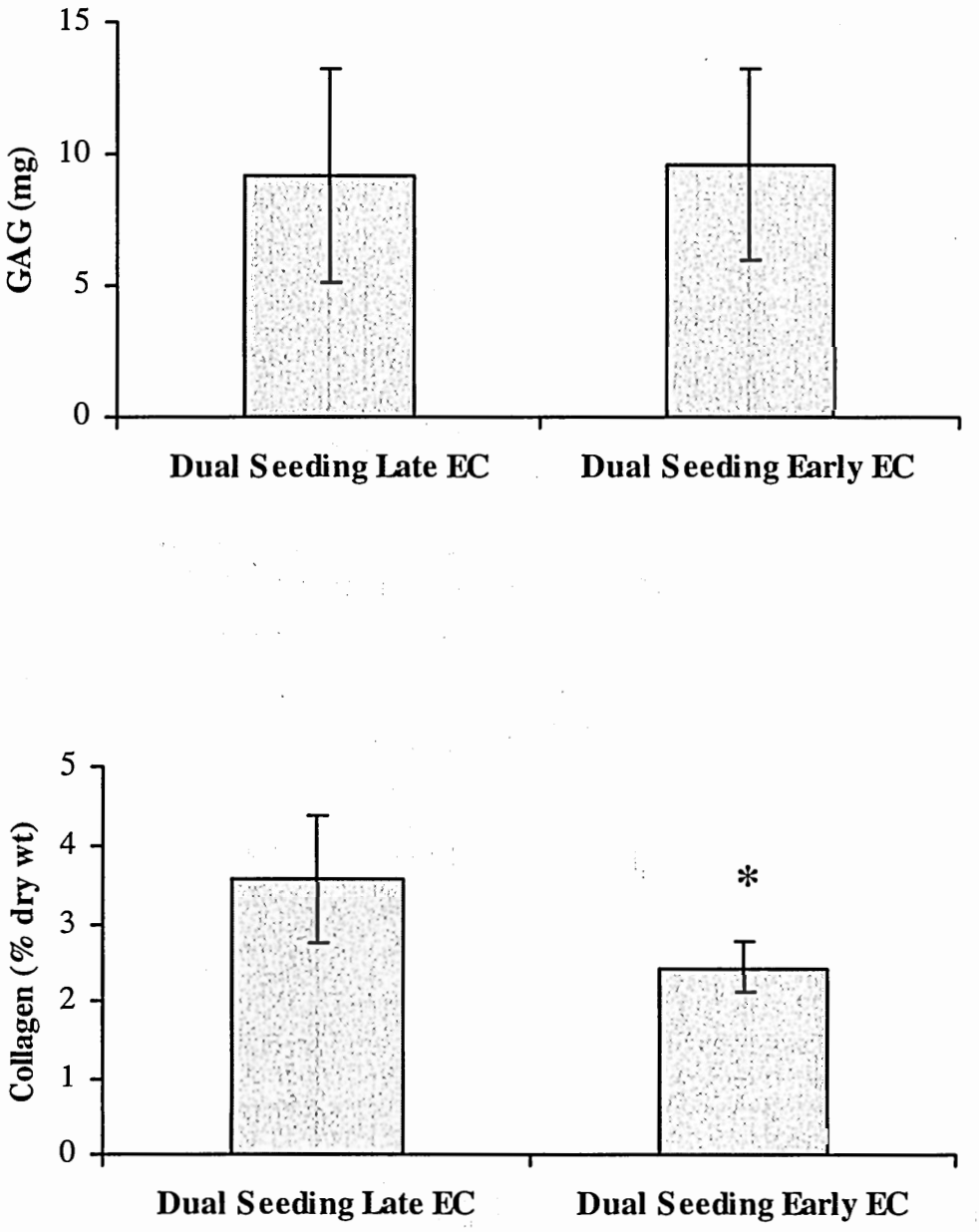

Figure 4.52 Biochemical Analysis of 25-Day Constructs Seeded with EC after 23 Days (Late Endothelialization) and after 10 Days (Early Endothelialization) of SMC Culture. These constructs were seeded with SMC through the lumen and on the external surface (dual seeding). Data are collected from a 5 mm construct ring. Data are mean ± standard deviation for N = 3 independent experiments with n = 2 constructs per experiment.

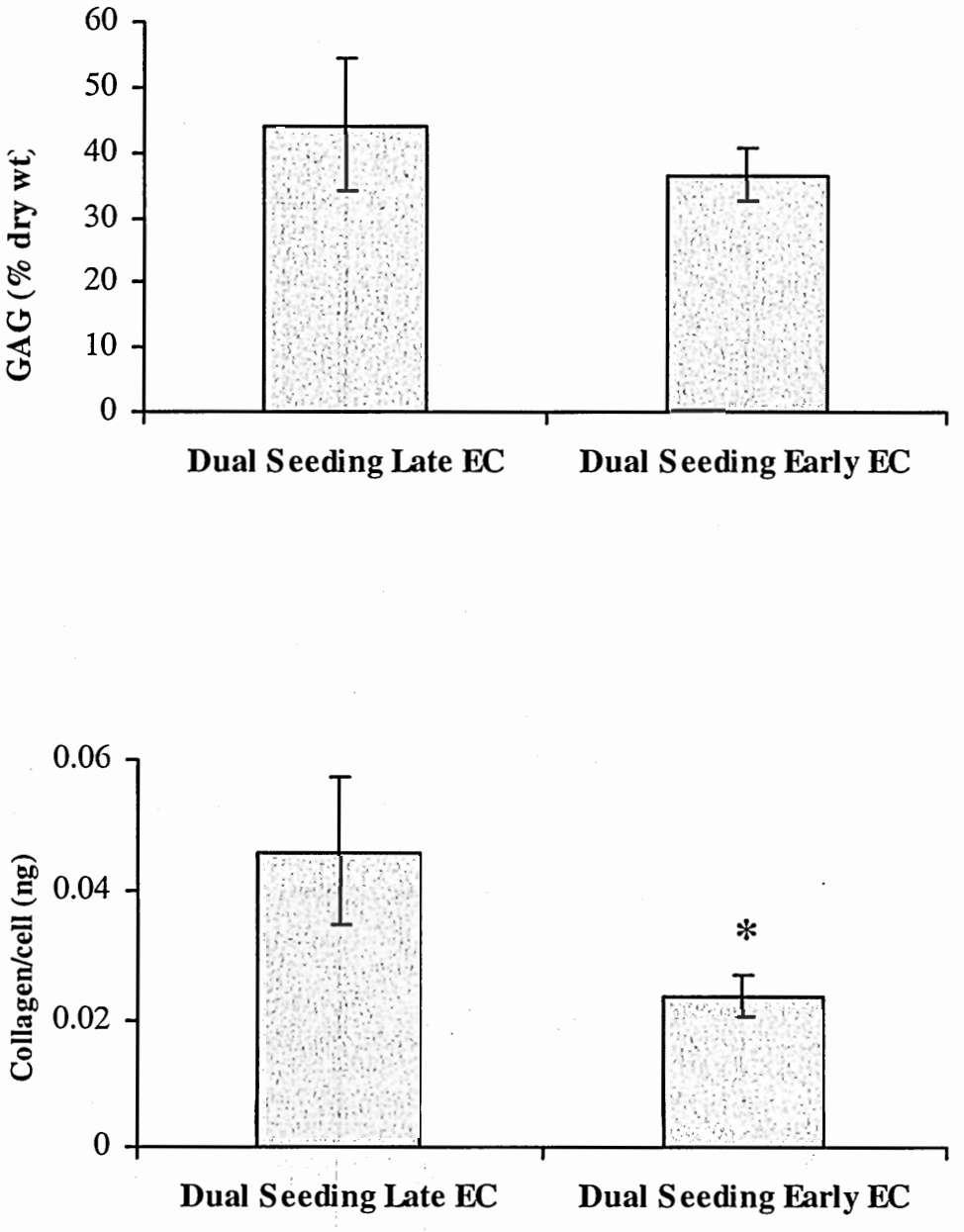

Figure 4.52 Biochemical Analysis of 25-Day Constructs Seeded with EC after 23 Days (Late Endothelialization) and after 10 Days (Early Endothelialization) of SMC Culture. These constructs were seeded with SMC through the lumen and on the external surface (dual seeding). Data are collected from a 5 mm construct ring. Data are mean ± standard deviation for N = 3 independent experiments with n = 2 constructs per experiment.

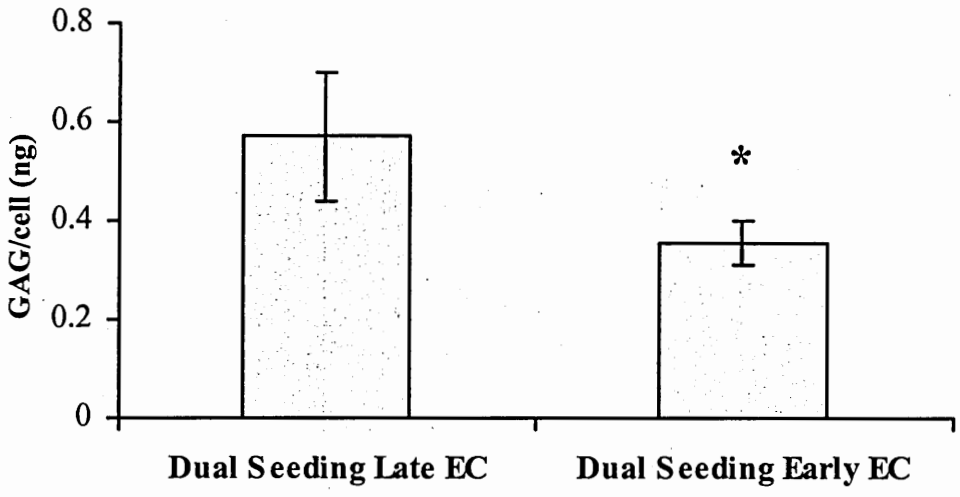

Figure 4.52 Biochemical Analysis of 25-Day Constructs Seeded with EC after 23 Days (Late Endothelialization) and after 10 Days (Early Endothelialization) of SMC Culture. These constructs were seeded with SMC through the lumen and on the external surface (dual seeding). Data are collected from a 5 mm construct ring. Data are mean ± standard deviation for N = 3 independent experiments with n = 2 constructs per experiment.

Figure 4.53 SMC and EC Distribution in Dual-Seeded Early EC Constructs. Cells are uniformly distributed across the wall (hematoxylin and eosin stain). A second lumen formation was observed in a construct near the lumen surface. Original magnification: 10X.

as in late EC cross-sections (Figure 4.54), consistent with the biochemical analysis data. Elastin staining was weaker in early EC compared to late EC constructs.

The effect of EC on SMC differentiation was also investigated. Smooth muscle α-actin expression in early EC constructs was intense near the lumen and the external surface areas but weak on the lumen surface (Figure 4.55). This is in contrast to single seeding and dual seeding late EC experiments, where smooth muscle α-actin expression was evident on the lumen surface (Figure 4.41), indicating that smooth muscle and endothelial cells co-populated the lumen surface. Calponin and myosin heavy chain expression was apparent near the lumen and the external surface of early EC constructs and showed the distribution of highly differentiated SMC (Figures 4.56 and 4.57). Myosin heavy chain expression in particular was more intense in early EC compared to late EC constructs (Figures 4.43 and 4.57). Therefore, longer term co-culture of EC and SMC led SMC into a more differentiated state.

Bioreactor medium samples were analyzed for glucose, lactate and pH. Lactate production was higher in early EC constructs compared to late EC constructs throughout the culture time, and significantly higher after 15 days ($p<0.03$) (Figure 4.58). Glucose and pH levels were similar under both protocols, and lactate to glucose ratio was significantly higher in early EC constructs after 25 days than in late EC constructs ($p<0.006$) (Table 4.11). Therefore, early EC led to an increase in cellular metabolic activity compared to late EC conditions.

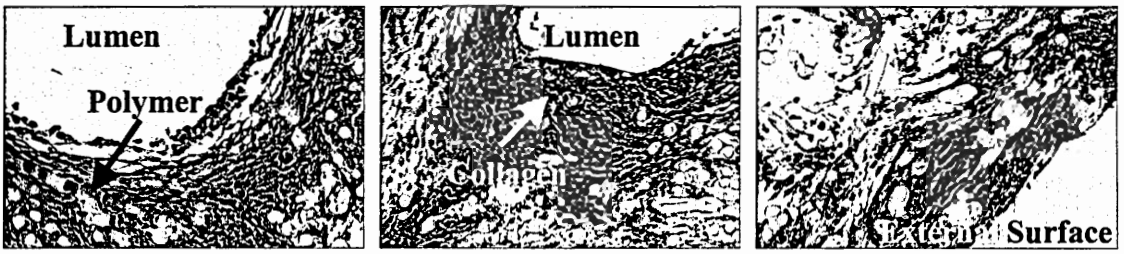

Figure 4.54 Collagen Deposition in 25-Day Dual-Seeded Early EC Constructs.
Collagen (stained blue by Masson's trichrome stain) was primarily deposited near the lumen and external surface of the constructs. Some polymer fragments (black arrow) are also stained blue. Original magnification: 20X.

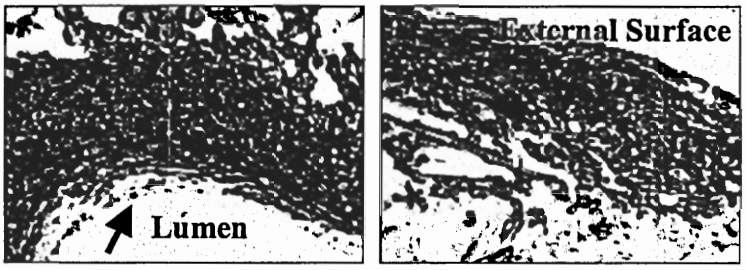

Figure 4.55 Smooth Muscle α-Actin Expression in Dual-Seeded Early EC Constructs.
Smooth muscle α-actin (SMA) positive cells are stained red close to the lumen and on the external surface. Cells on the lumen surface (black arrow) were negative for SMA. Original magnification: 10X.

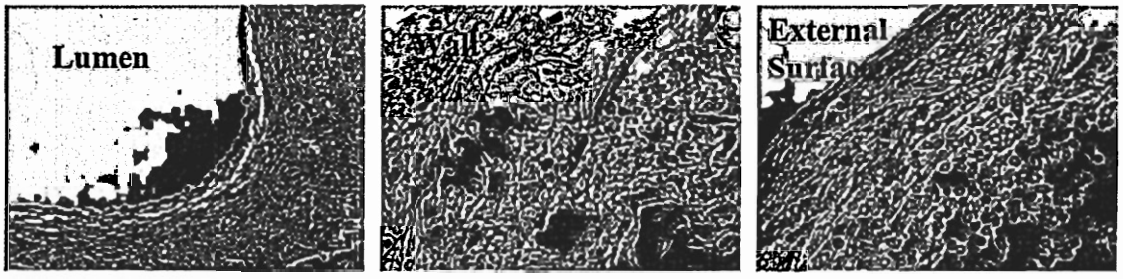

Figure 4.56 Calponin Expression in Dual-Seeded Early EC Constructs.
Cells stained positive for calponin (red) throughout the construct wall thickness. Original magnification: 10X.

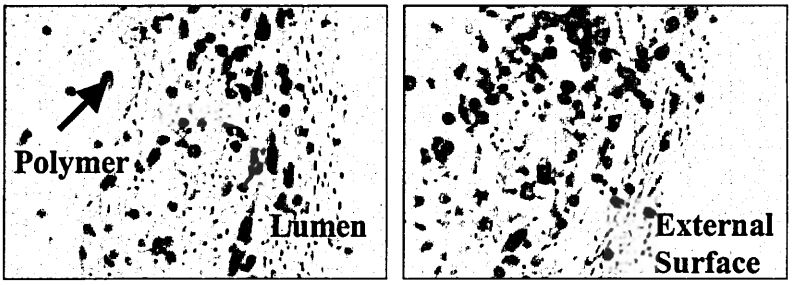

Figure 4.57 Myosin Heavy Chain Expression in Dual-Seeded Early EC Constructs. Myosin Heavy Chain positive cells near the lumen and external surfaces and polymer fibers (black arrow) stained red. Original magnification: 10X.

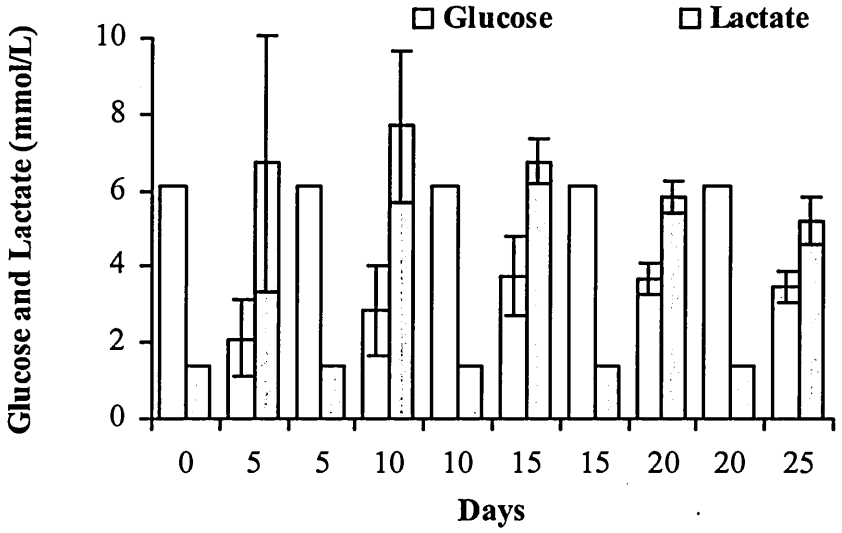

Figure 4.58 Glucose Uptake and Lactate Production in Dual Seeding Early EC Experiments.
Data are mean ± standard deviation for N = 3 independent experiments with n = 2 constructs per experiment.

Table 4.11 Lactate/Glucose Ratio and pH in Dual Seeding Late and Early EC Experiments.

Lactate/Glucose and pH values in spent medium are in bold. Data are mean ± standard deviation for N = 3 independent experiments with n = 2 constructs per experiment.

	pH		**Lactate/Glucose**	
Days	**Dual Seeding Late EC**	**Dual Seeding Early EC**	**Dual Seeding Late EC**	**Dual Seeding Early EC**
0	7.40	7.40	0.2	0.2
5	**6.75 ± 0.05**	**6.70 ± 0.04**	**2.5 ± 0.3**	**3.2 ± 1.6**
5	7.40	7.40	0.2	0.2
10	**6.64 ± 0.02**	**6.77 ± 0.08**	**4.7 ± 1.1**	**2.7 ± 0.9**
10	7.40	7.40	0.2	0.2
15	**6.73 ± 0.02**	**6.73 ± 0.02**	**2.0 ± 0.1**	**1.8 ± 0.3**
15	7.40	7.40	0.2	0.2
20	**6.67 ± 0.08**	**6.73 ± 0.01**	**2.0 ± 0.5**	**1.6 ± 0.1**
20	7.40	7.40	0.2	0.2
25	**6.78 ± 0.01**	**6.76 ± 0.04**	**0.8 ± 0.1**	**1.5 ± 0.1**

Scanning electron microscopy was used to gain insight into the surface morphology of early and late EC constructs. Figure 4.59 shows the confluent lumen surface of constructs seeded under both protocols and cell alignment in the flow direction. The external surface of the constructs was populated with cells that deposited extracellular matrix proteins and filled the space between the PGA fibers (Figure 4.59). A step (or uneven morphology) was also observed on the lumen surface, which could be the result of cells growing on PGA fibers that are not even. Figure 4.59 also shows a PGA fiber on the lumen surface of a late EC construct that is partially exposed to the flow as well as a cell at higher magnification that is spread and attached on extracellular matrix proteins. Therefore, early EC constructs had a more confluent lumen surface compared to late EC constructs with cells aligned in the flow direction.

PGA fiber degradation was also studied using scanning electron microscopy (Figure 4.60). PGA degrades by surface hydrolysis, and it was found that fiber diameter decreased over the course of 25-day experiments by approximately 26%. Fiber fracture followed three distinct patterns: jagged longitudinal, jagged transverse, and smooth transverse. The transverse sections also support the occurrence of shorter fiber fragments in long term cultures as opposed to long, intact fibers of purchased PGA scaffolds that have not been in contact with medium (Figure 4.35).

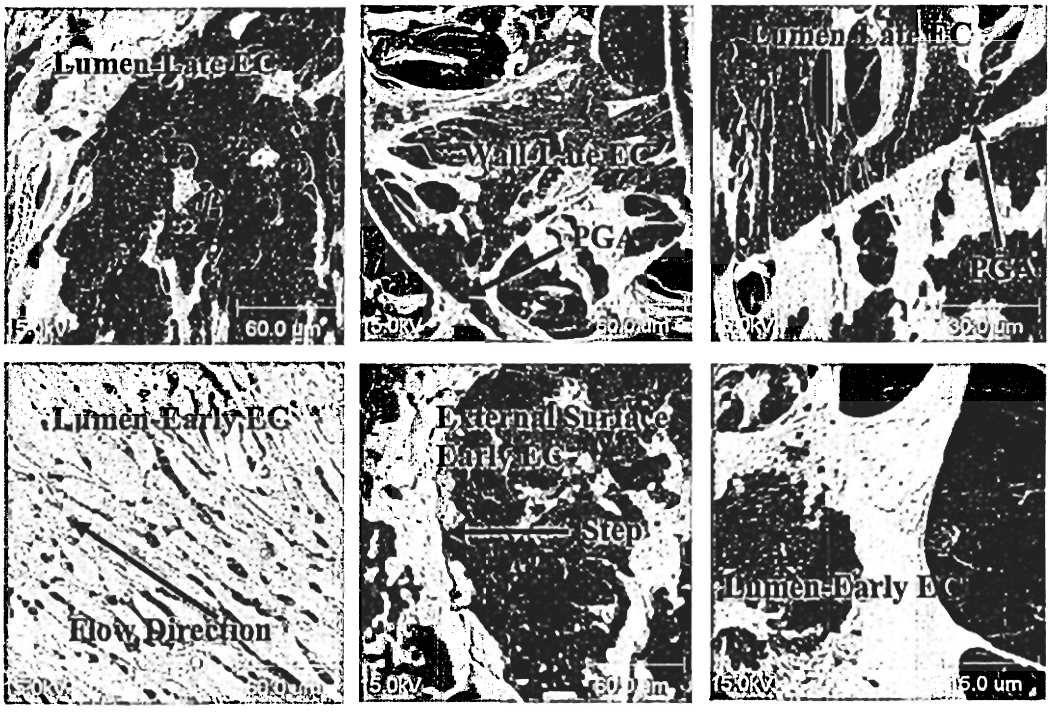

Figure 4.59 Ultrastructure of Dual-Seeded Late and Early EC Constructs.
Lumen surface was confluent in both late and early EC constructs and extracellular matrix proteins surrounded the PGA fibers in the construct wall. Cells enveloped PGA fibers on the lumen surface of late constructs (top right), while cell protrusions were observed in early EC constructs on the lumen surface. A step was seen in the external surface of an early construct possibly due to the underlying and uneven PGA fiber mesh.

Figure 4.60 PGA Degradation Patterns of Dual-Seeded Late EC Constructs.
Jagged longitudinal degradation (left), jagged transverse (middle) and smooth transverse hydrolysis (right).

Finally, Table 4.12 shows the lumen diameter and lumen inlet and outlet flow rates in late and early EC experiments. Lumen diameter was similar in both protocols as well as lumen inlet flow rates and shear stresses. This is in contrast to single-seeded constructs that had a smaller lumen diameter (Table 4.10). Time-averaged flow rates in early EC experiments followed the typical pattern of large fluctuations during the first 10 days of culture that were essentially eliminated by day 15 (Figure 4.61). These data show that wall permeability is significantly decreased by day 15 in early EC constructs due to cell proliferation and matrix deposition.

In summary, early endothelialization of dual-seeded constructs results in higher cell number, more uniform cell distribution, decreased extracellular matrix production, higher cellular metabolic activity, and more differentiated SMC compared to late EC. Therefore, 15-day co-culture of EC and SMC has a significant effect on various SMC functions compared to 2-day co-culture.

Table 4.12 Time-Averaged Flow Rate and Wall Shear Stress in 25-Day Dual Seeding Late and Early EC Experiments.
Data are mean ± standard deviation for N = 3 independent experiments with n = 2 constructs per experiment.

	Lumen Diameter (mm)	**Lumen Inlet Flow Rate ($\dot{Q}_{in}$) (ml/min)**	**Lumen Outlet Flow Rate ($\dot{Q}_{out}$) (ml/min)**	**Shear Stress based on $\dot{Q}_{out}$ (dynes/cm^2)**
Dual Seeding Late EC (N = 3 and n = 2)	3.0 ± 0.7	44.0 ± 11.6	34.8 ± 11.8	1.6
Dual Seeding Early EC (N = 3 and n = 2)	3.1 ± 0.7	56.0 ± 7.7	54.3 ± 6.7	2.1

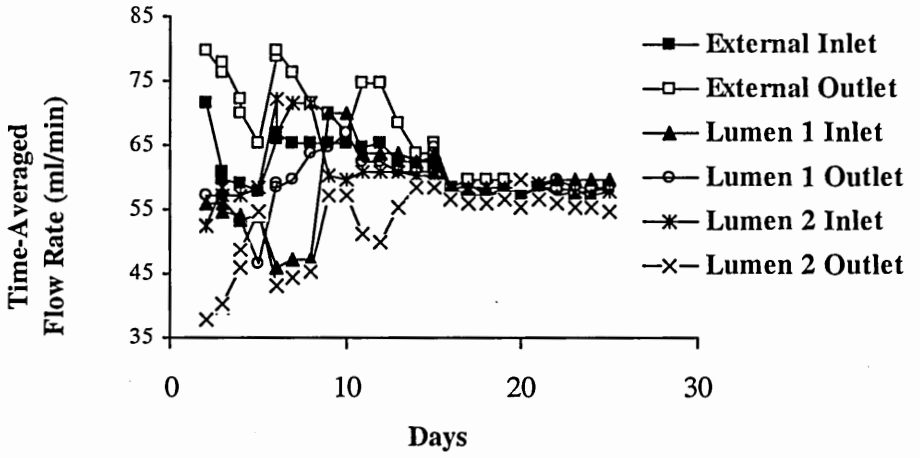

Figure 4.61 Time-Averaged Flow Rate of a Dual Seeding Early EC Experiment. Flow rates were monitored at the lumen inlet and outlet of each construct and at the inlet and outlet of the bioreactor external space flow loop.

IV.3.6 Mechanical Testing

The tensile strength of 5-mm long construct rings was measured using a ring tester apparatus. Two types of constructs had to be excluded from testing: constructs that did not have adequate handling ability (structural integrity), and constructs that had such a small inner diameter that they could not be mounted on the ring tester. Single-seeded late EC constructs did not have good handling ability and dual-seeded early EC constructs as well as a dual-seeded late EC construct had too small inner diameters and were very difficult to mount on the hooks without damaging the tissue. Based on these limitations, mechanical testing data are presented here to provide some information on the order of magnitude of the construct strength after 25 days of bioreactor culture. Three rings from two dual-seeded late EC constructs were tested as shown in Table 4.13.

Figure 4.62 shows the stress vs. displacement curve of a construct that follows the behavior of tissue materials (Dinnar, 1981). However, Figure 4.63 shows two peaks,

indicating non-homogeneous mechanical properties. In this case, the two materials are the lumen surface (first peak) and the external surface (second peak) tissues as observed by the video recording. As histological (Figure 4.40) and gross morphological (Figure 4.51) observations have shown, areas near the lumen and the external surface possess higher cellularity and more matrix proteins compared to the middle of cross-sections. The mechanical testing data support those observations as the lumen tissue fails first (first peak), followed by the external surface tissue (second peak). Figure 4.63 shows that the near lumen area of the construct has higher mechanical strength than the external surface tissue. It is also clear from these results and the video images acquired that after 25 days, the polymer scaffold is not contributing to the construct's mechanical strength because the polymer has undergone significant degradation.

Table 4.13 Ultimate Stress and Material Modulus of Dual-Seeded Late EC Constructs.

	Ultimate Stress (KPa)	**Elastic Modulus (KPa)**
Construct 1	2.5	1.2
Construct 2: Ring 1	5.3	10.5
Construct 2: Ring 2	16.9	33.9

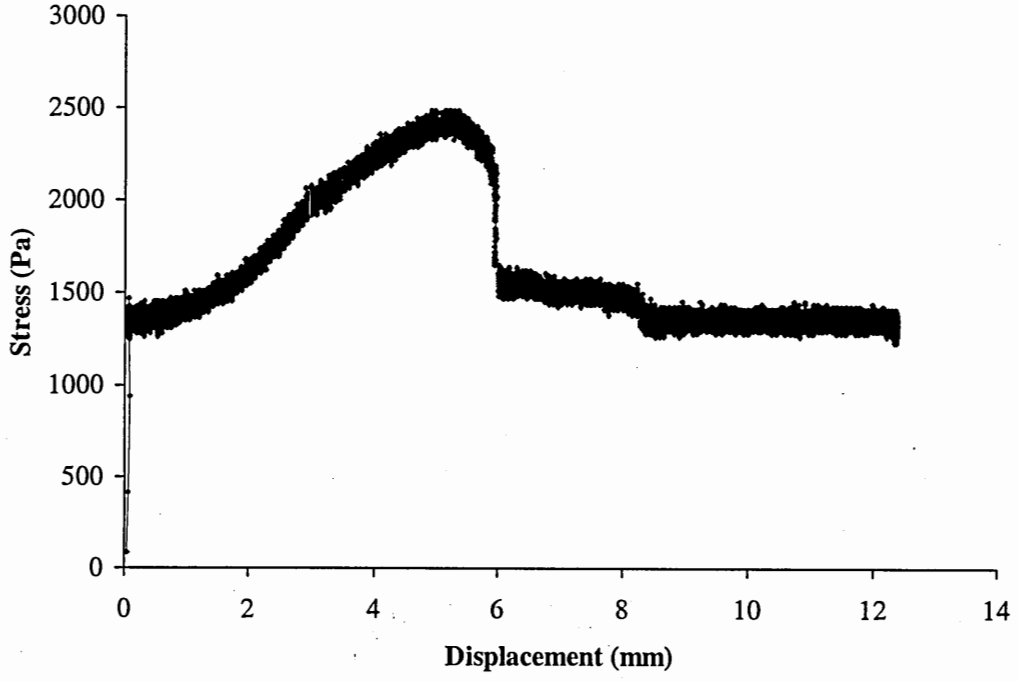

Figure 4.62 Stress vs. Displacement of Dual-Seeded Late EC Construct 1.

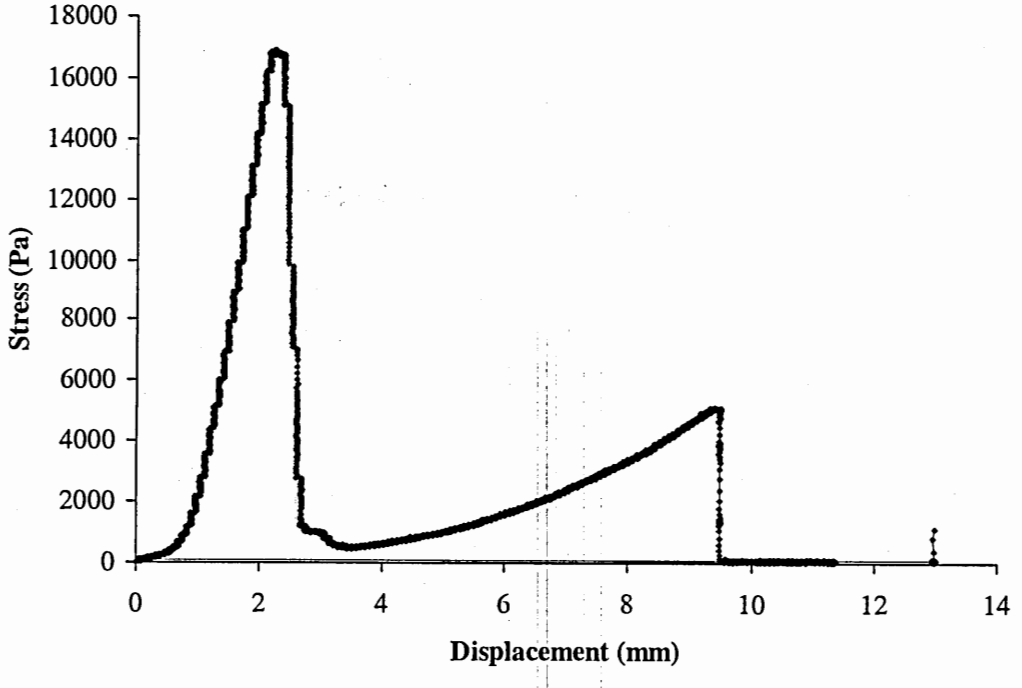

Figure 4.63 Stress vs. Displacement of Dual-Seeded Late EC Construct 2, Ring 2.

CHAPTER V

DISCUSSION

An enabling technology for tissue engineering is the development of bioreactors to promote growth of functional tissues for human implantation. This thesis describes a dual perfusion bioreactor system developed to address bioprocessing issues related to the engineering of small diameter vascular grafts. This bioreactor allows for the dynamic seeding of multiple cell types and incorporation of construct biomechanical stimulation (shear stress and pulsatility) toward the engineering of vascular tissue with complex architecture and differentiated function. Dual perfusion of the growing tissue-engineered constructs on both the lumen and the external surface facilitates nutrient diffusion and removal of PGA degradation products. Smooth muscle cell seeding under dynamic conditions leads to uniform cell distribution across the thickness of the construct wall in short term experiments. Smooth muscle cells deposit collagen, elastin and glycosaminoglycans in bioreactor experiments up to 35 days and express differentiated phenotype. Results are comparable in two- and three-module bioreactors demonstrating reproducibility of arterial tissue development in the modular bioreactor. Construct endothelialization early in culture resulted in increased cell number and reduced matrix production compared to late endothelialization. These arterial tissue culture results validate the bioreactor as a scaleable perfusion system for the simultaneous growth of multiple vascular grafts under similar conditions. Development of robust bioreactors and bioprocessing technologies is essential to produce functional tissue-engineered constructs to meet clinical demands. Since bioreactor biomechanical environment controls cell

differentiation and construct development, bioreactor design must be addressed in the early stages of tissue engineering research.

V.1 Static Cell Seeding

Preliminary cell seeding experiments were designed under static conditions using human, rat, and bovine aortic smooth muscle cells in PCL, PLLA and PGA scaffolds. These polymers are biocompatible and biodegradable and among the few synthetic absorbable materials with U.S. Food and Drug Administration approval for human clinical use. Early experiments investigated HASMC proliferation in PCL and PLLA scaffolds. HASMC proliferation data showed that higher initial cell densities result in higher cell number at harvest time in both polymers. This indicates that cell densities between 1,000 and 6,000 cells/mm^2 do not saturate the construct surface area. Since these polymer scaffolds are highly porous, higher initial cell densities than those used in monolayer cultures are necessary to seed 3D scaffolds. When a higher density of 12,000 cells/mm^2 was investigated, cell number increased in both polymers up to 7 days and significantly decreased by day 14. These results are in agreement with many research groups who have identified the surface properties of biocompatible, synthetic polymers as not cell-friendly and have used various techniques to increase cell attachment such as surface hydrolysis (Gao et al., 1998). Indeed, although scaffolds prepared from naturally derived biomaterials have intrinsic cell adhesion properties, cells adhere to synthetic scaffolds via extracellular matrix proteins that are adsorbed on the polymer surface (Lamba, 1998; Saltzman, 1997). Overnight prewetting of the scaffolds in complete culture medium containing 10% serum and human epidermal and fibroblast growth

factors did not increase cell attachment and proliferation in PLLA scaffolds. This could be due to transient protein adsorption on the polymer surface that are rapidly replaced by other proteins (such as albumin) that do not favor cell adhesion. The opposite trend was observed in PCL constructs. Cell number in prewetted constructs was higher than in dry ones at all time points and significantly higher after 30 days. Therefore, prewetting of the polymer surface did not affect cell attachment as predicted but had a positive effect on long term proliferation in PCL scaffolds. Although the exact mechanism is not known, this long term effect could be due to enhanced migration along the adsorbed proteins inside the scaffold resulting in overall higher cell numbers.

With the goal of improving cell seeding efficiency and proliferation, PCL and PLLA scaffolds were pretreated with NaOH, fibronectin (Fn), and NaOH+Fn, and seeded with SMC. Cell number increased significantly between days 1 and 14 in NaOH and NaOH+Fn treated PCL constructs, and the NaOH+Fn treated PCL constructs had a higher cell number than the control at day 14. These data suggest that different surface treatments can have a synergistic effect on cell proliferation that may not be observed in individual treatments. Sodium hydroxide leads to partial hydrolysis of the polymer, which could have a positive effect on protein adsorption by increasing the polymer's wettability and hydrophilicity. However, these surface pretreatments did not significantly increase cell attachment in PCL compared to the controls. Similar results were observed in experiments with PCL treated with collagen, gelatin, NaOH+collagen, and NaOH+gelatin. These results were unexpected as protein adsorption onto polymer surfaces is thought to increase cell attachment and spreading. However, Marois et al. reported that collagen and gelatin treated polyesters did not improve chick endothelial

cell adhesion significantly (Marois et al., 1999). It could be that cell adhesion was not affected because the adsorbed proteins were replaced by serum proteins present in the culture medium that do not promote cell adhesion. Depending on the affinity of the polymer surface for the various proteins in the culture medium, proteins used to pretreat the polymers might desorb and become replaced by proteins with higher affinity.

The third polymer scaffold used in static seeding experiments was PGA. This polymer is a biocompatible synthetic scaffold that has been shown to support cell attachment and proliferation. Its main limitation is that it degrades faster than PLLA, thereby releasing acidic glycolide monomers in the culture medium that can lower the pH and have adverse effects on cell viability (discussed in Chapter V.2). Even though modest HASMC proliferation rates were observed in PCL and PLLA scaffolds, HASMC and RASMC number increased four- and two-fold in PGA scaffolds within 6 days, respectively, showing that PGA promotes cell proliferation. One of the main differences of the PGA and PLLA scaffolds used in these experiments was their architecture. PGA scaffolds were a non-woven mesh of fibers whereas PLLA was a porous scaffold prepared by salt leaching. Therefore, the different proliferation rates of HASMC in these two polymers that have similar chemistry may be due to their different surface architecture.

In summary, modest cell proliferation was observed when HASMC were seeded in PCL and PLLA and SMC in PCL scaffolds. Various surface modifications did not significantly cell attachment compared to controls. These results could be inherent to static seeding limitations. In these static seeding experiments, high cell numbers were seeded into polymer discs in culture dishes and medium was replaced every two days.

However, the cell nutrient requirements may not be satisfied by the small medium volume used in culture dishes. This is in contrast to cell monolayers plated in culture dishes as cells are divided into more dishes/flasks as they become confluent. Cells proliferating in polymer scaffolds are dependent on the same medium and the medium volume is not increased with time. Additionally, there is no perfusion or mixing that could improve nutrient transport inside the scaffolds. These are important limitations of static culture methods that work excellently for cell monolayers but become inadequate for 3D tissue culture.

V.2 Cell and Scaffold Sourcing

A large variety of cell types and materials have been combined over the years to engineer vascular grafts. Both human and animal cells, vascular, dermal, progenitor and even cartilage cells have been utilized to culture arterial constructs with varying degrees of success. Some of the cell sourcing criteria that are considered in vascular tissue engineering are the following:

(1) The ability of the cells to produce extracellular matrix proteins. Indeed, this is a major consideration in cell source selection since perhaps the biggest limitation of tissue-engineered constructs is inadequate mechanical strength. Neonatal and newborn cells are among a few cell types that have been shown to produce elastin and collagen in vitro (Abraham et al., 1974), whereas human smooth muscle cells require long term culture for increased extracellular matrix production (L'Heureux et al., 1998).

(2) Use of cells from the same species as the animal model that will be used for in vivo experiments. Although human cells seem like the obvious cell source for the

development of vascular grafts, animal testing of the grafts must occur prior to human implantation to establish the product's safety and efficacy. Particularly because endothelial cells are highly immunogenic, heterografts require post-surgical administration of anti-coagulants. Therefore, it is preferable to harvest the animal's own cells, expand them in culture, develop the graft, and implant it in the same animal. With this approach, the efficacy and patency of the graft can be directly studied and any immune reaction will be due to the biomaterial used (if any). However, it should be stressed that the behavior of animal cells in animal models does not necessarily predict the behavior of human cells seeded in vascular grafts and implanted in patients.

(3) Use of primary or low passage fetal or neonatal cells that have a large proliferative capacity. McKee et al. have shown that adult human cells undergo 10-30 population doublings in vitro before becoming senescent (McKee et al., 2003). However, the same authors estimate that 45-60 SMC population doublings are necessary to produce mechanically-robust vascular grafts in vitro. Based on this observation, they infected SMC from young donors with the human telomerase reverse transcriptase subunit to arrest telomere shortening and extend the lifespan of SMC while maintaining their characteristics. Blood vessels cultured with infected SMC had a higher cell density, contained more viable cells compared to controls, and SMC maintained a differentiated phenotype. This study raises an important point since cell sourcing for grafts suitable for human implantation remains an open question in vascular tissue engineering.

(4) Use of stem cells that can differentiate into vascular cells in vitro. Kaushal et al. used endothelial progenitor cells isolated from sheep peripheral blood to seed decellularized porcine iliac vessels in vitro and implanted them in sheep for up to 130

days (Kaushal et al., 2001). Endothelial progenitor cell-seeded vessels were fully patent after 130 days as opposed to 75% of the control unseeded vessels that failed within 5 days of implantation. This approach is very promising for endothelial cell sourcing from patients since it only requires a blood sample. However, it remains to be investigated whether progenitor cells with endothelial cell phenotype can be harvested from humans and in sufficient numbers for the development of grafts suitable for implantation and with long term patency.

(5) Donor to donor and animal to animal variability can mask or otherwise alter experimental results. Continuous cell lines are rarely used in tissue engineering, unless a very specific study is undertaken, because infinite cell proliferation in vivo would lead to tumor-like growth and construct failure. Therefore, tissue engineers have to face the necessary evil of donor to donor and animal to animal variability of the cell source. Although statistical analysis such as multifactor ANOVA can isolate the effect of this variability versus the effect of another parameter that is being studied, cell source variability inevitably leads to large experimental variance. When the variance is large, a large number of independent experiments have to be performed to obtain significant results, which is both expensive and time-consuming. In some cases, this is not even feasible due to the limited number of cells that are available (e.g. from donors).

(6) Sequential seeding of individual cell types versus a cell mix. The majority of vascular tissue engineers seed individual cell types into biological or synthetic scaffolds sequentially in vitro (Niklason et al., 1999), or culture them separately and then laminate the cell layers (L'Heureux et al., 1998). This approach deprives cells from important cell-cell signaling cues that are essential in tissue function and remodeling in vivo. Shinoka

and coworkers seeded polymer scaffolds with mixed cells containing ovine endothelial cells, smooth muscle cells, and fibroblasts and implanted them into lambs for up to 169 days for the tissue engineering of pulmonary arteries and autologous aortic grafts. Interestingly, even though scaffolds were seeded with a mixed cell population, endothelial cells were found on the lumen surface of the harvested vessels and smooth muscle cells and fibroblasts populated the vessel wall. This important finding suggests that when mixed vascular cells seeded in synthetic scaffolds are implanted in vivo, they tend to migrate to their corresponding positions observed in native vessels.

Based on these six criteria, low passage bovine aortic cells were selected for and used in bioreactor experiments. The response of bovine endothelial cells to shear stress has been studied extensively and bovine vascular cells have been used successfully to create functional tissue-engineered vascular grafts (Niklason et al., 1999). Since the primary objective of this project was to develop a perfusion bioreactor system for the dynamic seeding and growth of blood vessels, it was deemed crucial to use a readily available source of primary cells that can be expanded in vitro to produce the large numbers of cells required in bioreactor experiments while still being at low passage.

Scaffold sourcing is another critical matter, mostly because of its paramount importance in the development of patent vascular grafts. The first question, however, is whether a scaffold should be used at all. Indeed, L'Heureux et al. were successful in developing tissue-engineered grafts composed solely of cells and their matrix while achieving high burst strength and differentiated function (L'Heureux et al., 1998). However, scale-up and bioreactor development suitable for this tissue engineering approach cannot be readily envisioned. Since the main research focus in this thesis has

been on the use of a scaffold material that can support cell growth and matrix production, the perfusion bioreactor system described in this thesis has been designed to accommodate any type of scaffold that can be mounted on the bioreactor holders. Furthermore, a biodegradable scaffold was preferred over a permanent one, because tissue-engineered products should eventually not contain any foreign material that could elicit immune response, should fully integrate with the surrounding native tissue, and adapt with physiologic/pathologic changes that take place in the human body.

The hardest decision perhaps was choosing a synthetic over a biological scaffold. Indeed, biological scaffolds such as hydrogels, collagen and fibrin gels, and collagen and elastin electrospun scaffolds offer numerous advantages over synthetic biomaterials. Collagen, for example, is an abundant extracellular matrix protein of the arterial wall that is secreted by vascular cells and involved in cell spreading, migration, and differentiation. Collagen also provides tensile strength and therefore has been used in vascular tissue engineering as a substrate for cell attachment. Elastin, another component of the vascular wall, provides elasticity to the tissue and is involved in various cell processes. Fibrin, a major structural protein in blood clots, has also been investigated as an alternative to collagen and used as a fibrin gel by fibrinolysis of fibrinogen (Grassl et al., 2002). The main advantage of these biologic materials is that they are natural cell substrates that can bind other extracellular matrix proteins such as fibronectin and increase cell adhesion and migration. In addition, collagen and elastin are the major contributors of the arterial wall's mechanical strength, an important parameter of tissue-engineered vascular grafts. However, previous work with these biologic materials has shown that cell proliferation and extracellular matrix production is limited in collagen and fibrin gels and cells

produce proteases that remodel the exogenous matrix proteins. Vascular cells, such as SMC, remodel their extracellular matrix, but the rate of remodeling appears to be higher in exogenous matrices compared to the cells' own matrix in vitro. This could be one of the reasons why tissue-engineered collagen gels have insufficient mechanical strength.

On the other hand, biodegradable polymeric scaffolds provide adequate initial mechanical strength and support cell proliferation and extracellular matrix production. These scaffolds can therefore be used transiently to achieve a tissue of sufficient mechanical strength composed of cells and their extracellular matrix as the polymer degrades. Based on these observations, biodegradable PGA non-woven felts were used in bioreactor experiments presented in this work. The major limitations of PGA are its synthetic nature, degradation products, and degradation rate.

As a synthetic biomaterial, PGA does not provide a substrate that is as cell-friendly for attachment as the protein substrates found in vivo. Various techniques have been used to improve cell attachment on PGA. PGA scaffolds have been partially hydrolyzed with 1 N NaOH (Gao et al., 1998), prewetted in culture medium (Burg et al., 2000; Kim et al., 1998), or in fibronectin solution (Kim et al., 1999a) to increase protein adsorption and cell adhesion. In this work, PGA was prewetted with culture medium C overnight at room temperature prior to cell seeding to increase adsorption of extracellular matrix proteins and growth factors in the felts.

Glycolic acid is the main degradation product of PGA hydrolysis and it either enters the TCA cycle or is excreted in urine in vivo (Williams and Mort, 1977). Glycolic acid production leads to reduced pH in the microenvironment of degrading PGA fibers. Acidic conditions can have an adverse effect on vascular cell viability and other cellular

processes such as proliferation and differentiation (Niklason et al., 1999). Hence removal of the degradation products from the cellular microenvironment is of paramount importance, and perfusion culture conditions assist in this regard. In our dual perfusion bioreactor, both the external and lumen surfaces of the scaffold are perfused with culture medium throughout the culture time. Due to the scaffold's high porosity, significant fluid flow through the construct wall takes place during the first 5-10 days of culture that is subsequently decreased as the wall is populated with cells and their matrix proteins. Therefore, PGA degradation products are not accumulated in the construct wall and are transported in the culture medium.

PGA scaffolds degrade within 6-8 weeks in vitro. In vascular tissue engineering, this time frame may be too short to achieve sufficient matrix production prior to polymer degradation. Indeed, culture conditions need to be optimized to obtain enough tissue formation within 6-8 weeks as the mechanical strength of the polymer is gradually diminishing (Niklason et al., 2001). On the other hand, in vitro culture longer than 6-8 weeks could become very costly and therefore undesirable. Acknowledging this limitation on culture time length, we have designed a bioreactor that can be used to manipulate culture conditions such as mechanical and biochemical parameters in order to minimize culture time. Specifically, dual perfusion improves nutrient transport inside the construct wall and accelerates tissue growth, and the independent lumen and external flows can be used to supply each loop with a medium composition specific to each cell type (lumen flow for EC and external flow for SMC).

The PGA non-woven felts used in bioreactor experiments were purchased in slab form and sutured along the length to create tubular scaffolds. It has been shown that this

technique is successful and that arterial constructs do not fail along the suture line during mechanical testing (Niklason et al., 1999). In our experiments, the lumen morphology appeared tear-shaped instead of circular during the first two weeks of culture but became more circular at later culture times. Construct harvesting resulted in lumen collapse and further analysis of lumen shape was not possible. However, histological and immunohistochemical analyses were performed on harvested constructs. We did not observe any difference in cell distribution or matrix production in the azimuthal direction, and the suture line could not be detected after 25 days of culture. Therefore, suturing of the scaffolds was deemed as a straightforward method of creating tubular scaffolds for bioreactor experiments.

V.3 Bioreactor Technology for Vascular Tissue Engineering

The bioreactor described in this work was successfully used for the development of small diameter tissue-engineered arterial constructs. Short-term bioreactor experiments showed uniform cell distribution as early as 4 days after seeding and uniform collagen deposition after 9 days in culture, indicating that dynamic seeding enables cell attachment, distribution and matrix production throughout the thickness of highly porous polymer scaffolds. Higher initial cell densities resulted in higher cell number at harvest for short term (< 16 days) culture (Figure 4.21). In addition, cell distribution was more organized with culture time, suggesting that cell seeding and attachment were followed by cell migration, extracellular matrix deposition and organization beyond approximately 4 days in a dynamic culture environment.

Although smooth muscle cells were uniformly distributed in the constructs after 4 and 9 days of bioreactor culture, in longer-term experiments high cellularity was observed close to the free surfaces of 16- and 25-day constructs exposed to flow. Regions of high cellularity co-localized with low polymer content (Figures 4.23 and 4.26). The preferential accumulation of cells near free surfaces may result from the following: smooth muscle cells being attracted to the free surfaces due to increased nutrient concentrations; the pH in the cellular microenvironment being at more physiological levels close to the surfaces and lower in the wall due to polymer degradation products (Agrawal and Athanasiou, 1997); the flow environment promoting cell migration toward the free surfaces through mechanosensing proteins on the surface of smooth muscle cells (Gosgnach et al., 2000; Ozaki et al., 1999).

Cell proliferation and matrix deposition decrease construct porosity and reduce nutrient transport through constructs, especially late in culture when bulk flow through matrix does not occur (Figure 4.28). This may increase cell migration toward the free surfaces of the construct, where nutrient concentrations are higher. However, histological analysis of harvested constructs does not reveal reduced cell viability within the core of the construct. Thus, it is not likely that nutrient limitations alone account for heterogeneous cellular distribution in the constructs.

PGA hydrolysis releases glycolic acid that may reduce culture medium pH locally near degrading polymer fibers (Gao et al., 1998). This may result in the accumulation of glycolic acid within the construct, and the creation of an acidic microenvironment that inhibits cell proliferation and/or function. Again, histological analysis does not support

the notion of nonviable cells within the construct, although further studies might reveal an inhibitory effect of PGA degradation products on cell function and differentiation.

A more plausible explanation for non-uniform distribution of smooth muscle cells within the construct wall is that cells in the construct periphery experience higher shear forces, especially early in culture when porosity and wall permeability are highest. This is consistent with previous reports that either shear stress (Sterpetti et al., 1993) or strain (Mills et al., 1997) increase smooth muscle cell proliferation rate. Thus, shear stress and cyclic strain experienced by the smooth muscle cells close to the free surfaces in the construct may increase cell proliferation compared to cells deeper in the construct. In addition, smooth muscle α-actin staining is more intense in the high cellularity areas suggesting that smooth muscle cells near free surfaces are more differentiated than cells within the construct. These observations further establish the importance of mechanical forces in arterial construct development and demonstrate that the bioreactor is an important tool to investigate and characterize the role of mechanical forces on artery tissue engineering.

Flow monitoring demonstrates that medium flow rates at the construct lumen inlet and outlet are initially different (Figure 4.28). Lumen inlet and outlet flow rates converge after approximately 10 days of culture, when lumen time-average flow becomes constant (Figure 4.28). This suggests a significant medium cross-flow through the porous construct wall early in culture that decreased as the construct becomes populated with cells and matrix. After 10 days in culture, construct inlet and outlet flow rates are equal, indicating that shear stress in the lumen is spatially homogeneous and shear stress calculations can be based on measured flow rates.

Measurements of flow rates as depicted in Figure 4.28 provide potential to monitor arterial construct growth in the bioreactor. For example, determination of a low flow rate through the construct wall may suggest when smooth muscle cell-seeded constructs should be endothelialized. In addition, lack of flow through the construct wall suggests that constructs can support increased lumen pressure, flow, or pulsatility to accelerate construct development. Further bioreactor studies will indicate the potential for in-line flow rate measurements as a predictive tool of construct development or suggest changes in bioreactor operation to enhance arterial construct growth.

In arterial constructs the endothelium provides an antithrombogenic layer and is the major contributor of signal transduction to other cell types that reside inside the vessel wall (Campbell and Campbell, 1986). To assess whether arterial construct dynamic endothelialization is feasible in the perfusion bioreactor, smooth muscle cell-seeded constructs were co-cultured with endothelial cells. Endothelial cell seeding occurred under dynamic flow conditions after 13 days of SMC-seeded construct growth without opening the bioreactor or compromising tissue sterility to create an arterial co-culture tissue substitute. Within 2 days, endothelial cells attached to the construct lumen and appeared to form a confluent lining (Figure 4.29). Thus, the bioreactor system supports straightforward introduction of endothelial cells to growing arterial constructs with similar to native artery architecture without first having to remove a mechanical support from the construct lumen (Niklason et al., 1999), separately create sheets of the different cell types (L'Heureux et al., 1998), or rotate the cell suspension (Nasseri, 2003).

V.4 Single and Dual Seeding of SMC in the Bioreactor

Small diameter arteries are tissues with hierarchical wall architecture. In our attempt to develop a blood vessel substitute, a PGA scaffold was seeded with SMC and EC. Therefore, tissue-engineered arterial constructs developed in the bioreactor did not have the three-layered structure of native vessels. Other groups have shown that the adventitia layer is not essential in creating a patent vessel substitute (Niklason et al., 1999) and fibroblasts were omitted in this thesis for simplicity. However, based on the dynamic seeding capability of the bioreactor, seeding of the construct's external surface with fibroblasts is possible. A fibroblast cell suspension can be perfused on the construct external surface for 24 hours once the media layer has been populated with SMC (after 10-15 days of SMC culture).

Since our perfusion bioreactor has fluid flow both through the lumen and on the external surface, we investigated the effect of seeding SMC on both surfaces. To this effect, SMC were seeded through the lumen of the scaffolds for 48 hours (single seeding), or through the lumen for 24 hours and on the external surface for an additional 24 hours (dual seeding). In both cases, EC were seeded only through the construct lumen on day 23 and constructs were harvested on day 25. Our hypothesis was that dual seeding will lead to increased cell attachment compared to single seeding, and result in uniform cell distribution and matrix deposition across the construct wall. Biochemical analysis of harvested constructs showed that cell number and density were similar under both protocols, and collagen and GAG per dry weight and per cell were higher in dual-seeded compared to single-seeded constructs, but this increase was not statistically significant. Although cell distribution was similar under the two seeding protocols,

collagen and elastin staining was more intense in dual-seeded compared to single-seeded constructs.

Although definite conclusions cannot be made solely based on biochemical analysis, histological analysis supported the biochemical data suggesting that matrix production is increased in dual-seeded compared to single-seeded constructs. These data were further supported by morphological observations. Dual-seeded constructs had better handling ability (i.e. structural integrity) than single-seeded constructs and were used in mechanical testing. Furthermore, single-seeded constructs had a smaller lumen diameter compared to dual-seeded constructs, indicating that SMC proliferated toward the lumen in single seeding since all scaffolds had the same inner diameter initially. This could be due to the higher cell seeding density in the construct lumen compared to dual seeding, where SMC are introduced both through the lumen and on the external surface. Therefore, dual-seeded constructs had higher matrix deposition and better handling ability compared to single-seeded constructs, and it was concluded that dual seeding of SMC in PGA scaffolds is superior to single seeding and leads to mechanically stronger arterial constructs. Based on this conclusion, the dual seeding protocol was used to compare early versus late endothelialization of constructs described in the following section.

The cell seeding efficiency of single and dual seeding was also compared and was similar in both cases. This was a surprising finding since the culture medium volume of the external flow loop is significantly larger than that of the lumen flow loop. It is consistent, however, with the scaffold's high porosity that allows cells to be distributed evenly in the total volume of the culture medium that is the same in both seeding

protocols. Therefore, the differences observed between the two protocols are most likely associated with differential cell attachment and migration rather than different initial cell numbers.

Since similar cell number attached to PGA scaffolds in single and dual seeding experiments, cell distribution in the medium was likely different in the two protocols. It is likely that cell density is higher inside the scaffold during single seeding (because cells are delivered through the lumen) compared to dual seeding (where cells are first perfused through the lumen and then on the scaffolds' external surface). Therefore, more cells may attach initially on the external surface of dual-seeded constructs compared to single seeding. In addition, cells preferentially populate the lumen and external surfaces of the constructs and deposit extracellular matrix proteins near the free surfaces. It can by hypothesized that in dual seeding, cells attach on the external surface and the lumen surface and are able to synthesize more matrix because nutrients are readily available. This might be in contrast to single seeding where SMC attach mostly on the lumen surface and have to compete for nutrients. If this phenomenon occurs, it is prevalent in the first couple of weeks of culture because after 25 days cells have migrated throughout the construct wall and are uniformly distributed (Figure 4.40).

In summary, two different SMC seeding protocols were investigated in the bioreactor that had an effect on cell proliferation, metabolic activity and extracellular matrix synthesis. Specifically, dual-seeded constructs contained more collagen, elastin and GAG compared to single-seeded constructs.

V.5 Early and Late Endothelialization of SMC-Seeded Constructs

The vascular wall has a multi-layered architecture with SMC, EC and fibroblasts residing predominantly in the media, intima, and adventitia layer, respectively. These different cell types participate in various processes and have different functions. However, each cell type is "dependent" on the other cells of the arterial wall, and all act as one entity towards the development, maintenance, remodeling, and regulation of the tissue under physiological and pathological conditions. Vascular tissue engineering research has focused on mimicking in vitro those components and environmental conditions of the native tissue that are deemed necessary for arterial graft replacement. For this purpose, SMC and EC are commonly used in vitro to create vascular graft substitutes. However, these two cell types are typically co-cultured for a few days in contrast to in vivo conditions, in which EC initiate vasculogenesis and angiogenesis and subsequently recruit SMC. Therefore, the in vitro approach of culturing SMC for an extended period of time and then introducing EC is the opposite of what takes place in vivo.

There are a number of reasons why tissue engineers often choose to endothelialize grafts toward the end of the culture time. First, SMC have a higher proliferative capacity compared to EC. When the two cell types are co-cultured without any physical barrier between them (this barrier is the internal elastic lamina in vivo), SMC tend to overtake EC in vitro. Second, a confluent monolayer of EC is desirable on the lumen surface of the grafts. If EC are seeded in a porous scaffold material, large number of the EC could be lost in the wall. Therefore, a SMC-seeded media layer is often developed first, followed by the endothelialization of the lumen. Third, EC retention and 100%

confluency on polymeric and even biological biomaterials has proved to be problematic, especially under fluid flow conditions. Consequently, endothelialized grafts are typically harvested shortly after the introduction of the EC to retain most of the attached cells.

However, endothelialization of arterial constructs late in culture negates cell signaling pathways between SMC and EC that are of paramount importance in vivo. In fact, SMC proliferation, migration, differentiation and extracellular matrix production has been shown to be affected by the presence of EC. It is evident that all the SMC processes that take place during vascular graft tissue engineering are influenced by EC. Our dual perfusion bioreactor was used to dynamically seed cells on PGA scaffolds at different times without compromising sterility. We have used these characteristics to compare the effect of late (co-culture of 2 days) versus early endothelialization (co-culture of 15 days) on arterial construct development and observed significant differences. Cell number was significantly increased in early EC constructs, which could be due to either increased SMC proliferation, EC proliferation, or both. It has been shown that proliferative EC induce SMC proliferation, which implies that both cell types are in a proliferative state and contribute to the increased cell number in early EC compared to late EC constructs.

SMC production of collagen and GAG was also affected by the early presence of EC. Early EC constructs contained significantly less collagen and GAG per cell compared to late EC constructs. Additionally, collagen per dry weight was significantly decreased in early compared to late EC constructs. This phenomenon could be linked to SMC differentiation. Indeed, decreased matrix production could be associated with a switch in SMC phenotypic expression toward a more contractile phenotype that is characterized by decreased matrix production compared to a more synthetic phenotype.

Even though smooth muscle α-actin and calponin expression were similar in both early and late EC constructs, myosin heavy chain expression was more intense in early compared to late EC constructs. This indicates that SMC are in a more contractile phenotype in early compared to late EC constructs, but it is not known whether SMC in early EC constructs differentiate at an earlier time in culture compared to late EC constructs. A likely explanation is that EC proliferate after seeding leading to increased SMC proliferation, and subsequently regulate SMC differentiation to a more contractile phenotype through cell signaling. This behavior slows down SMC proliferation and extracellular matrix production.

Cell distribution across the construct wall varied significantly between the two EC seeding protocols. Late EC constructs were characterized by higher cell density close to the lumen and the external surface, whereas early EC constructs had a more uniform cell distribution across the wall. This cell distribution could be due to the EC forming a monolayer on the lumen surface, thereby preventing excessive SMC proliferation in the lumen, and/or EC could increase SMC migration, leading to a more uniform cell distribution.

Longer term co-culture of SMC and EC resulted in increased cell proliferation, more uniform cell distribution and reduced extracellular matrix deposition compared to 2-day co-culture studies. Therefore, EC appear to induce SMC proliferation and migration, which is desirable during early culture times, at the expense of matrix deposition. EC seeding concurrently with SMC could provide SMC proliferation and distribution early in culture followed by extracellular matrix deposition.

These experiments led insight into SMC-EC interactions when the two cell types are co-cultured in a PGA scaffold in a perfusion bioreactor. It was observed that long term co-culture resulted in significant changes in cell number, collagen and GAG deposition per cell, and cell distribution and differentiation. Dynamic cell seeding in one bioreactor allows for the introduction of different cell types at different times in culture without compromising sterility and with few handling steps. This important bioreactor feature can be used for the seeding of scaffolds with any cell type toward the development of tissues with complex architecture.

V.6 Inter- and Intra-Construct Variability

Multi-module experiments were performed to explore the feasibility of bioreactor scale-up by increasing the number of constructs in the bioreactor. Inter-construct (construct to construct) variability analysis for a given bioreactor run is very important because reproducible results are essential. Each construct cultured in the same bioreactor and under the same conditions should have similar properties. Results demonstrate that constructs seeded with the same smooth muscle cells in adjacent modules yielded similar cellularity (Figure 4.24) and matrix deposition. This suggests that a perfusion bioreactor design with a common culture medium reservoir can be used to develop multiple homogeneous constructs.

Data collected from two-module bioreactor experiments was used to analyze the inter-construct and intra-construct (middle versus edge of each construct) variability in terms of cell number and collagen deposition. Figure 5.1 compares cell number and Figure 5.2 compares collagen content in the middle section of construct 1 versus the

middle section of construct 2 in dual seeding with early and late EC. There were no statistically significant differences between the two constructs in either case. This shows that constructs cultured in a two-module bioreactor under dual seeding with late and early EC have similar cell numbers and collagen content for each experimental protocol.

Furthermore, we investigated whether the middle of the constructs had different properties than the edges in terms of cell number and collagen content. Figure 5.3 shows that there was no statistically significant difference between the middle section of the constructs and their edges in dual seeding with early EC experiments. Single and dual seeding late EC experimental data were not analyzed because there were not sufficient numbers of constructs to draw statistical conclusions.

In every experiment, a 5 mm long section from the middle of each construct is used for biochemical analysis. In some experiments, additional sections were taken from the edges. Since the total construct length was approximately 25 mm, 5-mm long sections from the edges were not harvested for each experiment. Sections taken from the constructs were used not only for biochemical analysis, but also for histology, scanning electron microscopy, and occasionally for mechanical testing and confocal microscopy. Therefore, intra-construct variability was studied from two dual seeding early EC independent experiments with 2-3 sections from each experiment. Since the inter-construct variability analysis showed that there are no statistically significant differences between the two constructs cultured in a given bioreactor, we pooled the data of the two experiments and sample size increased to 4 samples for the middle sections and 6 for the edges of the constructs.

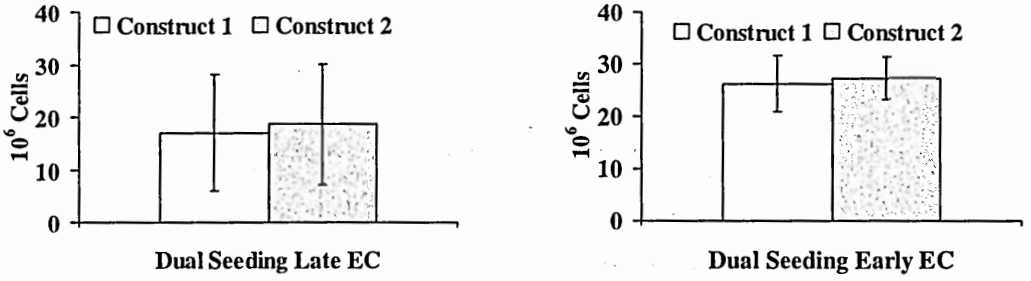

Figure 5.1 Construct to Construct Variability in Cell Number in Two Module Bioreactors in Dual Seeding Late and Early EC Experiments.
Data are collected from a 5 mm construct ring. Data are mean ± standard deviation for N = 3 independent experiments with n = 1 construct per experiment.

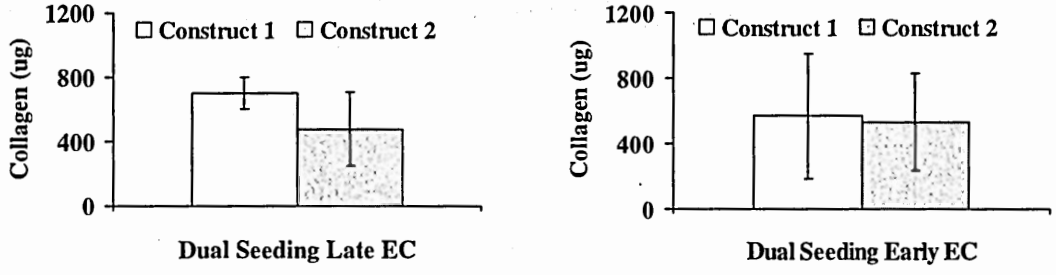

Figure 5.2 Construct to Construct Variability in Collagen Content in Two Module Bioreactors in Dual Seeding Late and Early EC Experiments.
Data are collected from a 5 mm construct ring. Data are mean ± standard deviation for N = 3 independent experiments with n = 1 construct per experiment.

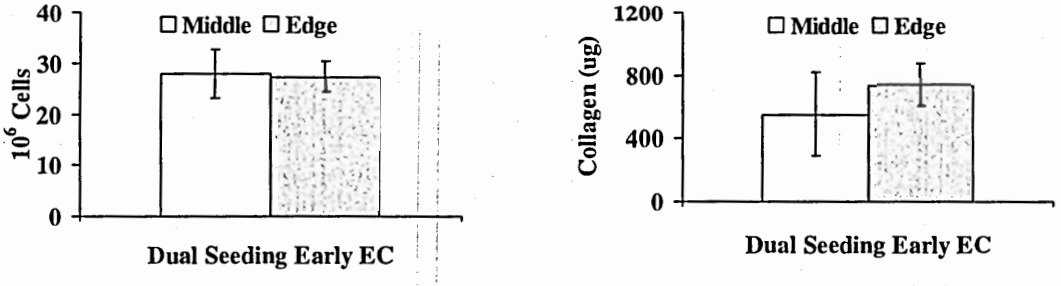

Figure 5.3 Middle to Edge of the Construct Variability in Cell Number and Collagen Content in Two Module Bioreactors in Dual Seeding Early EC Experiments.
Data are collected from a 5 mm construct ring. Data are mean ± standard deviation for N = 2 independent experiments with n = 2-3 construct per experiment.

In summary, we showed that construct cell number and collagen content was similar across the construct's length and between constructs cultured in the same bioreactor. Additionally, histological analysis of sections from the construct middle versus the edge showed similar staining pattern, reinforcing the biochemical data.

V.7 Dual Perfusion Bioreactor Limitations

Existing arterial construct culture technologies have capitalized on both shear and cyclical strain to promote development of functional tissue-engineered blood vessel substitutes (Girton et al., 1999; He and Matsuda, 2002; Huynh et al., 1999; Kim et al., 1998; Seliktar et al., 2000). Niklason *et al.* have developed a perfusion bioreactor, in which smooth muscle cells are injected into a porous scaffold (Niklason et al., 2001; Niklason et al., 1999). Smooth muscle cells in the scaffold are cyclically stretched by pulsatile flow through a silicone tube. Cyclical stretching significantly increases construct burst pressure compared to unstretched constructs. Although the authors generated functional and patent small diameter grafts using animal cells, the bioreactor design exhibits limited potential for scale-up and bioprocessing. Significantly, smooth muscle cell seeding is done individually for each construct and involves opening each bioreactor vessel for cell suspension injection. In addition, the silicone tubing must be removed prior to lumen endothelialization, introducing considerable complexity to the culture process. L'Heureux *et al.* have developed a patent and vaso-responsive vascular construct composed solely of human cells and extracellular matrix by growing cell sheets in culture flasks. Constructs are fabricated by wrapping fibroblast, smooth muscle and endothelial cell sheets around each other and culturing them to prevent delamination

(L'Heureux et al., 1998; L'Heureux et al., 2001). Scale-up of this approach may be labor- and cost-intensive to meet the patient demand in a time-efficient manner. Nasseri *et al.* developed recently a dynamic cell seeding system, in which a hybridization oven was used to seed myofibroblasts under rotation (Nasseri, 2003). A large percentage of cells adhered to the polymer scaffolds and infiltrated the construct wall in experiments up to 10 days. Other recent bioreactor designs are difficult to evaluate because limited data of vascular graft growth is available (Sodian et al., 2002; Thompson, 2002).

The dual perfusion bioreactor presented in this work was designed to address limitations of current vascular tissue engineering bioreactors. The main limitations that we identified are the following:

(1) Dual perfusion to improve nutrient transport to the constructs. Arterial constructs grown in our bioreactor are perfused with culture medium both through the lumen and on their external surface decreasing the transport distance in half. This characteristic does not mimic physiologic conditions, in which only the lumen is exposed to blood flow. However, in vivo, the vasa vasorum provides nutrients to the adventitia of large arteries. Since a vasa vasorum analog has not yet been reproduced in vitro, we perfused the external surface with medium. We have used 5 mm thick PGA scaffolds in our bioreactor experiments, therefore nutrients and cellular waste/polymer degradation products need only diffuse half of that distance, thereby preventing the formation of a necrotic core.

(2) Ability to seed cells on scaffolds under dynamic conditions in the bioreactor. Dynamic cell seeding in the same bioreactor that is used for growth is a step toward long term aseptic culture and the development of a time- and cost-efficient bioprocess.

Handling steps are minimized and the bioprocess can be automated. In our bioreactor, the flow loops were switched manually but there is the potential for automation by regulating the appropriate connectors by a computer. Equally important, however, is the ability to seed different cell types into the scaffolds at different times, thereby mimicking the multi-layered architecture of the arterial wall.

(3) Reproducible production of multiple constructs. Our bioreactor is composed of modules assembled in series, so that scale-up of construct development is feasible by the mere addition of additional modules. Reproducibility is ensured by having one culture medium reservoir that is used for the lumen and external flow loops. In addition, all constructs share the external space of the bioreactor, thereby allowing cell-cell signaling and enhanced growth conditions, for example by growth factor secretion.

However, like every other man-made device, our bioreactor has limitations. Dynamic cell seeding in the dual perfusion bioreactor results in low seeding efficiency. This could be due to the design itself or the large medium volume that is diluting the cell suspension. The bioreactor rests on an incubator shelf horizontally with the constructs parallel to the surface. Except for the fluid flow facilitated by pumps, there is no rotation of the bioreactor or mixing that can keep the cells in suspension during seeding and increase cell seeding efficiency. Short term experiments have shown that cells are uniformly distributed across the construct wall (Figures 4.22 and 4.25). Therefore, perfusion alone appears sufficient for uniform cell seeding. Alternatively, the large medium volume could be diluting the cell suspension resulting in low cell seeding efficiencies. The total medium volume of the bioreactor loop is 1 L but cells are suspended in 50 ml of medium in the syringes used for seeding. However, as the cell

suspension is pumped through the porous scaffolds, cells are diluted in the total medium volume as shown by the cell seeding efficiency experiments described in Chapter IV.

Furthermore, the bioreactor is run using syringe and peristaltic pumps that have high incidence of failure or malfunction. The pumps are operated independently by the user and not by a computer, which introduces experimental variability. Therefore, a computer-controlled bioreactor with incorporated pumps, although costly, would allow smoother operation, higher reliability, and fewer lost experiments.

Potential modifications of the current bioreactor design that address some of the limitations discussed above are described in Chapter VI.

V.8 Challenges of Vascular Graft Development in the Dual Perfusion Bioreactor

There were two major challenges related to the vascular graft development aspect of this thesis. The first was the significantly lower ECM content compared to native vessels and the second was the difficulty of identifying EC in the constructs. Both 25- and 35-day experiments yielded collagen synthesis in the order of 2-4% of the construct dry weight (Tables 4.2 and 4.6 and Figures 4.38 and 4.52). Furthermore, elastin content was so low that it could only be detected by immunohistochemical analysis. However, GAG content was 44% after 25 days and 57% of the construct dry weight after 35 days of culture. Histological analysis showed that SMC express differentiated phenotype as early as 16 days in the bioreactor (Figure 4.23). Therefore, it appears that SMC switch to a more contractile phenotype characterized by reduced matrix synthesis early in bioreactor culture. Strategies to increase ECM production through medium supplementation and mechanical stimulation are discussed later in this Chapter.

Construct endothelialization took place at different times in culture, i.e. after 10 days in early and after 23 days in late endothelialization. The constructs were stained with different EC-specific markers to investigate the distribution of EC. Most of the markers studied (such as platelet and vascular endothelial cell adhesion molecules, PECAM-1 and VCAM-1) were not reactive to bovine cells. Species reactivity was established with vWF but the antibody did not show sufficient specificity (Figure 4.44). Indeed, the antibody stained polymer fragments throughout the construct wall, and staining was diffuse in the extracellular matrix and not localized in or around cells. Therefore, the distribution of EC could not be directly studied in these experiments. Use of a different cell species with available EC-specific antibodies could elucidate the fate of EC seeded on the constructs.

The materials used, aside from the bioreactor itself, and the implemented conditions likely introduced additional limitations. First, bovine aortic SMC and EC were used in all bioreactor experiments. Despite the advantages of using these cells, there is a major drawback: arterial constructs created with bovine cells cannot be used in animal studies without administering anti-coagulants and cannot be implanted for long term evaluation as xenografts. Animal models thought to mimic the human vasculature include canine and baboon, and such models are preferred for in vivo experiments prior to clinical studies. However, the main objective of this thesis did not include animal studies and bovine cells helped validate the bioreactor.

Second, PGA is not the best biomaterial for the engineering of vascular grafts. In addition to its high degradation rate, the acidic degradation products may cause adverse immune reactions in vivo and affect cell function in vitro. Additionally, the PGA surface

properties can be modified to increase its biocompatibility but the only pretreatment we investigated was prewetting with culture medium. Perhaps other surface modifications (e.g. growth factor grafting) could increase cell attachment and migration leading to high cell seeding efficiency and uniform cell distribution across the thickness of the scaffolds. The polymer scaffold wall thickness could also be decreased to improve nutrient transport and cell distribution. Alternatively, a non-degradable scaffold could be used on the external surface of the constructs to increase mechanical strength while cells are producing extracellular matrix proteins.

Third, the culture medium composition was not specifically optimized for the cells and polymer scaffold used in these experiments. The culture medium composition used was a combination of recipes reported elsewhere (Imberti et al., 2002; Niklason et al., 1999). Although culture medium composition and addition of various components has been studied extensively, no "gold standard" has been found for a given type of experiment. Therefore, the culture medium used aimed at providing growth factors that result in cell proliferation, and contained ascorbic acid and amino acids that promote extracellular matrix synthesis. Neither the composition, nor the concentrations were optimized for these experiments. However, the medium composition was modified during the culture time by removing the externally-added growth factors (basic fibroblast and epidermal growth factors) from the medium after 10 days of culture. We have observed from short term experiments that significant cell proliferation occurs during the first 9 days of bioreactor culture, and we were interested in decreasing proliferation and increasing matrix production. During in vitro vascular graft development, there are different events that take place at different times. In our bioreactor the following

chronological sequence would be desirable: SMC attachment, SMC proliferation and migration, SMC production of extracellular matrix, and SMC phenotypic switch to a more contractile phenotype. EC seeding could take place at any time during these events. It can be foreseen that each phase could require a different culture medium that would facilitate each event.

Fourth, the mechanical environment provided in the bioreactor was not modified significantly during the culture time. If we consider the ideas presented above, it becomes clear that differential mechanical cues during culture time could significantly assist or enhance cell attachment, migration, proliferation, matrix production, and differentiation. There are many lessons to be learned from developmental biology in this matter. Indeed, during angiogenesis SMC (pericytes) are recruited by EC prior to any blood flow, i.e. there is no cyclic strain experienced by the SMC. Yet, solely by SMC-EC signaling cues, SMC migrate and proliferate to create the new vessel. Therefore, mechanical stimuli could be modified with culture time to promote specific cellular processes as described in Chapter VI.

CHAPTER VI

CONCLUSIONS AND RECOMMENDATIONS

Great advances have been made recently in vascular tissue engineering (Campbell et al., 1999; L'Heureux et al., 1998; Niklason et al., 1999). However, concepts such as dynamic cell seeding, scaleability, and reproducibility have not been directly explored. This thesis has led insight into parameters that are considered important in vascular graft development.

The dual perfusion bioreactor developed in this work can be used for dynamic seeding of SMC and EC into PGA scaffolds. Cell seeding and tissue maturation took place in the same bioreactor, thereby minimizing handling steps that increase contamination risk. SMC adhered to the polymer fibers, were uniformly distributed across the construct wall, deposited extracellular matrix proteins and expressed a differentiated phenotype. Therefore, the nutrient environment and pulsatile shear stress provided by the bioreactor support arterial construct growth.

The independent lumen and external flow loops were used to compare single (lumen only) to dual (lumen and external surface) seeding of SMC. Higher cell number and matrix content was found in dual-seeded constructs indicating that the cell seeding method affects long term growth and tissue properties.

Dynamic cell seeding allowed the introduction of EC at different times during the culture: after 10 days (early EC) and after 23 days (late EC) of SMC dual-seeded constructs. Long term co-culture (15 days) of EC and SMC resulted in significantly higher cell number and lower collagen and GAG content compared to short term

co-culture (2 days). These results show that EC regulate SMC functions and control the amount of extracellular matrix produced. This finding gives tissue engineers one more parameter that can be used for optimal growth of vascular grafts in vitro. Specifically, increasing EC seeding density would decrease EC and SMC proliferation (proliferating EC increase SMC proliferation) and possibly enhance SMC extracellular matrix production.

The dual perfusion bioreactor is scaleable and two-module experiments showed no significant variation between constructs cultured in the same bioreactor. Additionally, there were no significant differences in composition and architecture along the length of the arterial constructs. Therefore, reproducibility is feasible in this bioreactor as also shown from a short term three-module bioreactor experiment. However, future work is required to address some of the limitations described in Chapter V and further advance vascular graft development in bioreactors.

The cell seeding density used in these experiments was rather low (approximately $43x10^3$ cells/ml) considering the total medium volume that the cell suspension was diluted into due to the scaffold's porosity. As a result, cell seeding efficiency was low, and high cell proliferation rates are required to achieve native tissue density (10^8 cells/cm^3) (Ziegler and Nerem, 1994). However, seeding efficiency and tissue cell density can be increased by doubling initial cell seeding number and reducing the total medium volume (i.e. increasing cell seeding density). The latter technique can be achieved by closing one of the flow loops during the seeding phase. For example, while cells are seeded through the lumen the external flow loop can be clamped shut and vice versa. This will reduce the medium volume from 1100 ml (in a two-module bioreactor)

to 300 ml, and likely increase cell seeding density. A more sophisticated way of further reducing the medium volume during lumen seeding would be to use a biodegradable sleeve around the constructs. This material should have high degradation rates, and degrade within 24 hours. Such an approach would decrease the medium volume from 1100 ml to 50 ml and significantly increase cell seeding density. These manipulations are necessary to attain high tissue density within short culture times and render the process time-efficient.

The polymer scaffold used in the bioreactor experiments has been employed successfully by many groups in vascular tissue engineering (Niklason et al., 1999; Nikolovski and Mooney, 2000; Shum-Tim et al., 1999). One limitation of this biomaterial is the release of acidic degradation products into the culture environment that lower medium pH (Agrawal and Athanasiou, 1997) and probably negatively affect cell viability and function. The bioreactor described here efficiently addressed nutrient and waste product transport by perfusing both the lumen and the external surface of the constructs, thereby reducing the transport distance in half. However, the scaffolds used were 5 mm thick, which brings the transport distance to 2.5 mm. This distance is close to the maximum distance that oxygen, and other perhaps nutrients, can diffuse to in tissues considering oxygen diffusivity and metabolic consumption by mammalian cells in native tissue. At the initial stages of the experiments, the scaffold is 97% porous and nutrients/waste products are advected into the wall. However, as cells proliferate and deposit matrix proteins wall permeability is decreased and diffusion comes into play. These observations are consistent with histological data that show an area sparsely populated with cells and high in polymer content in the middle of the cross-sections.

Therefore, PGA scaffolds 2 mm thick would overcome any diffusion-related transport limitations of nutrients, and cell and polymer waste products.

A current limitation of the bioreactor loop is that medium replenishment is not continuous. In the majority of the experiments described, medium is replaced every 5 days by draining the bioreactor into the medium reservoir, discarding spent medium, and adding fresh medium. This approach not only adds handling steps to the process, but it also results in spikes in pH, glucose, and lactate. Therefore, forming a continuous medium replenishment loop with three medium reservoirs (fresh, working, and spent medium reservoirs) would help maintain fairly constant levels of pH, glucose, and lactate in the medium.

The mechanical environment experienced by the cells has a significant effect on arterial construct development. The mechanical cues necessary for vascular graft development in vitro have not been completely identified. Pulsatile shear stress, strain and tension are mechanical components cells are exposed to in vivo but not by all cell types and not at all times. During vasculogenesis, SMC are recruited by EC and proliferate to form the arterial wall before the initiation of blood flow. Clearly, EC and SMC are not exposed to those mechanical forces, and rely on cell-cell signaling pathways. Furthermore, SMC are not directly exposed to shear stress in vivo, except in injury and disease situations. In an attempt to mimic the in vivo conditions, the mechanical cues used in bioreactor experiments should be not only cell- but also time-dependent. It appears logical that both shear stress and pressure should be increased gradually during culture to allow for strong cell attachments and subsequently tissue differentiation. Low shear stress (1-3 dynes/cm^2) should be used in the first 5 days of

culture to allow cells to form firm attachments to their extracellular matrix. Shear stress should be gradually increased to 15 dynes/cm^2 after day 5 until day 10 and maintained at that level for the duration of the experiments. Pressure should also increase gradually as the arterial constructs mature. Atmospheric pressure should be used for the first 5 days of culture and gradually increased to 100 mmHg by day 15. Pressure can then be further increased to 150 mmHg for the duration of the experiment. This regimen will provide the mechanical cues that SMC are exposed to in vivo.

The nutrient environment should also be time-dependent. In these experiments, externally-added growth factors were removed from the medium after 10 days of culture to reduce cell proliferation and facilitate differentiation. Indeed, it was observed that SMC expressed contractile markers and were in a highly differentiated state. However, collagen and particularly elastin content were significantly lower than the in vivo content. Therefore, medium composition as a function of time should be further investigated for increased matrix production and mechanical strength.

Combining these strategies with the dual perfusion bioreactor can render this system a useful tool not only for engineering vascular grafts but also an in vitro model of the arterial wall that can be used to study cell-cell and cell-biomaterial interactions. Furthermore, this bioreactor can be exploited as a laboratory-scale device to address large-scale bioprocessing-related questions of vascular graft development.

APPENDIX

B.1 Raw Data for Cell Proliferation in Short Term Experiments.

Harvest Date	B/R Modules	Cells	Days	Cell Seeding # ($x10^{-6}$)	Cell Harvest # (10^{-6})	Text Reference
1/31/02	1	SMC	4	9.9	41.3	Figure 4.21
2/13/02	1	SMC	9	11.3	43.1	Figure 4.21
3/29/02	1	SMC	16	25.3	68.7	Figure 4.21
3/8/02	3	SMC	8	6.6	15.1	Figure 4.24
3/8/02				6.6	15.4	
3/8/02				6.6	18.8	

B.2 Raw Data for Cell Proliferation and Extracellular Matrix Production in 25-Day Experiments.

Harvest Date	8/11/02	12/12/02	12/12/02
B/R Modules = 1	Cells = SMC	Days = 25	
Experiment	1	2	3
Cell Seeding # ($x10^{-6}$)	47	47	47
Cell Harvest # (10^{-6})	122.5	91.7	93.0
Cell Harvest # per g Dry Wt (10^{-6})	1,065	1,019	968
Collagen (mg)	1.3	2.0	2.6
Collagen per Dry Wt (%)	1.1	2.0	2.5
Collagen per Cell (pg)	10.6	19.9	25.9
GAG (mg)	19.2	19.7	18.3
GAG per Dry Wt (%)	16.7	21.9	19.1
GAG per Cell (pg)	157.1	214.9	197.0
Text Reference	Table 4.2	Table 4.2	Table 4.2

B.3 Raw Data for Cell Proliferation and Extracellular Matrix Production in 35- and 15-Day Experiments.

Harvest Date	9/18/02	11/3/02
B/R Modules	1	1
Cells	SMC	SMC + EC
Days	35	15
Cell Seeding # ($x10^{-6}$)	70.9	47
Cell Harvest # (10^{-6})	99.1	128.5
Cell Harvest # per g Dry Wt (10^{-6})	929.7	221.0
Collagen (mg)	1.2	1.1
Collagen per Dry Wt (%)	2.5	0.8
Collagen per Cell (pg)	27.0	34.5
GAG (mg)	12.4	23.9
GAG per Dry Wt (%)	56.7	16.8
GAG per Cell (pg)	610.0	760.4
Text Reference	Table 4.6	Table 4.4

B.4 Raw Data for Cell Proliferation in 25-Day Single Seeding Late Endothelialization Experiments.

Harvest Date	3/29/03	4/8/03	4/22/03	4/22/03	5/13/03	5/13/03
B/R Modules	2		2		2	
Cells	SMC + EC	SMC + EC	SMC + EC	SMC + EC	SMC + EC	SMC + EC
Days	15	25	25	25	25	25
Experiment	1	1	2	2	3	3
Construct	1	2	1	2	1	2
Cell Seeding # ($x10^{-6}$)	93.3	93.3	93.3	93.3	93.3	93.3
Cell Harvest # (10^{-6}) (5 mm ring)	Edge: 15.2	Middle: 12.9 Edge 1: 12.4 Edge 2: 16.8	Middle: 25.6	Middle: 21.1 Edge 1: 30.5 Edge 2: 18.2	Middle: 14.2	Middle: 14.5
Cell Harvest # per g Dry Wt (10^{-6}) (5 mm ring)	Edge: 390.1	Middle: 644.2 Edge 1: 653.0 Edge 2: 765.1	Middle: 1,024.8	Middle: 705.0 Edge 1: 708.5 Edge 2: 673.1	Middle: 786.5	Middle: 689.7
Text Reference	None	Figure 4.38	Figure 4.38	Figure 4.38	Figure 4.38	Figure 4.38

B.5 Raw Data for Extracellular Matrix Production in 25-Day Single Seeding Late Endothelialization Experiments.

Harvest Date	3/29/03	4/8/03	4/22/03	4/22/03	5/13/03	5/13/03
B/R Modules	2		2		2	
Days	15	25	25	25	25	25
Experiment	1	1	2	2	3	3
Construct	1	2	1	2	1	2
Collagen (mg) (5 mm ring)	Edge: 1.1	Middle: 0.4 Edge 1: 0.4 Edge 2: 1.1	Middle: 1.3	Middle: 0.4 Edge 1: 0.3 Edge 2: 0.3	Middle: 0.5	Middle: 0.5
Collagen per Dry Wt (%) (5 mm ring)	Edge: 2.9	Middle: 2.1 Edge 1: 2.0 Edge 2: 5.0	Middle: 5.4	Middle: 1.2 Edge 1: 0.6 Edge 2: 1.3	Middle: 3.0	Middle: 2.4
Collagen per Cell (ng) (5 mm ring)	Edge: 0.08	Middle: 0.03 Edge 1: 0.03 Edge 2: 0.06	Middle: 0.05	Middle: 0.02 Edge 1: 0.01 Edge 2: 0.02	Middle: 0.04	Middle: 0.04
GAG (mg) (5 mm ring)	Edge: 9.5	Middle: 6.9 Edge 1: 13.6 Edge 2: 7.7	Middle: 3.6	Middle: 7.1 Edge 1: 10.1 Edge 2: 10.2	Middle: 8.4	Middle: 8.5
GAG per Dry Wt (%) (5 mm ring)	Edge: 24.3	Middle: 34.5 Edge 1: 71.5 Edge 2: 34.8	Middle: 14.5	Middle: 23.5 Edge 1: 23.4 Edge 2: 37.9	Middle: 46.9	Middle: 42.6
GAG per Cell (ng) (5 mm ring)	Edge: 0.6	Middle: 0.5 Edge 1: 1.1 Edge 2: 0.5	Middle: 0.1	Middle: 0.3 Edge 1: 0.3 Edge 2: 0.6	Middle: 0.6	Middle: 0.6
Text Reference	None	Figure 4.38	Figure 4.38	Figure 4.38	Figure 4.38	Figure 4.38

B.6 Raw Data for Cell Proliferation in 25-Day Dual Seeding Late Endothelialization Experiments.

Harvest Date	2/11/03	2/11/03	5/20/03	5/20/03	5/27/03	5/27/03
B/R Modules	2		2		2	
Cells	SMC + EC	SMC + EC	SMC + EC	SMC + EC	SMC + EC	SMC + EC
Days	25	25	25	25	25	25
Experiment	1	1	2	2	3	3
Construct	1	2	1	2	1	2
Cell Seeding # ($x10^{-6}$)	93.3	93.3	93.3	93.3	93.3	93.3
Cell Harvest # (10^{-6}) (5 mm ring)	Middle: 15.0	Middle: 24.4	Middle: 29.0	Middle: 26.0	Middle: 7.2 Edge: 12.6	Middle: 5.5 Edge: 9.2
Cell Harvest # per g Dry Wt (10^{-6}) (5 mm ring)	Middle: 748.0	Middle: 659.0	Middle: 966.7	Middle: 1,040.3	Middle: 598.4 Edge: 571.8	Middle: 681.6 Edge: 763.7
Text Reference	Figure 4.38	Figure 4.38	Figure 4.38	Figure 4.38	Figure 4.38	Figure 4.38

B.7 Raw Data for Extracellular Matrix Production in 25-Day Dual Seeding Late Endothelialization Experiments.

Harvest Date	2/11/03	2/11/03	5/20/03	5/20/03	5/27/03	5/27/03
B/R Modules	2		2		2	
Days	25	25	25	25	25	25
Experiment	1	1	2	2	3	3
Construct	1	2	1	2	1	2
Collagen (mg) (5 mm ring)	Middle: 0.6	Middle: 0.2	Middle: 0.8	Middle: 0.7	Middle: 0.7 Edge: 0.9	Middle: 0.5 Edge: 1.5
Collagen per Dry Wt (%) (5 mm ring)	Middle: 3.0	Middle: 0.6	Middle: 2.7	Middle: 2.6	Middle: 5.9 Edge: 4.2	Middle: 6.8 Edge: 12.2 (not used)
Collagen per Cell (ng) (5 mm ring)	Middle: 0.04	Middle: 0.01	Middle: 0.03	Middle: 0.03	Middle: 0.10 Edge: 0.07	Middle: 0.10 Edge: 0.16
GAG (mg) (5 mm ring)	Middle: 7.1	Middle: 14.6	Middle: 4.7	Middle: 15.2	Middle: 8.3 Edge: 4.3	Middle: 10.5 Edge: 8.6
GAG per Dry Wt (%) (5 mm ring)	Middle: 35.7	Middle: 39.5	Middle: 15.5	Middle: 60.8	Middle: 69.6 Edge: 19.6	Middle: 131.1 (not used) Edge: 71.7
GAG per Cell (ng) (5 mm ring)	Middle: 0.5	Middle: 0.6	Middle: 0.2	Middle: 0.6	Middle: 1.2 Edge: 0.3	Middle: 1.9 Edge: 0.9
Text Reference	Figure 4.38	Figure 4.38	Figure 4.38	Figure 4.38	Figure 4.38	Figure 4.38

B.8 Raw Data for Cell Proliferation in 25-Day Dual Seeding Early Endothelialization Experiments.

Harvest Date	6/10/03	6/10/03	6/24/03	6/24/03	8/5/03	8/5/03
B/R Modules	2		2		2	
Cells	SMC + EC	SMC + EC	SMC + EC	SMC + EC	SMC + EC	SMC + EC
Days	25	25	25	25	25	25
Experiment	1	1	2	2	3	3
Construct	1	2	1	2	1	2
Cell Seeding # ($x10^{-6}$)	93.3	93.3	93.3	93.3	93.3	93.3
Cell Harvest # (10^{-6}) (5 mm ring)	Middle: 31.8 Edge: 26.5	Middle: 30.4 Edge: 24.2	Middle: 20.9 Edge 1: 29.9 Edge 2: 26.9	Middle: 28.9 Edge 1: 24.2 Edge 2: 31.8	Middle: 25.8	Middle: 22.6
Cell Harvest # per g Dry Wt (10^{-6}) (5 mm ring)	Middle: 1,223.0 Edge: 1,202.5	Middle: 1,012.3 Edge: 967.7	Middle: 871.5 Edge 1: 1,148.4 Edge 2: 960.8	Middle: 904.3 Edge 1: 1,208.2 Edge 2: 1,026.4	Middle: 1,033.5	Middle: 835.3
Text Reference	Figure 4.52	Figure 4.52	Figure 4.52	Figure 4.52	Figure 4.52	Figure 4.52

B.9 Raw Data for Extracellular Matrix Production in 25-Day Dual Seeding Early Endothelialization Experiments.

Harvest Date	6/10/03	6/10/03	6/24/03	6/24/03	8/5/03	8/5/03
B/R Modules	2		2		2	
Days	25	25	25	25	25	25
Experiment	1	1	2	2	3	3
Construct	1	2	1	2	1	2
Collagen (mg) (5 mm ring)	Middle: 0.2 Edge: 0.7	Middle: 0.7 Edge: 0.6	Middle: 0.6 Edge 1: 0.9 Edge 2: 0.7	Middle: 0.7 Edge 1: 0.6 Edge 2: 0.9	Middle: 0.9	Middle: 0.2
Collagen per Dry Wt (%) (5 mm ring)	Middle: 0.6 Edge: 3.1	Middle: 2.3 Edge: 2.4	Middle: 2.7 Edge 1: 3.3 Edge 2: 2.5	Middle: 2.2 Edge 1: 3.2 Edge 2: 3.0	Middle: 3.6	Middle: 0.7
Collagen per Cell (ng) (5 mm ring)	Middle: 0.005 Edge: 0.03	Middle: 0.02 Edge: 0.02	Middle: 0.03 Edge 1: 0.03 Edge 2: 0.03	Middle: 0.02 Edge 1: 0.03 Edge 2: 0.03	Middle: 0.04	Middle: 0.01
GAG (mg) (5 mm ring)	Middle: 10.4 Edge: 3.5	Middle: 8.6 Edge: 5.5	Middle: 10.0 Edge 1: 7.9 Edge 2: 8.1	Middle: 12.5 Edge 1: 9.3 Edge 2: 8.9	Middle: 12.9	Middle: 17.7
GAG per Dry Wt (%) (5 mm ring)	Middle: 40.0 Edge: 16.1	Middle: 28.7 Edge: 22.1	Middle: 41.6 Edge 1: 30.5 Edge 2: 28.9	Middle: 38.9 Edge 1: 46.5 Edge 2: 28.9	Middle: 51.6	Middle: 65.5
GAG per Cell (ng) (5 mm ring)	Middle: 0.3 Edge: 0.1	Middle: 0.3 Edge: 0.2	Middle: 0.5 Edge 1: 0.3 Edge 2: 0.3	Middle: 0.4 Edge 1: 0.4 Edge 2: 0.3	Middle: 0.5	Middle: 0.8
Text Reference	Figure 4.52	Figure 4.52	Figure 4.52	Figure 4.52	Figure 4.52	Figure 4.52

REFERENCES

Abraham, P. A., Smith D. W., and Carnes W. H. (1974). Synthesis of soluble elastin by aortic medial cells in culture. *Biochem Biophys Res Commun* 58, 597.

Agrawal, C. M., and Athanasiou K. A. (1997). Technique to control pH in vicinity of biodegrading PLA-PGA implants. *J Biomed Mater Res* 38, 105.

American Heart Association. Heart Disease and Stroke Statistics - 2003 Update. 2003.

Anderson, J. M. Perspectives on the in vivo responses of biodegradable polymers. In: Hollinger J, ed. Biomedical applications of synthetic biodegradable polymers, 1995.

Antonelli-Orlidge, A., Saunders K. B., Smith S. R., and D'Amore P. A. (1989). An activated form of transforming growth factor beta is produced by cocultures of endothelial cells and pericytes. *Proc Natl Acad Sci U S A* 86, 4544.

Assoian, R. K., and Marcantonio E. E. (1996). The extracellular matrix as a cell cycle control element in atherosclerosis and restenosis. *J Clin Invest* 98, 2436.

Bassiouny, H., Sakaguchi Y., and Glagov S. Non-invasive imaging of atherosclerosis. In: Mercuri M, McPherson DD, Bassiouny H, Glagov S, eds. Carotid Atherosclerosis: From Induction to Complication: Kluwer Academic Publishers, 1997.

Benbrahim, A., L'Italien G. J., Kwolek C. J., Petersen M. J., Milinazzo B., Gertler J. P., Abbott W. M., and Orkin R. W. (1996). Characteristics of vascular wall cells subjected to dynamic cyclic strain and fluid shear conditions in vitro. *J Surg Res* 65, 119.

Berglund, J. D., Mohseni M. M., Nerem R. M., and Sambanis A. (2003). A biological hybrid model for collagen-based tissue engineered vascular constructs. *Biomaterials* 24, 1241.

Bhat, V. D., Truskey G. A., and Reichert W. M. (1998). Fibronectin and avidin-biotin as a heterogeneous ligand system for enhanced endothelial cell adhesion. *J Biomed Mater Res* 41, 377.

Burg, K. J., Holder W. D., Jr., Culberson C. R., Beiler R. J., Greene K. G., Loebsack A. B., Roland W. D., Eiselt P., Mooney D. J., and Halberstadt C. R. (2000). Comparative study of seeding methods for three-dimensional polymeric scaffolds. *J Biomed Mater Res* 52, 576.

Burke, A. P., Farb A., Malcom G. T., Liang Y. H., Smialek J., and Virmani R. (1997). Coronary risk factors and plaque morphology in men with coronary disease who died suddenly. *N Engl J Med* 336, 1276.

Cameron, A., Davis K. B., Green G., and Schaff H. V. (1996). Coronary bypass surgery with internal-thoracic-artery grafts--effects on survival over a 15-year period. *N Engl J Med* 334, 216.

Campbell, G. CJH: Phenotypic Modulation of Smooth Muscle Cells in Primary Culture. Vacular Smooth Muscle in Culture. CRC Press, 1985.

Campbell, J. H., and Campbell G. R. (1986). Endothelial cell influences on vascular smooth muscle phenotype. *Annu Rev Physiol* 48, 295.

Campbell, J. H., Efendy J. L., and Campbell G. R. (1999). Novel vascular graft grown within recipient's own peritoneal cavity. *Circ Res* 85, 1173.

Carey, D. J. (1991). Control of growth and differentiation of vascular cells by extracellular matrix proteins. *Annu Rev Physiol* 53, 161.

Carrier, R. L., Rupnick M., Langer R., Schoen F. J., Freed L. E., and Vunjak-Novakovic G. (2002). Perfusion improves tissue architecture of engineered cardiac muscle. *Tissue Eng* 8, 175.

Carson, F. Histotechnology: A Self-Instructional Text. 1990.

Casscells, W. (1992). Migration of smooth muscle and endothelial cells. Critical events in restenosis. *Circulation* 86, 723.

Chamley-Campbell, J. H., and Campbell G. R. (1981). What controls smooth muscle phenotype? *Atherosclerosis* 40, 347.

Chepda, T., Cadau M., Girin P., Frey J., and Chamson A. (2001). Monitoring of ascorbate at a constant rate in cell culture: effect on cell growth. *In Vitro Cell Dev Biol Anim* 37, 26.

Clyman, R. I., McDonald K. A., and Kramer R. H. (1990). Integrin receptors on aortic smooth muscle cells mediate adhesion to fibronectin, laminin, and collagen. *Circ Res* 67, 175.

Conte, M. S. (1998). The ideal small arterial substitute: a search for the Holy Grail? *Faseb J* 12, 43.

Cordewener, F. W., Dijkgraaf L. C., Ong J. L., Agrawal C. M., Zardeneta G., Milam S. B., and Schmitz J. P. (2000). Particulate retrieval of hydrolytically degraded poly(lactide-co-glycolide) polymers. *J Biomed Mater Res* 50, 59.

Cotran, R. S., Kumar V., and Robbins S. L. Robbins Pathologic Basis of Disease. W.B. Saunders Company, 1994.

Davies, P. F. (1986). Vascular cell interactions with special reference to the pathogenesis of atherosclerosis. *Lab Invest* 55, 5.

Davisson, T., Sah R. L., and Ratcliffe A. (2002). Perfusion increases cell content and matrix synthesis in chondrocyte three-dimensional cultures. *Tissue Eng* 8, 807.

Desmouliere, A., and Gabbiani G. Smooth muscle cell and fibroblast biological and functional features: similarities and differences. In: Schwartz SM, Mecham RP, eds. The vascular smooth muscle cell: molecular and biological responses to the extracellular matrix: Academic Press, Inc., 1995.

Deutsch, M., Meinhart J., Fischlein T., Preiss P., and Zilla P. (1999). Clinical autologous in vitro endothelialization of infrainguinal ePTFE grafts in 100 patients: a 9-year experience. *Surgery* 126, 847.

Didisheim, P., and Watson J. T. Cardiovascular applications. In: Ratner BD, Hoffman AS, Schoen FJ, Lemons JE, eds. Biomaterials Science: An Introduction to Materials in Medicine: Academic Press Inc., 1996.

Dinnar, U. Cardiovascular Fluid Dynamics. CRC Press, Inc., 1981.

Dunkern, T. R., Paulitschke M., Meyer R., Buttemeyer R., Hetzer R., Burmester G., and Sittinger M. (1999). A novel perfusion system for the endothelialisation of PTFE grafts under defined flow. *Eur J Vasc Endovasc Surg* 18, 105.

Farndale, R. W., Sayers C. A., and Barrett A. J. (1982). A direct spectrophotometric microassay for sulfated glycosaminoglycans in cartilage cultures. *Connect Tissue Res* 9, 247.

Fillinger, M. F., O'Connor S. E., Wagner R. J., and Cronenwett J. L. (1993). The effect of endothelial cell coculture on smooth muscle cell proliferation. *J Vasc Surg* 17, 1058.

Frid, M. G., Kale V. A., and Stenmark K. R. (2002). Mature vascular endothelium can give rise to smooth muscle cells via endothelial-mesenchymal transdifferentiation: in vitro analysis. *Circ Res* 90, 1189.

Fung, Y. C. Biomechanics Circulation. Springer, 1996.

Gao, J., Niklason L., and Langer R. (1998). Surface hydrolysis of poly(glycolic acid) meshes increases the seeding density of vascular smooth muscle cells. *J Biomed Mater Res* 42, 417.

Giddens, D. P., Zarins C. K., and Glagov S. (1990). Response of arteries to near-wall fluid dynamic behavior. *Appl Mech Rev* 43, S98.

Girton, T. S., Oegema T. R., Grassl E. D., Isenberg B. C., and Tranquillo R. T. (2000). Mechanisms of stiffening and strengthening in media-equivalents fabricated using glycation. *J Biomech Eng* 122, 216.

Girton, T. S., Oegema T. R., and Tranquillo R. T. (1999). Exploiting glycation to stiffen and strengthen tissue equivalents for tissue engineering. *J Biomed Mater Res* 46, 87.

Glagov, S., Bassiouny H. S., Giddens D. P., and Zarins C. K. (1995). Pathobiology of plaque modeling and complication. *Surg Clin North Am* 75, 545.

Gosgnach, W., Challah M., Coulet F., Michel J. B., and Battle T. (2000). Shear stress induces angiotensin converting enzyme expression in cultured smooth muscle cells: possible involvement of bFGF. *Cardiovasc Res* 45, 486.

Gospodarowicz, D., Hirabayashi K., Giguere L., and Tauber J. P. (1981). Factors controlling the proliferative rate, final cell density, and life span of bovine vascular smooth muscle cells in culture. *J Cell Biol* 89, 568.

Graham, M. F., Willey A., Adams J., Yager D., and Diegelmann R. F. (1995). Role of ascorbic acid in procollagen expression and secretion by human intestinal smooth muscle cells. *J Cell Physiol* 162, 225.

Grassl, E. D., Oegema T. R., and Tranquillo R. T. (2002). Fibrin as an alternative biopolymer to type-I collagen for the fabrication of a media equivalent. *J Biomed Mater Res* 60, 607.

Greisler, H. P., Gosselin C., Ren D., Kang S. S., and Kim D. U. (1996). Biointeractive polymers and tissue engineered blood vessels. *Biomaterials* 17, 329.

Hayat, M. Principles and Techniques of Electron Microscopy: Biological Applications. 2000.

Hayter, A. Probability and Statistics for Engineers and Scientists. 1996.

He, H., and Matsuda T. (2002). Arterial replacement with compliant hierarchic hybrid vascular graft: biomechanical adaptation and failure. *Tissue Eng* 8, 213.

Herring, M., Gardner A., and Glover J. (1978). A single-staged technique for seeding vascular grafts with autogenous endothelium. *Surgery* 84, 498.

Heydarkhan-Hagvall, S., Helenius G., Johansson B. R., Li J. Y., Mattsson E., and Risberg B. (2003). Co-culture of endothelial cells and smooth muscle cells affects gene expression of angiogenic factors. *J Cell Biochem* 89, 1250.

Hiles, M. C., Badylak S. F., Lantz G. C., Kokini K., Geddes L. A., and Morff R. J. (1995). Mechanical properties of xenogeneic small-intestinal submucosa when used as an aortic graft in the dog. *J Biomed Mater Res* 29, 883.

Hoerstrup, S. P., Zund G., Schnell A. M., Kolb S. A., Visjager J. F., Schoeberlein A., and Turina M. (2000). Optimized growth conditions for tissue engineering of human cardiovascular structures. *Int J Artif Organs* 23, 817.

Hoerstrup, S. P., Zund G., Sodian R., Schnell A. M., Grunenfelder J., and Turina M. I. (2001). Tissue engineering of small caliber vascular grafts. *Eur J Cardiothorac Surg* 20, 164.

Hollinger, J. O., and Battistone G. C. (1986). Biodegradable bone repair materials. Synthetic polymers and ceramics. *Clin Orthop*, 290.

Hungerford, J. E., and Little C. D. (1999). Developmental biology of the vascular smooth muscle cell: building a multilayered vessel wall. *J Vasc Res* 36, 2.

Hutmacher, D., Hurzeler M. B., and Schliephake H. (1996). A review of material properties of biodegradable and bioresorbable polymers and devices for GTR and GBR applications. *Int J Oral Maxillofac Implants* 11, 667.

Huynh, T., Abraham G., Murray J., Brockbank K., Hagen P. O., and Sullivan S. (1999). Remodeling of an acellular collagen graft into a physiologically responsive neovessel. *Nat Biotechnol* 17, 1083.

Imberti, B., Seliktar D., Nerem R. M., and Remuzzi A. (2002). The response of endothelial cells to fluid shear stress using a co-culture model of the arterial wall. *Endothelium* 9, 11.

Junqueira, L. C., Bignolas G., and Brentani R. R. (1979). Picrosirius staining plus polarization microscopy, a specific method for collagen detection in tissue sections. *Histochem J* 11, 447.

Kanda, K., Matsuda T., and Oka T. (1993). Mechanical stress induced cellular orientation and phenotypic modulation of 3-D cultured smooth muscle cells. *Asaio J* 39, M686.

Kangasniemi, and Opas. Structure of the arterial wall: Oulu University Library, 1997.

Kaushal, S., Amiel G. E., Guleserian K. J., Shapira O. M., Perry T., Sutherland F. W., Rabkin E., Moran A. M., Schoen F. J., Atala A., Soker S., Bischoff J., and Mayer J. E., Jr. (2001). Functional small-diameter neovessels created using endothelial progenitor cells expanded ex vivo. *Nat Med* 7, 1035.

Kim, B. S., and Mooney D. J. (1998a). Development of biocompatible synthetic extracellular matrices for tissue engineering. *Trends Biotechnol* 16, 224.

Kim, B. S., and Mooney D. J. (1998b). Engineering smooth muscle tissue with a predefined structure. *J Biomed Mater Res* 41, 322.

Kim, B. S., Nikolovski J., Bonadio J., and Mooney D. J. (1999a). Cyclic mechanical strain regulates the development of engineered smooth muscle tissue. *Nat Biotechnol* 17, 979.

Kim, B. S., Nikolovski J., Bonadio J., Smiley E., and Mooney D. J. (1999b). Engineered smooth muscle tissues: regulating cell phenotype with the scaffold. *Exp Cell Res* 251, 318.

Kim, B. S., Putnam A. J., Kulik T. J., and Mooney D. J. (1998). Optimizing seeding and culture methods to engineer smooth muscle tissue on biodegradable polymer matrices. *Biotechnol Bioeng* 57, 46.

Ko, I. K., and Iwata H. (2002). Simple method for increasing cell-attachment ability of biodegradable polyester. *Ann N Y Acad Sci* 961, 288.

Ku, D. N. ARC: Vascular Grafts. In: Bronzino JD, ed. The Biomedical Engineering Handbook: CRC Press, 2000.

Ku, D. N., Giddens D. P., Zarins C. K., and Glagov S. (1985). Pulsatile flow and atherosclerosis in the human carotid bifurcation. Positive correlation between plaque location and low oscillating shear stress. *Arteriosclerosis* 5, 293.

Kutryk, M. Complications of coronary stenting Coronary Stenting: Current Perspectives. A companion to the book of coronary stents, 1999.

Kypreos, K. E., and Sonenshein G. E. (1998). Basic fibroblast growth factor decreases type V/XI collagen expression in cultured bovine aortic smooth muscle cells. *J Cell Biochem* 68, 247.

Lamba, N. M. K., Baumgartner, J.A., Cooper, S.L. Cell-synthetic surface interactions. In: Jr. CWP, ed. Frontiers in Tissue Engineering. New York: Elsevier Science, 1998.

Lee, K. Y., Peters M. C., Anderson K. W., and Mooney D. J. (2000). Controlled growth factor release from synthetic extracellular matrices. *Nature* 408, 998.

L'Heureux, N., Paquet S., Labbe R., Germain L., and Auger F. A. (1998). A completely biological tissue-engineered human blood vessel. *Faseb J* 12, 47.

L'Heureux, N., Stoclet J. C., Auger F. A., Lagaud G. J., Germain L., and Andriantsitohaina R. (2001). A human tissue-engineered vascular media: a new model for pharmacological studies of contractile responses. *Faseb J* 15, 515.

Lieber, B. B., and Giddens D. P. (1990). Post-stenotic core flow behavior in pulsatile flow and its effects on wall shear stress. *J Biomech* 23, 597.

Lu, L., Peter S. J., Lyman M. D., Lai H. L., Leite S. M., Tamada J. A., Uyama S., Vacanti J. P., Langer R., and Mikos A. G. (2000). In vitro and in vivo degradation of porous poly(DL-lactic-co-glycolic acid) foams. *Biomaterials* 21, 1837.

Lytle, B. W., Loop F. D., Cosgrove D. M., Ratliff N. B., Easley K., and Taylor P. C. (1985). Long-term (5 to 12 years) serial studies of internal mammary artery and saphenous vein coronary bypass grafts. *J Thorac Cardiovasc Surg* 89, 248.

Mann, B. K., Tsai A. T., Scott-Burden T., and West J. L. (1999). Modification of surfaces with cell adhesion peptides alters extracellular matrix deposition. *Biomaterials* 20, 2281.

Marois, Y., Sigot-Luizard M. F., and Guidoin R. (1999). Endothelial cell behavior on vascular prosthetic grafts: effect of polymer chemistry, surface structure, and surface treatment. *Asaio J* 45, 272.

McKee, J. A., Banik S. S., Boyer M. J., Hamad N. M., Lawson J. H., Niklason L. E., and Counter C. M. (2003). Human arteries engineered in vitro. *EMBO Rep* 4, 633.

Merrilees, M. J. Synthesis of glycosaminoglycans and proteoglycans. In: Campbell JH, Campbell GR, eds. Vascular smooth muscle in culture: CRC Press, Inc., 1985.

Merrilees, M. J., Campbell J. H., Spanidis E., and Campbell G. R. (1990). Glycosaminoglycan synthesis by smooth muscle cells of differing phenotype and their response to endothelial cell conditioned medium. *Atherosclerosis* 81, 245.

Merrilees, M. J., and Scott L. (1981). Interaction of aortic endothelial and smooth muscle cells in culture. Effect on glycosaminoglycan levels. *Atherosclerosis* 39, 147.

Mikos, A. G., Thorsen A. J., Czerwonka L. A., Bao Y., Langer R., Winslow D. N., and Vacanti J. P. (1994). Preparation and Characterization of Poly(L-Lactic Acid) Foams. *Polymer* 35, 1068.

Mills, I., Cohen C. R., Kamal K., Li G., Shin T., Du W., and Sumpio B. E. (1997). Strain activation of bovine aortic smooth muscle cell proliferation and alignment: study of strain dependency and the role of protein kinase A and C signaling pathways. *J Cell Physiol* 170, 228.

Nasseri, B. A., Pomerantseva, I., Kaazempur-Mofrad, M.R., Sutherland, F.W.H., Perry, T., Ochoa, E., Thompson, C.A., Mayer, J.E., Oesterle, S.N., Vacanti, J.P. (2003). Dynamic rotational seeding and cell culture system for vascular tube formation. *Tissue Eng* 9, 291.

Neidert, M. R., Lee E. S., Oegema T. R., and Tranquillo R. T. (2002). Enhanced fibrin remodeling in vitro with TGF-beta1, insulin and plasmin for improved tissue-equivalents. *Biomaterials* 23, 3717.

Niklason, L. E. (1999). Techview: medical technology. Replacement arteries made to order. *Science* 286, 1493.

Niklason, L. E., Abbott W., Gao J., Klagges B., Hirschi K. K., Ulubayram K., Conroy N., Jones R., Vasanawala A., Sanzgiri S., and Langer R. (2001). Morphologic and mechanical characteristics of engineered bovine arteries. *J Vasc Surg* 33, 628.

Niklason, L. E., Gao J., Abbott W. M., Hirschi K. K., Houser S., Marini R., and Langer R. (1999). Functional arteries grown in vitro. *Science* 284, 489.

Nikolovski, J., and Mooney D. J. (2000). Smooth muscle cell adhesion to tissue engineering scaffolds. *Biomaterials* 21, 2025.

Orlidge, A., and D'Amore P. A. (1987). Inhibition of capillary endothelial cell growth by pericytes and smooth muscle cells. *J Cell Biol* 105, 1455.

Owens, G. K. (1995). Regulation of differentiation of vascular smooth muscle cells. *Physiol Rev* 75, 487.

Ozaki, T., Iizuka K., Suzuki M., Murakami T., Kitabatake A., and Kawaguchi H. (1999). Threshold-dependent DNA synthesis by pure pressure in human aortic smooth

muscle cells: Gialpha-dependent and -independent pathways. *Biochem Biophys Res Commun* 256, 212.

Pei, M., Solchaga L. A., Seidel J., Zeng L., Vunjak-Novakovic G., Caplan A. I., and Freed L. E. (2002). Bioreactors mediate the effectiveness of tissue engineering scaffolds. *Faseb J* 16, 1691.

Powell, R. J., Hydowski J., Frank O., Bhargava J., and Sumpio B. E. (1997). Endothelial cell effect on smooth muscle cell collagen synthesis. *J Surg Res* 69, 113.

Puchtler, H., Waldrop F. S., and Valentine L. S. (1973). Polarization microscopic studies of connective tissue stained with picro-sirius red FBA. *Beitr Pathol* 150, 174.

Ratcliffe, A. (2000). Tissue engineering of vascular grafts. *Matrix Biol* 19, 353.

Ratcliffe, A., and Niklason L. E. (2002). Bioreactors and bioprocessing for tissue engineering. *Ann N Y Acad Sci* 961, 210.

Reisman, M. Management of complications Guide to Rotational Atherectomy: Physicians' Press, 1997.

Risau, W. (1995). Differentiation of endothelium. *Faseb J* 9, 926.

Rocnik, E. F., Chan B. M., and Pickering J. G. (1998). Evidence for a role of collagen synthesis in arterial smooth muscle cell migration. *J Clin Invest* 101, 1889.

Roeder, R., Wolfe J., Lianakis N., Hinson T., Geddes L. A., and Obermiller J. (1999). Compliance, elastic modulus, and burst pressure of small-intestine submucosa (SIS), small-diameter vascular grafts. *J Biomed Mater Res* 47, 65.

Ross, R. (1971). The smooth muscle cell. II. Growth of smooth muscle in culture and formation of elastic fibers. *J Cell Biol* 50, 172.

Saini, S. Bioreactor for the production of tissue engineered cartilage: defining operating parameters for optimal construct growth Chemical Engineering. Atlanta: Georgia Institute of Technology, 2001.

Saltzman, W. M. Cell interactions with polymers. In: R. Lanza RL, and W. Chick, ed. Principles of Tissue Engineering. Austin, TX: R.G. Landers, 1997.

Sanborn, T. A. Early results of laser angioplasty using bare fiberoptics. In: Sanborn TA, ed. Laser Angioplasty: A.R. Liss, 1989.

Sapirstein, W., Zuckerman B., and Dillard J. (2001). FDA approval of coronary-artery brachytherapy. *N Engl J Med* 344, 297.

Saunders, K. B., and D'Amore P. A. (1992). An in vitro model for cell-cell interactions. *In Vitro Cell Dev Biol* 28A, 521.

Schmidt, C. E., and Baier J. M. (2000). Acellular vascular tissues: natural biomaterials for tissue repair and tissue engineering. *Biomaterials* 21, 2215.

Schoen, F. J. Blood Vessels. In: Cotran RS, Kumar V, Robbins SL, eds. Robbins Pathologic Basis of Disease: W.B. Saunders Company, 1994.

Scott-Burden, T., Tock C. L., Schwarz J. J., Casscells S. W., and Engler D. A. (1996). Genetically engineered smooth muscle cells as linings to improve the biocompatibility of cardiovascular prostheses. *Circulation* 94, II235.

Seifalian, A. M., Tiwari A., Hamilton G., and Salacinski H. J. (2002). Improving the clinical patency of prosthetic vascular and coronary bypass grafts: the role of seeding and tissue engineering. *Artif Organs* 26, 307.

Seliktar, D. Dynamic mechanical conditioning regulates the development of cell-seeded collagen constructs in vitro: Implications for tissue-engineered blood vessels. Atlanta: Georgia Institute of Technology, 2000.

Seliktar, D., Black R. A., Vito R. P., and Nerem R. M. (2000). Dynamic mechanical conditioning of collagen-gel blood vessel constructs induces remodeling in vitro. *Ann Biomed Eng* 28, 351.

Shin'oka, T., Imai Y., and Ikada Y. (2001). Transplantation of a tissue-engineered pulmonary artery. *N Engl J Med* 344, 532.

Shireman, P. K., and Pearce W. H. (1996). Endothelial cell function: biologic and physiologic functions in health and disease. *AJR Am J Roentgenol* 166, 7.

Shum-Tim, D., Stock U., Hrkach J., Shinoka T., Lien J., Moses M. A., Stamp A., Taylor G., Moran A. M., Landis W., Langer R., Vacanti J. P., and Mayer J. E., Jr. (1999). Tissue engineering of autologous aorta using a new biodegradable polymer. *Ann Thorac Surg* 68, 2298.

Sodian, R., Lemke T., Fritsche C., Hoerstrup S. P., Fu P., Potapov E. V., Hausmann H., and Hetzer R. (2002). Tissue-engineering bioreactors: a new combined cell-seeding and perfusion system for vascular tissue engineering. *Tissue Eng* 8, 863.

Stadler, E., Campbell J. H., and Campbell G. R. (1989). Do cultured vascular smooth muscle cells resemble those of the artery wall? If not, why not? *J Cardiovasc Pharmacol* 14 Suppl 6, S1.

Stegemann, J. P., and Nerem R. M. (2003). Altered response of vascular smooth muscle cells to exogenous biochemical stimulation in two- and three-dimensional culture. *Exp Cell Res* 283, 146.

Sterpetti, A. V., Cucina A., D'Angelo L. S., Cardillo B., and Cavallaro A. (1993). Shear stress modulates the proliferation rate, protein synthesis, and mitogenic activity of arterial smooth muscle cells. *Surgery* 113, 691.

Szycher, M. (1998). Review of cardiovascular devices. *J Biomater Appl* 12, 321.

Tagami, M., Nara Y., Kubota A., Sunaga T., Maezawa H., Fujino H., and Yamori Y. (1986). Morphological and functional differentiation of cultured vascular smooth-muscle cells. *Cell Tissue Res* 245, 261.

Thompson, C. A. (2002). A Novel Pulsatile, Laminar Flow Bioreactor for the Development of Tissue-Engineered Vascular Structures. *Tissue Eng* 8, 1083.

Thyberg, J., Hedin U., Sjolund M., Palmberg L., and Bottger B. A. (1990). Regulation of differentiated properties and proliferation of arterial smooth muscle cells. *Arteriosclerosis* 10, 966.

Thyberg, J., Nilsson J., Palmberg L., and Sjolund M. (1985). Adult human arterial smooth muscle cells in primary culture. Modulation from contractile to synthetic phenotype. *Cell Tissue Res* 239, 69.

Tiwari, A., Salacinski H. J., Hamilton G., and Seifalian A. M. (2001). Tissue engineering of vascular bypass grafts: role of endothelial cell extraction. *Eur J Vasc Endovasc Surg* 21, 193.

Tjia, J. S., Aneskievich B. J., and Moghe P. V. (1999). Substrate-adsorbed collagen and cell secreted fibronectin concertedly induce cell migration on poly(lactide-glycolide) substrates. *Biomaterials* 20, 2223.

Tranquillo, R. T., Girton T. S., Bromberek B. A., Triebes T. G., and Mooradian D. L. (1996). Magnetically orientated tissue-equivalent tubes: application to a circumferentially orientated media-equivalent. *Biomaterials* 17, 349.

Waybill, P. N., Chinchilli V. M., and Ballermann B. J. (1997). Smooth muscle cell proliferation in response to co-culture with venous and arterial endothelial cells. *J Vasc Interv Radiol* 8, 375.

Waybill, P. N., and Hopkins L. J. (1999). Arterial and venous smooth muscle cell proliferation in response to co-culture with arterial and venous endothelial cells. *J Vasc Interv Radiol* 10, 1051.

Weinberg, C. B., and Bell E. (1986). A blood vessel model constructed from collagen and cultured vascular cells. *Science* 231, 397.

Wight, T. N. (1989). Cell biology of arterial proteoglycans. *Arteriosclerosis* 9, 1.

Wight, T. N. Arterial wall. In: Comper W, ed. Extracellular matrix: Harwood Academic Publishers, 1996.

Williams, D. F., and Mort E. (1977). Enzyme-accelerated hydrolysis of polyglycolic acid. *J Bioeng* 1, 231.

Woessner, J. F. (1961). The determination of hydroxyproline in tissue and protein samples containing small proportions of this imino acid. *Archives Biochemistry and Biophysics*, 93440.

Ye, Q., Zund G., Jockenhoevel S., Schoeberlein A., Hoerstrup S. P., Grunenfelder J., Benedikt P., and Turina M. (2000). Scaffold precoating with human autologous extracellular matrix for improved cell attachment in cardiovascular tissue engineering. *Asaio J* 46, 730.

Ziegler, T., Alexander R. W., and Nerem R. M. (1995). An endothelial cell-smooth muscle cell co-culture model for use in the investigation of flow effects on vascular biology. *Ann Biomed Eng* 23, 216.

Ziegler, T., and Nerem R. M. (1994). Tissue engineering a blood vessel: regulation of vascular biology by mechanical stresses. *J Cell Biochem* 56, 204.

VITA

Chrysanthi (Sandy) Tsiagkli was born on April 25, 1974 in Athens, Greece. She grew up in Greece and graduated from high school in 1992. Sandy took the college entrance exam in Greece and was admitted to the School of Geology at the University of Athens. In 1993, she was admitted to the National Technical University of Athens where she pursued her Bachelor's degree in the School of Mining and Metallurgical Engineering. Sandy completed her 5-year program in 1998 and graduated first in her class.

In the fall of 1998, Sandy started the Ph.D. program in Biomedical Engineering at Georgia Institute of Technology under the advisement of Dr. Timothy M. Wick. Sandy was married to Kenneth Williams in the summer of 2002 and changed her last name to Williams. She will complete her Ph.D. in Bioengineering in the fall of 2003 and move to Minnetonka, Minnesota, to pursue a career in the medical devices industry.